EAST ENGINEERING LIBRARY

JUL 2 1948

TEXTILE RESEARCH JOURNAL

VOLUME XVIII June, 1948 NUMBER 6

PUBLICATION OF

TEXTILE RESEARCH INSTITUTE, INC.

AND

THE TEXTILE FOUNDATION

Editorial Office: 10 East 40th Street, New York 16, N. Y.

TEXTILE RESEARCH JOURNAL

VOL. XVIII, No. 6 June, 1948

In This Issue

Rheological Measurements with the Rotational Viscometer
Earl K. Fischer and Charles H. Lindsley 325

A Theory of Commercial Yarn Testing
Charles J. Geyer, Jr., C. H. Reichardt, and George Halsey 338

Cellulose Behavior with Filtered Sunlight
P. J. Fynn, J. E. Sands, and K. S. Campbell 350

A Permeability Method for Determining Fiber Fineness
John P. Elting and James C. Barnes 358

An Electron-Microscopical Examination of Rayon
Charles W. Hock 366

A Microscopical Technique for Determining Latex Distribution in Tire Cords
Ines V. deGruy and Mary L. Rollins 371

Book Reviews 374

Abstracts 376

Editor: Julian S. Jacobs *Managing Editor:* Julia M. Crisp

Associate Editors

H. J. Ball
Earl E. Berkley
Henry Eyring
Gustavus J. Esselen
Earl K. Fischer
Milton Harris
K. L. Hertel
H. Mark
E. R. Schwarz
Kyle Ward, Jr.

TEXTILE RESEARCH JOURNAL, published monthly at Prince and Lemon Streets, Lancaster, Pa., is devoted to the interest of research in textile and allied industries. It is the official publication of Textile Research Institute, Inc., and the Textile Foundation.

Manuscripts and communications should be sent to the editorial offices, 10 East 40th Street, New York 16, N. Y.

Subscription rates: General—$15.00 per annum; additional for postage, 50 cents to Canada, $1.00 to all other countries. Special—$10.00 per annum for United States and Canadian students, teachers, educational institutions, public libraries, governmental libraries and departments, plus 50 cents for postage to Canada. Single copies, $1.50 each.

Entered as second-class matter, April 27, 1945, at the postoffice at Lancaster, Pa., under the Act of August 24, 1912.

Contents copyrighted 1948 by Textile Research Institute, Inc.

Advertising rates supplied on request.

TEXTILE RESEARCH JOURNAL

VOL. XVIII, No. 6 June, 1948

Rheological Measurements with the Rotational Viscometer*

Earl K. Fischer and Charles H. Lindsley

Institute of Textile Technology, Charlottesville, Virginia

Abstract

The rotating cylinder viscometer in various forms has found wide use for the measurement of viscosity and the study of so-called anomalous flow. Starch pastes, pigment dispersions, printing pastes, and coatings are examples of materials used in the textile industry which exhibit complex flow properties. Identification of the different kinds of flow and measurement in terms of valid physical units are necessary before the properties of these materials can be correctly described. It can be expected that with adequate specification of flow properties more effective control in mill processes will become possible. This article is concerned with essential features of instrumentation, definition, and computation.

THE ADVANTAGES of the cylindrical rotational viscometer are so numerous that it deserves wider use for industrial measurements. It may be used on suspensions as well as on clear liquids and it is suitable for determination of viscosities over a wide range at variable rates of shear. Different types of flow properties may be identified, and the data may be expressed in dimensionally consistent units. As it is commonly used, however, the data cannot be expressed in rational units, and, as a consequence, the literature is cluttered with meaningless measurements. The unsatisfactory state of instrumentation in this field is in part responsible, since commercially available instruments of moderate cost need modification before they can be used to best advantage.

This paper presents details on the modification of one of these instruments, the well-known Stormer viscometer. The mechanical changes required are comparatively simple and can be made at small cost. The modified instrument makes possible a measurement of viscosities which is based on accepted physical principles and yields data of moderate precision which are easily reproducible. Because the operation of rotational viscometers has not been systematized, a preliminary discussion on terminology and an analysis of the basic factors for this measurement have been included here. Experimental results,

*This paper is based on part of the material presented at the Chemical Research Conferences, American Association for the Advancement of Science, at Colby Junior College, New London, N. H., July, 1947.

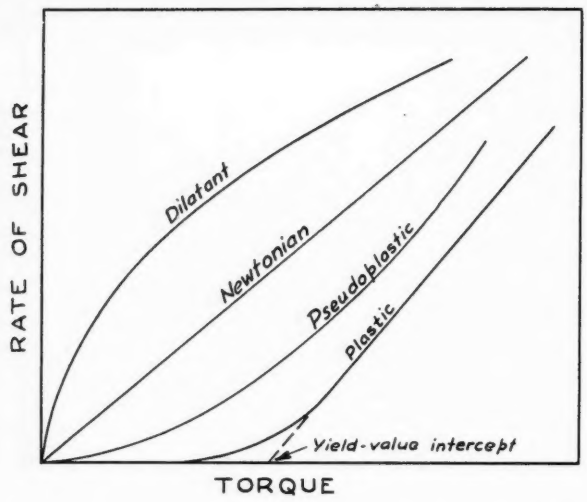

FIG. 1. *Generalized curves showing four types of flow measured on rotational viscometers.*

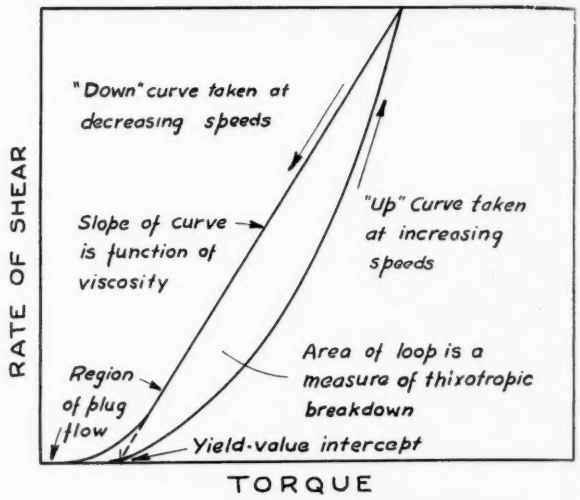
"Down" curve taken at decreasing speeds
Slope of curve is function of viscosity
"Up" Curve taken at increasing speeds
Area of loop is a measure of thixotropic breakdown
Region of plug flow
Yield-value intercept
RATE OF SHEAR
TORQUE

FIG. 2. *Generalized curve showing thixotropic flow measured on a rotational viscometer.*

drawn from a large number of data accumulated over the past several years, have been selected for illustration. As this paper is concerned with instrumentation, theory on the mechanism of flow is not included. Additional information on viscometers of all types will be found in the monograph by Barr [1].

It seems appropriate at this time to express our point of view regarding industrial instruments and measurements. Rheological measurements of all types are finding increasing utility in a variety of industries. Frequently it is necessary to devise an instrument for a specific purpose, but too often little attention is given to the principles upon which the measurement is made or the units in which the data are expressed. Completely empirical results obtained on special-purpose instruments are frequently of value in control of processes and charting of day-to-day variation, and they are a great advance over individual judgment. When interpretation of the results in terms of physical properties is attempted, however, difficulties arise. Adoption of a standard empirical test by a standardizing authority offers the advantage that a uniform procedure is followed by all persons making the measurement, but such standardization is not a substitute for measurement of a physical property capable of exact definition. Moreover, in the case of rheological measurements on pastes and suspensions, concealed systematic errors are inherent in the use of some well-established instruments.

A few examples of such difficulties will serve for illustration. One form of efflux viscometer is a cup with an orifice of standard size. The time of outflow, the basic datum, depends on the make and size of the instrument, which must be specified if the measurements are to have permanent reference value. More serious objections can be raised: (1) the flow from the orifice is not laminar, and it is not possible to derive a valid mathematical relationship between time of flow and viscosity, although the instrument can be calibrated with liquids of known viscosity; (2) the driving force (stress), and hence the rate of shear, diminishes as the material flows from the cup, a serious limitation for materials which exhibit anomalous flow properties; (3) in the case of a thixotropic material (see below) the quantity remaining in the cup may be determined by the amount of agitation it received prior to testing. Despite these limitations the efflux viscometer in various forms is widely used in many industries.

The capillary viscometer is very satisfactory for measuring viscosities of simple liquids and solutions. It is virtually useless, however, on suspensions or turbid liquids, for any obstruction in the capillary introduces unsuspected errors in the time of flow. Furthermore, it yields only a single figure for time, unless an arrangement is made to apply variable pressure and thus obtain a series of readings at different rates of flow. Even with this arrangement, new material is continually entering the capillary and the effects of extended shearing on the same volume

of material cannot be observed. Similar limitations may be noted with the falling-sphere viscometer. Shearing is not uniform and cannot be estimated or controlled, and the effect of continuous shear on a given volume of material cannot be studied.

Definitions

Several types of flow may be distinguished when rate of shear is plotted as ordinate against shearing stress as abscissa. This is the conventional method for representing data obtained with rotational viscometers. (Stress is applied as torque in rotational viscometers.) Figures 1 and 2 show idealized flow curves; actual experimental curves are presented later. Units of measurements are given in Table I and definitions follow.

A *Newtonian liquid* flows when acted on by any force however small. The rate of flow is directly proportional to the shearing force, as shown by the straight line extending to the origin in Figure 1. Many of the materials used in industry do not behave like true or Newtonian liquids but exhibit, instead, more complicated properties which are often designated *anomalous*. One very common non-Newtonian type is *plastic flow*. Materials exhibiting this property do not flow until the applied shearing stress exceeds a certain minimum value. It acts as if a barrier had to be surmounted before flow can occur. This minimum shearing stress, designated the *yield value*, is indicated by an intercept on the stress axis. When the yield value has been exceeded, laminar or streamline flow takes place. At lower values, the material is not being sheared uniformly: this is the region of plug flow.

Plastic flow is frequently associated with an internal structure which is temporarily destroyed by stirring or shaking but re-forms on standing. This property, designated *thixotropy*, is illustrated by Figure 2. Originally the term was applied to a reversible gel-sol-gel transformation: a thixotropic material was defined as a gel which seemingly liquefied on stirring but returned to the gel state on standing. When studied in a viscometer (preferably of the rotating-cup type) this change in flow properties is termed *thixotropic breakdown* [4, 5]. At any given rate of shear the shearing stress decreases until a steady state is reached in which further breakdown is balanced by re-formation of structural units. At higher rates of shear the balance is shifted in the direction of further breakdown. By taking a series of readings starting at low rates of shear and increasing to an arbitrarily fixed limit, and then continuing the measurement with a second series of readings at decreasing rates of shear, a loop in the flow curve is obtained. One measure of thixotropic breakdown is the area of the loop between the two curves. The difficulty in defining thixotropy lies in the fact that the behavior is dependent not only on the properties of the material under study but also on the method and rate of measurement. Thus, if shearing is not continued until a balance has been established, the viscometer reading obtained will represent some intermediate state. If the re-formation of structural units is very rapid, thixotropic breakdown may be completely overlooked.

Another type of flow is designated *pseudoplastic*. A substance which exhibits this property flows more readily as it is stirred or sheared, but there is no reversible structural breakdown as found in thixotropic flow. The curve for this type of flow is convex to the torque axis.

A fourth type is *dilatant flow*. A dilatant material shows increased resistance to flow as it is agitated or sheared, but when allowed to stand without disturbance it reverts to its original condition. In some respects dilatancy is the reverse of pseudoplasticity; the curve illustrating this property is concave to the torque axis.

It is in attempting to compute viscosities from experimental data that attention should be given to the type of flow exhibited. *Viscosity* is that property of a material in flow which gives rise to retarding forces. The *coefficient of viscosity* is the factor of proportionality between rate of shear and stress in the Newton equation, $\tau = \eta \frac{dv}{dx}$, where τ is the shearing stress, v is the relative velocity of the bounding surfaces, and x is the separation. Very

TABLE I. VISCOMETRIC UNITS

Property	Symbol	Unit	Dimensions
Viscosity (Newtonian)	η or μ*	Poise	dyne-sec/cm² $[ML^{-1}T^{-1}]$
Fluidity	ϕ	Rhe	cm²/sec/dyne $[M^{-1}LT]$
Plastic viscosity	U	Poise	dyne-sec/cm² $[ML^{-1}T^{-1}]$
Mobility	μ	Rhe	cm²/sec/dyne $[M^{-1}LT]$
Yield value	f	—	dynes/cm² $[ML^{-1}T^{-2}]$
Thixotropic breakdown	M	—	dyne-sec/cm² $[ML^{-1}T^{-1}]$
Rate of shear	S	—	Reciprocal seconds $[T^{-1}]$
Shearing stress	τ	—	dynes/cm² $[ML^{-1}T^{-2}]$

* International Critical Tables and many authorities prefer η.

frequently this quantity η is called the "viscosity" of the material. This dual use of the term leads to confusion, since *viscosity* as a property belongs to all materials capable of flow, whereas *viscosity*, meaning *coefficient of viscosity*, should be applied only to Newtonian materials.

Because *viscosity*, as a measure, has a limited meaning, it should be qualified when used to designate other types of flow. When applied to plastic flow, it is now frequently called *plastic viscosity*, with the intended meaning of *coefficient of plastic viscosity*, or the ratio of stress, in excess of the yield value, to the corresponding rate of shear. Both Newtonian and plastic viscosity are computed from the reciprocal of the slope of the line in the flow curve. The ratio of stress, or stress minus yield value, to rate of shear in these cases is constant.

For pseudoplastic and dilatant materials, however, this simple concept is not applicable. The ratio of stress to rate of shear changes continuously. In pseudoplastic materials the ratio decreases and in dilatant materials the ratio increases with rate of shear. Consequently, the rate of shear must be specified if a value analogous to viscosity is to be computed from the data. Despite some ambiguity, the term *apparent viscosity* has had long use. Unfortunately, what has been called apparent viscosity has been calculated from a single point on the stress-*vs.*-rate-of-shear curve, and the assumption is made that the flow curve is a straight line extending from this point to the origin, giving in effect a hypothetical (but completely erroneous) curve for a Newtonian material.* Throughout this paper the term *apparent viscosity* is applied to the differential rate of change of stress with change in rate of shear ($d\tau/dS$) at any specified rate of shear. It is thus unambiguously defined and is an exact analog of true or Newtonian viscosity.

Examples of the different types of flow which can be studied on a rotational viscometer follow.

Newtonian Liquids
- Pure substances (*e.g.*, glycerin, water, etc.)
- Oils (except highly viscous oils at high rates of shear)
- Many solutions, especially of low-molecular-weight compounds

Plastic Materials
- Pigment dispersions, including paints, printing inks, textile printing pastes

Pseudoplastic Materials
- Many high-polymer "solutions"
- Cooked starch pastes
- Emulsions

Dilatant Materials
- Deflocculated pigment dispersions with high proportion of suspended solid
- Starch slurries (uncooked) at 40–50 percent by weight of starch

Basic Factors in Operation of Rotational Viscometers

In any measurement of viscosity by means of a concentric-cylinder viscometer, the following factors must be considered: (1) the retarding torque produced by the liquid being sheared in the annular space between the two cylinders; (2) the contribution of end traction on the inner cylinder to the total traction (the end-effect); (3) the variation in rate of shear between cup and bob. These will be considered in turn.

The Retarding Torque

In rotational viscometers equilibrium is established when the driving force is balanced by the retarding force arising in the material being sheared. At equilibrium, the rate of rotation is constant and the following relation holds [8]:

$$T = 4\pi r^2 \eta h \omega, \tag{1}$$

where T is the applied torque, η the viscosity, and ω the rate of rotation. The factors r^2 and h are found from the dimensions of the cup and bob used: $r^2 = R_c^2 \times R_b^2/(R_c^2 - R_b^2)$, where R_c and R_b are the radii of the cup and bob; h is the height of the bob.

For materials exhibiting plastic viscosity, the equation by Reiner and Riwlin [10] is now considered to describe adequately the anomalous results obtained. This equation may be written in the following form:

$$U = \frac{T}{4\pi r^2 h \omega} - \frac{f}{\omega} \ln \frac{R_c}{R_b}, \tag{2}$$

where U is the plastic viscosity (poises) and f is the yield value (dynes/cm.^{2}); the other symbols have the same significance as above. When f is 0, equation (2) reduces to equation (1). The yield

* Difficulties in nomenclature have been discussed in an interesting paper by L. H. Cragg, *J. Colloid Sci.* 1, 261–9 (1946). Recommendations have been made for a uniform system. Most of these terms, however, are not concerned with the type of measurements discussed in this paper.

value may be expressed in terms of the intercept (T_f) on the torque axis of the linear portion of the flow curve, thus:

$$f = \frac{T_f}{4\pi r^2 h \ln R_c/R_b}. \quad (3)$$

Green [3] has examined equations (2) and (3) critically and found experimental support for them.

For equation (1) it is immaterial whether the bob is driven and the cup remains stationary (as in the Stormer viscometer) or whether the cup is rotated (as in the MacMichael and Interchemical instruments). When the Stormer is used, it is convenient to replace T by Wgl, where W is the load (in grams), g the acceleration of gravity (980 cm./sec./sec.), and l the effective length of the lever arm on which the load acts (dependent on the gear ratio and diameter of the drum on which the cord is wound). One usually replaces ω in radians per second by r.p.m. by inclusion of the factor $2\pi/60$. After these substitutions, equation (1) may be solved for η:

$$\eta = \frac{60gl}{8\pi^2} \times \frac{1}{r^2 h} \times \frac{W}{\text{rpm}} = K \times \frac{1}{r^2 h} \times \frac{W}{\text{rpm}}. \quad (4)$$

For the MacMichael type of viscometer, the torque is measured by the deflection δ (in degrees) and the torsional constant, c, of the wire or spring attached to the bob ($T = c \cdot \delta$), and equation (1) becomes:

$$\eta = \frac{60c}{8\pi^2} \times \frac{1}{r^2 h} \times \frac{\delta}{\text{rpm}} = K' \times \frac{1}{r^2 h} \times \frac{\delta}{\text{rpm}}. \quad (4a)$$

The End-Effect

In the derivation of the preceding equations, it has been assumed that the cylinders were without ends, or, rather, that the traction of the viscous liquid on the ends of the inner cylinder was negligible in comparison with the traction on the cylindrical surface. A detailed study by the authors [9] of this end-effect showed that it is by no means negligible. Several ways of taking account of the effect have been tried, among which may be mentioned: (1) calibration of the instrument with standard liquids of known viscosity to obtain an empirical instrument constant to use instead of K/r^2h or K'/r^2h in equation (4) or (4a); (2) reduction in relative motion of the liquid above and below the bob by means of "guard rings" or other mechanical features; (3) use of a bob with a cylindrical surface much greater than the area of the ends; (4) experimental measurement of the end-effect so that it may be included in calculations of viscosity and yield value. In the paper cited [9], a brief review of the first three ways was given with references to their application in experiments. The fourth method was carefully investigated. The end-effect can be expressed in terms of increased length of bob. In equation (4) or (4a) the actual length h is replaced by an effective length h^*, where $h^* = h + h_0$, and h_0 is the end-effect expressed as added length. The magnitude of h_0 is nearly the same for bobs of different diameters (from 2.5 to 4.2 cm.) for a given clearance between cup and bob; as the clearance increases, h_0 also increases. For a given cup and bob, the end-effect is nearly constant for all viscosities above 1 poise (measured to 154 poises). The separation between the bottom of the bob and the cup is without effect as long as it is greater than about 1.3 cm.; the end-effect becomes larger as the bottom of the bob and the cup are brought closer together.

By use of one bob partially immersed to varying depths (single-bob method) or by use of two bobs of the same radius but of different length (multiple-bob method), it is possible to determine the viscosity of a liquid without actual evaluation of the end-effect. Let h_1 and h_2 be the length of the immersed portion of the single bob or the total length of each of the two bobs used in the second method; and let P_1 and P_2 be the corresponding values for the ratio W/rpm or δ/rpm in equation (4) or (4a). Then it can easily be shown (see reference 9, equation (2)) that:

$$\eta = \frac{K}{r^2} \times \frac{P_1 - P_2}{h_1 - h_2}, \quad (5)$$

where K and r have the meaning previously given, and can be calculated from known constants and dimensions of the instrument. When Newtonian liquids are being studied, P is constant at values of r.p.m. below turbulence, so that average values may be substituted in equation (5).

In practice it has been found more convenient to determine a value for h_0 for a given cup and bob combination and then to use $h + h_0$ instead of h in equation (4) or (4a). Then η can be found from a single value of P. To find h_0 one uses the same data used in equation (5) to determine η, along with that value of η, for it is clear that

$$h^* = h + h_0 = \frac{K}{r^2} \times \frac{P}{\eta}.$$

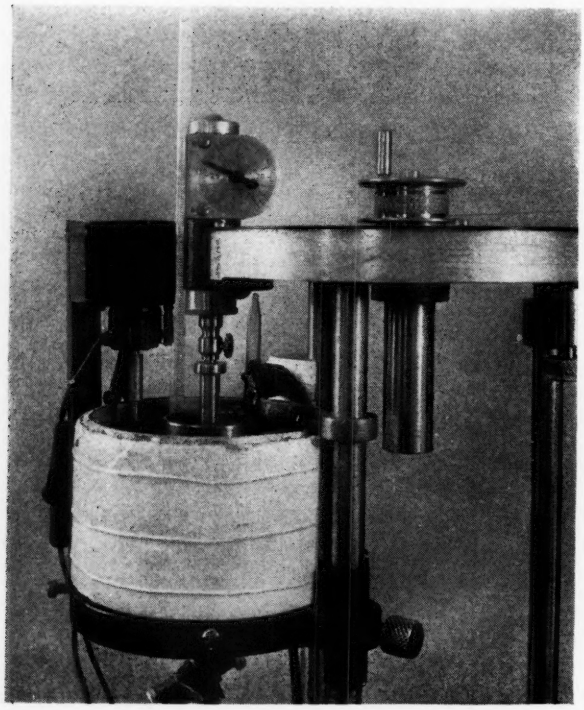

FIG. 3. *Viscometer assembly.*

Hence

$$h_0 = \frac{K}{r^2} \times \frac{P_1}{\eta} - h_1 = \frac{K}{r^2} \times \frac{P_2}{\eta} - h_2. \qquad (6)$$

There is some loss in accuracy in using a single value for h_0 over the whole viscosity range above 1 poise, but the greater convenience in measurement usually compensates for the loss, unless maximum accuracy is demanded. Below 1 poise, a separate value for h_0 must be found for each 0.1-poise interval because of the marked variation in end-effect with viscosity in this range. This can be done by either of the methods already described or by calibration with samples of known viscosity.

Rate of Shear

The rate of shear S (or the velocity gradient) in a rotational viscometer is determined by the rate of rotation, radius of the bob, and clearance between cup and bob. For any angular velocity ω, S is not uniform throughout the annular space, but depends on the distance x from the axis of rotation [6, 7]:

$$S = \frac{2R_c^2 \times R_b^2}{R_c^2 - R_b^2} \times \frac{\omega}{x^2}. \qquad (7)$$

The mean value $\bar{S}$ of S throughout the annular space may be found as follows:

$$\bar{S} = \int_{R_b}^{R_c} S dx \Big/ \int_{R_b}^{R_c} dx = \frac{2R_cR_b}{R_c^2 - R_b^2} \times \omega$$

$$= \frac{4\pi}{60} \cdot \frac{r^2}{R_c \times R_b} \times \text{rpm}. \qquad (8)$$

As was shown in the earlier paper, for small clearances S may be taken as equal to $\bar{S}$, within the usual experimental error. Even for relatively large clearances when there is considerable variation in S throughout the liquid, it was found that the average value was close to $\bar{S}$. For non-Newtonian liquids, where different values for apparent viscosity are found at different rates of shear, the mean value of η_a is found experimentally to be approximately the

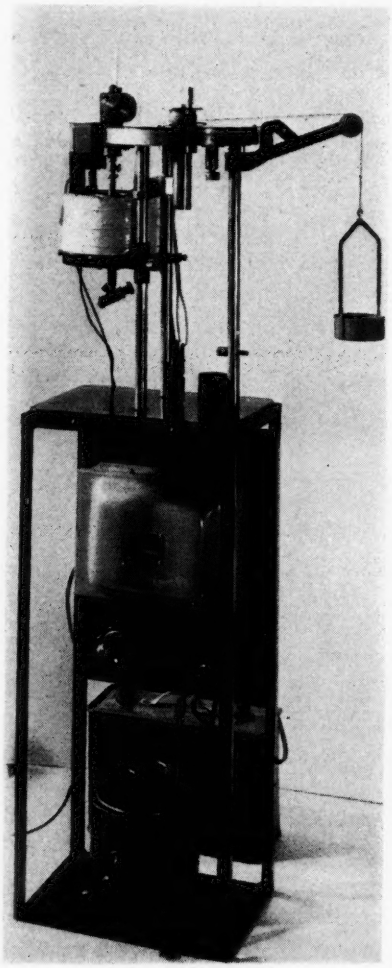

FIG. 4. *View of viscometer showing water bath, cup and bob in operating position, and accessory equipment.*

same for large and small clearances, so that the effect of variable rate of shear apparently balances out. The portions of liquid under high shear with corresponding low apparent viscosity are counterbalanced by other portions where the effects are reversed, and the over-all measurement gives a value in agreement with that found when the variation in S is negligible.

Experimental Details

Instrument Modifications

The following modifications were made on a commercial-model Stormer viscometer. A constant-temperature water bath was constructed using the aluminum cup supplied with the instrument. The cup was wound with a layer of asbestos paper attached with a thin layer of sodium silicate solution. Twenty turns of No. 22 (B & S gage) Nichrome resistance wire were then wound over the asbestos, and the winding was covered with several layers of the asbestos paper. This heater was connected to a fixed-point thermoregulator and relay through a Variac voltage control. For stirring, a small motor with an impeller agitator was attached to the support for the cup. Although the water bath held a relatively small volume of water, the temperature control was satisfactory when the Variac was set to give a uniform cycle of heating and cooling. With this arrangement, temperature control was maintained within ±0.1°C at 30°C. Higher temperatures, to 90°C, were obtained by changing to the appropriate thermoregulator and using a higher Variac setting. It was also found helpful to extend, by 12 cm., the arm carrying the pulley over which passed the cord holding the weight carrier. Laboratory weights were used to vary the load, and a fine nylon thread was used to support the weights. The instrument, with an angle-iron support and accessory equipment, is shown in Figures 3 and 4.

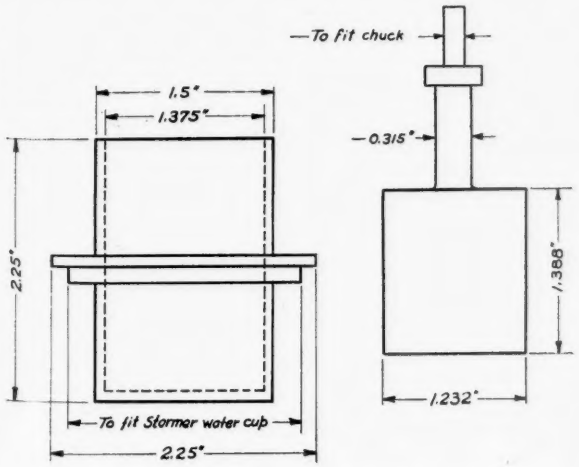

FIG. 5. *Machine drawing for cup 1, bob 1.*

TABLE II. DIMENSIONS OF CUPS AND BOBS

		Radius (cm.)	Height (cm.)
Cup	1	1.746	5.2
	2	2.342	4.9
Bob	1	1.565	3.53
	13 (plastic)	1.565	3.53
	4	2.104	3.49

The cup and bob or paddle supplied by the manufacturer are unsuited to measurement of viscosity in rational units. Accordingly, they were replaced by several cylindrical cups and bobs, of various diameters, accurately machined from brass (Figure 5). One bob was made of "Synthane," a laminated plastic, for use at high temperatures in order to reduce heat conduction. With different combinations, different clearances and hence a variety of rates of shear at a given r.p.m. were possible. Table II gives the dimensions (for the cups, inside dimensions are given).

Procedure for Using Viscometer

The cup and bob selected for a particular test are carefully aligned in the viscometer, the cup being raised to about 1.3 cm. from the bottom of the bob. The cup is filled nearly to the top with the sample, and the bob is then rotated slowly for a few minutes to help bring the contents to the temperature of the bath. At least ten measurements of the time of rotation with different loads are taken, and the results are plotted as illustrated in Figures 5 to 10. Special precautions necessary when measuring non-Newtonian liquids are noted later.

Calculations

To find the apparent viscosity from the experimental data, the following working equations are used (*cf.* equations 4 and 8):

$$\eta_a = K_v \cdot W/\text{rpm}; \tag{9}$$

$$\bar{S} = k_s \times \text{rpm}. \tag{9a}$$

Here $K_v = K/r^2(h + h_0)$ and $k_s = 0.209r^2/R_c \times R_b$. As seen from equation (4), K is an instrument constant, not involving the dimensions of cup and bob, while both K_v and k_s depend on the combination used. Values for these constants are given in

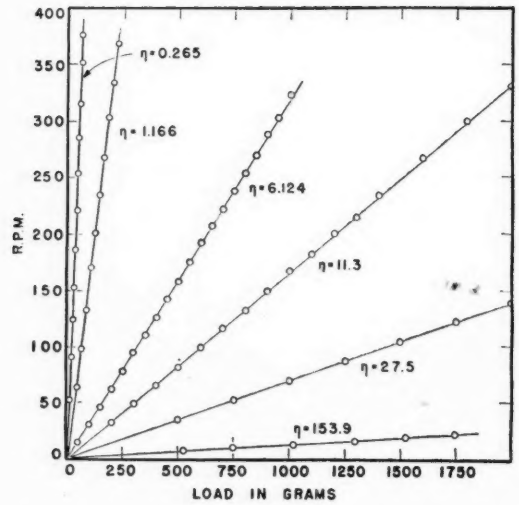

FIG. 6. *Experimental values for load and r.p.m. for oils showing Newtonian flow.*

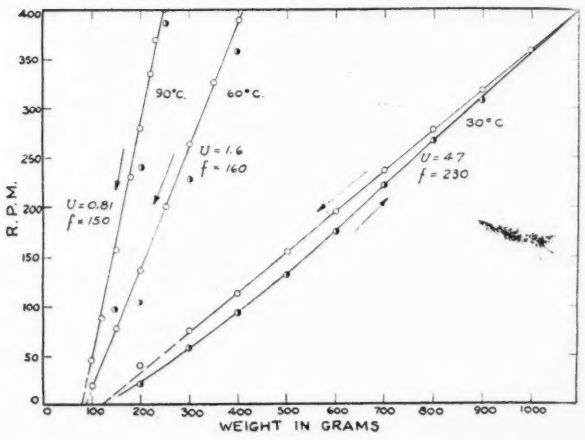

FIG. 7. *Plastic and thixotropic flow properties of a titanium dioxide dispersion in linseed oil.*

Table III. It should be recalled that the value for h_0, and hence the values of K_v and k_s, can be assumed constant for a given cup and bob only when the apparent viscosity is greater than 1 poise.

It is clear that K_v may be determined by calibration with standards of known viscosity. Such liquids may be obtained from the National Bureau of Standards [12] to cover a wide range of viscosity. The ratio W/rpm is found experimentally for one or more of these standards. Substitution of that value and the certified viscosity in equation (9) permits immediate evaluation of K_v.

With these constants, η_a and $\bar{S}$ are calculated for any observed W and r.p.m. For purposes of comparison, however, it is generally desirable to state the apparent viscosity for some particular rate of shear, say 100 sec^{-1}. Since only by coincidence will one of the experimental rates of shear correspond to this particular value, some method of interpolation is desired. This may be accomplished in any of several ways. To begin with, the r.p.m. corresponding to the given rate of shear is found from equation (9*a*). Then on the graph of r.p.m. *vs.* load, the tangent is drawn to the curve at that value for r.p.m. and its slope is found by direct measurement. The reciprocal of this slope multiplied by the appropriate K_v gives the value for η_a.

Alternatively, an empirical equation for W in terms of r.p.m. may be found; η_a may then be expressed as a function of r.p.m., thus:

$$\eta_a = K_v \cdot dW/d\,(\text{rpm}). \qquad (10)$$

Two forms of empirical equation have been used, a quadratic and an exponential. In the first case, data obtained with the Stormer viscometer are most conveniently fitted to an equation of the form:

$$\text{rpm} = a + bW + cW^2. \qquad (11)$$

The three constants are determined by some method

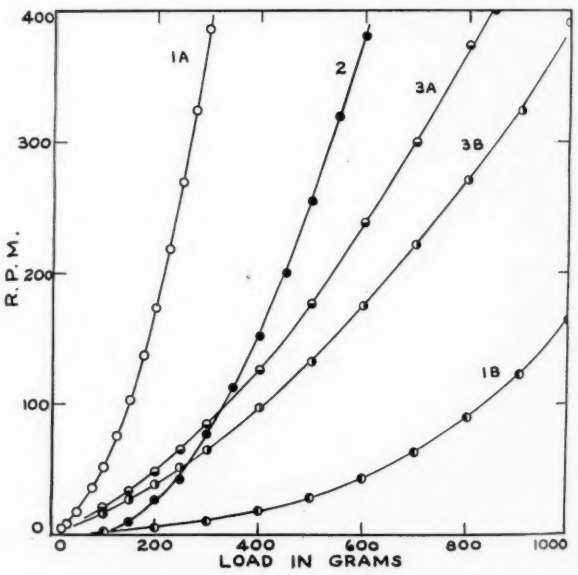

FIG. 8. *Experimental curves for materials showing pseudoplastic flow. (1A—sodium alginate, 1% in water; 1B—at 2% concentration; 2—acid-modified cornstarch paste, 10% (dry basis); 3A—methyl cellulose solution, 4000 cps. grade 1.95% (dry basis); 3B—1500 cps. grade 2.29% (dry basis). All solutions in water. Measurements at 30°C except for starch pastes, which were at 90°C. Cup 1, bob 1.)*

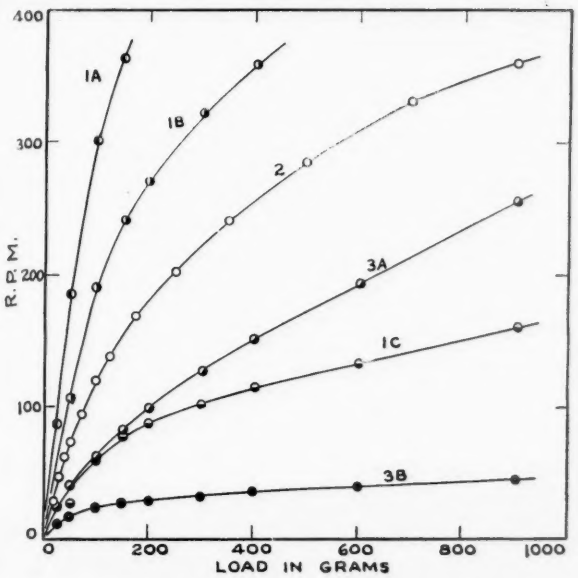

FIG. 9. *Experimental curves for materials showing dilatant flow. (1A—iron oxide suspension, 11.3 vol.% in aqueous solution of sodium lignin sulfonate 10%; 1B —same, iron oxide, 11.7 vol.%; 1C—same, iron oxide, 12.4 vol.%; 2—barium sulfate, 39.2 vol.%, suspension in aqueous solution of sodium lignin sulfonate; 3A—starch suspension in ethylene glycol, 46.9 vol.%; 3B—same, 50.8 vol.%. T = 30°C. Cup 2, bob 1.)*

of computation (*e.g.*, by least squares), and W as a function of r.p.m. is readily found:

$$W = (b^2 - 4ac + 4c \times \text{rpm})^{\frac{1}{2}}/2c - b/2c. \quad (11a)$$

The reciprocal of the slope of the curve of r.p.m. *vs.* W is given by the first derivative, and therefore

$$\eta_a = K_v \cdot dW/d\,(\text{rpm}) = K_v/(b^2 - 4ac + 4c \cdot \text{rpm})^{\frac{1}{2}}. \quad (12)$$

From equation (12), η_a is readily found for any r.p.m.—*i.e.*, for any rate of shear.

When the rotating-cup type of viscometer is used, the solution is somewhat simpler, for the data may be immediately expressed in the form:

$$\delta = a + b \cdot \text{rpm} + c \cdot (\text{rpm})^2. \quad (13)$$

Then

$$\eta_a = K_v' d(\delta)/d\,(\text{rpm}) = K_v' \cdot (b + 2c \cdot \text{rpm}). \quad (14)$$

TABLE III. WORKING CONSTANTS FOR DIFFERENT CUP AND BOB COMBINATIONS (K = 99.0)

	r^2	h_o	K_v	K_s	K_f
Cup 1—Bob 1 or 13	12.46	0.58	1.93	0.95	1.85
Cup 2—Bob 1 or 13	4.43	1.00	4.94	0.25	1.28
Cup 2—Bob 4	22.95	0.82	1.00	0.97	0.98

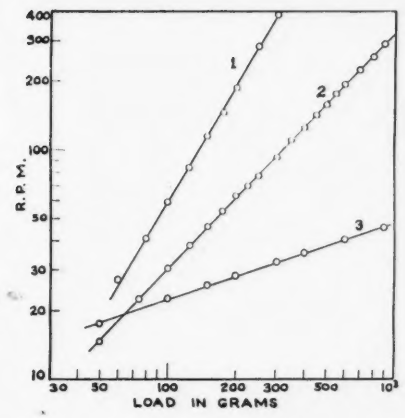

FIG. 10. *Log-log plot of data obtained with pseudoplastic (curve 1), Newtonian (curve 2), and dilatant (curve 3) flow. (1—sodium alginate solution, 1% concentration; 2—NBS standard oil; 3—starch suspension in ethylene glycol, 50.8 vol.%. T = 30°C.)*

In many instances the exponential form of empirical equation is useful:

$$W = A\,(\text{rpm})^n \quad \text{or} \quad \delta = A\,(\text{rpm})^n. \quad (15)$$

Then

$$\eta_a = K_v \cdot nA\,(\text{rpm})^{n-1} \quad (16)$$
$$= K_v \cdot nW/\text{rpm}, \quad \text{or} \quad K_v' \cdot n\delta/\text{rpm}. \quad (16a)$$

It is interesting to note in passing that different types of flow are readily classified by the value of n. When $n = 1$, the material shows Newtonian flow properties, η being independent of rate of shear, as is seen at once from equation (16). For n between 0 and 1, the material is pseudoplastic, and for n greater than 1 it is dilatant. An equation of the form (15) cannot be used to represent plastic materials, because the yield value prevents the curve r.p.m. *vs.* W from passing through the origin.

Only two constants appear in equation (15), whereas there are three in equations (11) and (13). This is true because in the former case it is implicit that the curve passes through the origin; if the same assumption is made in equations (11) and (13), $a = 0$ and only two constants, b and c, remain. Actually, as one sees from equation (16*a*), only n must be determined, provided the value for W corresponding to the desired r.p.m. can be readily found; this can be done, as is shown below.

To determine n, it is convenient to plot the experimental data on log-log paper (see Figure 10); such a plot is equivalent to the equation:

$$\log W = \log A + n \log \text{rpm}. \quad (17)$$

TABLE IV. COMPARISON OF EXPERIMENTAL VALUES OF r.p.m. FOR DIFFERENT LOADS WITH VALUES CALCULATED FROM EMPIRICAL EQUATIONS (1% sodium alginate solution)

Load, W (g.)	r.p.m. (expt'l)	r.p.m., calc'd from eq. (18)	r.p.m., calc'd from eq. (20)	r.p.m., calc'd from eq. (22)
40	15.0	14.6	13.8	14.9
60	26.9	26.7	26.7	26.6
80	41.1	41.4	42.7	41.3
100	59.2	59.0	61.3	59.0
125	84.1	84.9	88.2	85.2
150	114.5	115.2	118.6	115.6
175	149.0	149.7	152.4	150.4
200	189.3	188.7	189.3	189.2
250	282.0	279.8	272.2	279.4
300	387.0	388.2	366.2	385.6

Hence, if this type of equation is applicable, a straight line results; its slope can be found by direct measurement and the reciprocal is equal to n. From the same plot, one reads off the value of W for the particular value of r.p.m. Substitution of these values of n, W, and r.p.m. in equation (16a) gives η_a.

As an illustration of the several methods of computing the apparent viscosity, the experimental data for a colloidal solution containing 1 percent sodium alginate are given in Table IV. Suppose the apparent viscosity at four rates of shear—50, 100, 200, and 300 sec^{-1}—are required. Since the data were obtained with cup 1, bob 1, for which $k_s = 0.955$, these rates of shear correspond to 47.8, 95.5, 191.0, and 286.5 r.p.m. Tangents were drawn to the curve (IA, Figure 8) at these points, and their slopes measured; multiplication by $K_c = 1.93$ gives the apparent viscosity as shown:

Rate of shear, sec^{-1}	47.8	95.5	191.0	286.5
$\Delta W/\Delta$ rpm	1.192	0.924	0.564	0.456
η_a, poises	2.30	1.78	1.09	0.88

The data were also used to find an empirical quadratic equation:

$$\text{rpm} = -1.01 + 0.251W + 0.00349W^2. \quad (18)$$

From this one finds that

$$\eta_a = K_c dW/d\,\text{rpm} = 16.3/(5.53 + \text{rpm})^{\frac{1}{2}}. \quad (19)$$

The values of η_a calculated from this equation are shown in the fourth column of Table V.

TABLE V. CALCULATION OF APPARENT VISCOSITY OF SODIUM ALGINATE SOLUTION AT SEVERAL RATES OF SHEAR BY DIFFERENT METHODS

Rate of shear (sec^{-1})	r.p.m.	Apparent viscosity (poises) From curve	From eq. (19)	From eq. (21)	From eq. (23)
50	47.8	2.30	2.24	2.13	2.23
100	95.5	1.78	1.63	1.63	1.62
200	191.0	1.09	1.17	1.25	1.18
300	286.5	0.88	0.96	1.07	0.98

The same data were used to determine an equation of the form of equation (17) (see curve 1, Figure 10):

$$\log W = 0.901 + 0.615 \log \text{rpm}. \quad (20)$$

Then

$$\eta_a = 1.188W/\text{rpm}. \quad (21)$$

When the selected values for r.p.m. and corresponding values for W (calculated from equation (20)) were substituted in equation (21) the values of η_a shown in the fifth column of Table V were obtained. These differ considerably from those obtained from the graph or from equation (19). The explanation lies in the fact that the simple two-constant equation of the form $W = A\,(\text{rpm})^n$ is inadequate to provide a suitable fit for the experimental data. The inclusion of an additive constant, $W = A\,(\text{rpm})^n + B$, results in a much more satisfactory fit. Such an empirical equation may be solved by the method given by Davis [2, pp. 11–14]; one finds

$$W = 12.81\,(\text{rpm})^{0.538} - 14.7 \quad (22)$$

and the corresponding expression for apparent viscosity:

$$\eta_a = 1.04(W + 14.7)/\text{rpm}. \quad (23)$$

Values calculated from equation (23) are given in the last column of Table V; the agreement with those found from the quadratic equation or by graphical solution is excellent. In general, the experimental data do not justify such elaborate calcu-

TABLE VI. VISCOSITIES OF CERTIFIED STANDARD OILS AT 30°C DETERMINED EXPERIMENTALLY BY MULTIPLE BOB METHOD

Sample	Average viscosity (from 3 bob combinations) (poises)	Certified viscosity (poises)	Deviation (%)
K-5	0.264	0.2648	−0.3
M-11	1.16	1.166	−0.5
N-13	6.27	6.124	+2.2
OB-1	156.	153.9	+1.4

TABLE VII. VISCOSITIES DETERMINED BY CORRECTING BOB LENGTH FOR END-EFFECT
$\eta = (K/r^2h^*) \times$ (load/rpm)

Combination		Cup 1, bob 1		Cup 2, bob 1		Cup 2, bob 4	
Sample	Viscosity, known (poises)	Viscosity, detm'd (poises)	Deviation (%)	Viscosity, detm'd (poises)	Deviation (%)	Viscosity, detm'd (poises)	Deviation (%)
NBS: M-11	1.166	1.16	−0.5	—	—	1.15	−1.4
N-13	6.124	5.90	−3.7	5.97	−2.5	6.00	−2.0
OB-1	153.9	151.	−1.9	—	—	148.	−3.8
Litho-varnishes							
No. 00000	1.5	1.49	0.0	1.52	0.0	1.45	0.0
No. 1 Trans.	9.2	9.3	+1.1	9.0	−2.2	9.3	+1.1
No. 1 Reg.	11.6	11.7	+0.9	12.0	+3.4	11.6	0.0
No. 3 Reg.	27.5	27.9	+1.5	27.0	−1.8	27.5	0.0

lations, one method only sufficing. All three (or four) methods were employed for illustrative purposes to show what sort of results could be obtained by each. Neither of the empirical equations (11) or (15) is applicable to plastic materials because of the yield value. If, however, the intercept W_f on the stress axis (see Figure 6) is subtracted from the value of the load W for any r.p.m., then plastic viscosity may be found by replacing W by $W - W_f$ in the appropriate equations. (For the MacMichael type, $(\delta - \delta_f)$ is used, where δ_f is the corresponding intercept.) Thus the general equation (9) becomes

$$U = K_v \cdot (W - W_f)/\text{rpm}. \qquad (24)$$

The constant K_v has the same numerical value as before.

To express yield value in c.g.s. units, equation (3) may be written in the following form, after the usual substitutions have been made:

$$f = \frac{2\pi}{60} \frac{1}{2.303 \log R_c/R_b} \times \frac{K}{r^2(h + h_0)} \times W_f$$
$$= \frac{0.0455 K_r}{\log R_c/R_b} \times W_f = K_f \times W_f. \qquad (25)$$

The constant K_f involves the same factors as K_v and hence depends on the cup and bob used; its value for three combinations is given in Table III.

Examples of Types of Flow

The possible utility of the modified Stormer viscometer is illustrated with typical measurements on oils (Newtonian), pigment dispersions (plastic, thixotropic), starch and other lyophilic colloids (pseudoplastic), and uncooked starch slurry (dilatant). These examples are drawn from a large number of experimental data. Since this paper is concerned chiefly with instrumentation, theoretical matters connected with the possible causes of the different kinds of flow are not included. The reader is referred to Hatschek [7] and Scott Blair [11] for an introductory discussion.

Experimental data on the standard oils which exhibited Newtonian flow are given in Figure 6. It will be noted that excellent alignment of the points is obtained and all the lines pass through the origin. Computed viscosities using the method of multiple bobs are given in Table VI. Deviation from the certified value is within ±2 percent. In practice, however, it is simpler to use a single bob and apply the correction for the end-effect. Results obtained with this method are collected in Table VII [6]. It should be noted that the certified values for viscosity have not been used in computing the values listed in Tables VI and VII. Over this range the correction for end-effect may be applied to give viscosities with an accuracy of ±5 percent.

Plastic flow is commonly observed in pigment dispersions such as paints and textile printing pastes. Data on a representative composition prepared by dispersing titanium dioxide in a bodied linseed oil are presented in Figure 7. The pigment concentration was 15 percent. It will be noted that the data when plotted form a loop, indicating thixotropic structure, and that the points taken at decreasing rates of shear fall on straight lines with a positive intercept on the weight (torque) axis. The computed plastic viscosities and yield values are shown on the graph for three temperatures.

Colloidal solutions of starch, methyl cellulose, alginates, gelatin, water-soluble gums, etc. exhibit pseudoplastic flow, as shown in Figure 8. For most of these colloidal materials the curves measured at both increasing and decreasing rates of shear are,

TABLE VIII. CHANGE IN APPARENT VISCOSITY WITH RATE OF SHEAR
(Starch pastes, 10% dry basis)

Starch No.	Cooking time (hr.)	Fluidity rating*	Apparent viscosity (Poises) Rate of shear (sec^{-1}) 3.6	18	300
10A	1.0	20	22.0	9.7	1.4
9D	1.0	20	9.7	4.2	1.2
5	0.5	40	9.5	3.7	1.0
5	1.0	40	7.5	3.2	1.0
3	1.0	80	6.2	4.1	—
1	0.5	—	1.4	1.2	0.65

* Alkali fluidity values supplied by manufacturers.

within experimental error, identical. At the gel point, however, a structure is formed which, once broken down by shearing, does not re-form with the same initial physical properties. Since the criterion of thixotropy is a reversible, isothermal sol-gel transition, these materials should not be considered thixotropic.

Computation of apparent viscosities of pseudoplastic materials may be made by the tangent method described earlier. Data on starch pastes are given in Table VIII, computed at different rates of shear. These pastes were prepared by heating in a double boiler at 92°C. Differences in the pasting characteristics may be observed in this way.

Dilatant flow is infrequently encountered in textile-mill operations. Examples are shown in Figure 9. Dilatancy becomes evident at about 42 volume percent of starch and is extreme at 50 volume percent. Entirely similar properties are observed in aqueous suspensions of ungelatinized starch granules. The measurements on dilatancy are difficult if the clearance between cup and bob is small, for the composition on shearing becomes granular (*i.e.*, appears to form lumps) and pulls away from the surfaces. For this reason the measurements were made with cup 2, bob 1, with a clearance of 0.78 cm. The average rate of shear is less certain in this case. It will be observed that the curves are regularly concave to the weight axis.

Log-log plots of data obtained from Newtonian, pseudoplastic, and dilatant flow are shown in Figure 10. It will be observed that an equation of the form of (15) may be used to describe the curves. As was pointed out above, for Newtonian flow $n = 1$; for pseudoplastic flow, $n < 1$; and for dilatant flow, $n > 1$. This generalization holds unequivocally for Newtonian oils and in many cases of pseudoplastic flow; for dilatant flow, however, the precision of the measurements is lower, and for some materials (*e.g.*, iron oxide in water) the curve departs from a straight line, especially at low rates of shear.

Accuracy and Precision

The Stormer viscometer modified as described above has been shown to be capable of measurement of viscosity of Newtonian materials to an accuracy better than ± 5 percent, without dependence on viscosity standards, over a range from 1 to 150 poises. The use of two or more bobs of the same radius but different lengths yields the most accurate results. In practice, however, it is much easier to use a single bob and to apply the correction for the end-effect. Below 1 poise the correction for end-effect becomes increasingly large, as has been shown, and should be found by calibration with a standard the viscosity of which is near that of the material to be measured. Alternatively the method of multiple bobs, without calibration, may be employed for low viscosities. A series of K_F values may be calculated for each 0.1 poise difference.

The computation of yield value from equations (3) and (25) is subject to greater uncertainty than the calculation of viscosity. There are, moreover, no materials that can be used as reference standards, and it is unlikely that any plastic substance can be made sufficiently stable to serve as a standard. Green [3] states that an accuracy of ± 20 percent may be expected in yield-value measurements on a rotational viscometer. This may seem an inordinately large error. When it is realized, however, that many instruments are quite incapable of distinguishing different types of flow properties, yielding information of only the crudest sort, then even this accuracy will be seen as a distinct contribution.

The precision of the measurements will, of course, be within narrower limits if careful technique is followed and the necessary precautions are observed. It is estimated that viscosities of Newtonian liquids can be duplicated with ± 2 percent and plastic viscosities, using a standardized technique, to ± 5 percent. Differences in magnitude in yield value of the order of 25 dynes/cm^2 can be distinguished.

With Newtonian liquids such as oils it is sufficient to obtain 5 to 10 readings at different loads since these will be enough to establish and confirm the linearity of the curve. With plastic compositions (which are usually thixotropic as well) it is neces-

sary to obtain more points for both increasing loads and decreasing loads. Either of two procedures may be followed: (1) taking a series of readings from the lowest to the largest weight and then following the same sequence of loads in reverse, back to the lowest weight; or (2) running the viscometer with the weight which gives the maximum rate of shear desired until a constant value of the time for 100 revolutions is observed; then decreasing the weight in convenient steps, as in procedure (1), and taking a reading at each load. It is seen that in either case a maximum load or rate of shear must be selected; the basis for such selection lies in the purpose for which the measurements are being made. The sequence of readings with smaller and smaller weights should be completed without interruption, whichever procedure is followed. If this precaution is not observed, thixotropic "build-up" (the reverse of structural break-down) will result and the points will not fall on a straight line.

Summary

1. To obtain consistent results with the rotating cylinder viscometer, the following basic factors should be considered: (*a*) a measure of the retarding torque produced by the liquid being sheared in the annular space between the two cylinders; (*b*) determination of the magnitude of end traction on the inner cylinder (the end-effect); and (*c*) variation in the rate of shear between the cylinders. The influence of these factors on viscometric measurements is discussed.

2. Details for the modification of a commercial viscometer are given. The modified instrument is suitable for the identification and measurement of different kinds of flow properties often designated as anomalous. Data are obtained in c.g.s. units. This instrument is capable of an accuracy of ± 2 percent (as checked against viscosity standards) on materials exhibiting Newtonian flow.

3. On plastic-thixotropic, pseudoplastic, and dilatant materials the reproducibility of the measurements depends partly on the stability of the colloidal systems under investigation and partly on the conditions for the measurement. The importance of rate of shear in these cases is emphasized. When the term *apparent viscosity* (η_a) is used in connection with pseudoplastic or dilatant materials, the rate of shear at which η_a is computed should be given.

4. Methods of computation of apparent viscosity are described. In all cases, an experimental curve of rate of shear *vs.* shearing stress (r.p.m. *vs.* weight in the case of the modified Stormer viscometer) is essential. Values for η_a at any rate of shear may be found from the slope of the tangent drawn to the curve at the desired rate of shear, or the experimental data may be fitted to an empirical equation and from this equation a relation between η_a and rate of shear may be derived.

Literature Cited

1. Barr, G., "Monograph of Viscometry," London, Oxford University Press, 1931.
2. Davis, D. S., "Empirical Equations and Nomography," New York, McGraw-Hill Co., 1943.
3. Green, H., *Ind. Eng. Chem., Anal. Ed.* **14**, 576–85 (1942).
4. Green, H., and Weltmann, R. W., *Ind. Eng. Chem., Anal. Ed.* **15**, 201–6 (1943); *J. Applied Phys.* **15**, 414–20 (1944).
5. Green, H., and Weltmann, R. W., Chap. 15, "Thixotrophy," pp. 328–47, in *Colloid Chemistry*, Vol. VI, J. Alexander, Ed., New York, Reinhold Publishing Corp., 1946.
6. Fischer, E. K., and Lindsley, C. H., *J. Colloid Sci.* **3**, 111–28 (1948).
7. Hatschek, E., "Viscosity of Liquids," London, G. Bell & Sons, Ltd., 1928.
8. Lamb, H., "Hydrodynamics," 6th Ed., London, Cambridge University Press, 1932, p. 587.
9. Lindsley, C. H., and Fischer, E. K., *J. Applied Phys.* **18**, 988–96 (1947).
10. Reiner, M., and Riwlin, R., *Kolloid-Z.* **43**, 1–5 (1927); Reiner, M., *J. Rheology* **1**, 5–10 (1929).
11. Scott Blair, G. W., "An Introduction to Industrial Rheology," Philadelphia, P. Blakiston's Sons, & Co., 1938; "A Survey of General and Applied Rheology," New York, Pitman Publishing Corp., 1944.
12. Swindells, J. F., *J. Colloid Sci.* **2**, 177–84 (1947).

A Theory of Commercial Yarn Testing*

Charles J. Geyer, Jr., C. H. Reichardt,† and George Halsey‡**

Contribution of the Textile Foundation, Frick Chemical Laboratory of Princeton University, and the American Viscose Corporation

Abstract

A method has been devised for the application of the theory of the three-element shear model of Eyring and coworkers to textiles which does not necessitate the location of the "basic spring line" and thus is readily applicable to both yarn and fiber tests and to the commercial inclined-plane and pendulum-type testers. It is also applicable as a first approximation to those textiles which do not possess a "basic spring line" as such. The method employs the conventional spring constants or elastic moduli but determination of the viscous constants involves the magnitude of the relaxation in constant-rate-of-elongation experiments (or the magnitude of the creep in constant-rate-of-loading experiments) from the upper envelope per interval of time. The relationship has been employed to establish the correlation between the viscoelastic properties of "slashed" and "unslashed" viscose tire-cord rayon yarns and also to show the identity of single-filament stress-strain relationships with those of yarns of normal twist of the same textile. The simplicity of technique which enables this method to be used as a routine laboratory test for the determination of the viscoelastic properties of textiles is an advantage over previous methods, which were often unsatisfactory from both a theoretical and an experimental viewpoint.

I. Introduction

It might be expected, a priori, that tests which measure the stress-strain relationships of yarns and filaments of the same textile would agree when the yarns are manufactured of continuous filaments. With cotton and other staple fibers, where the yarns are constructed of short lengths held together by friction, agreement would not be expected, as another variable has entered the relationship.

A feature in the manufacture of a continuous-filament yarn, or of any yarn, for that matter, which does not allow a yarn to be considered as being merely a bundle of filaments is the twist. It has been determined, however, that the twist of a yarn, at least up to about 5 turns per inch, does not change significantly the stress-strain characteristics of a textile. On the other hand, the twist given to two yarns in manufacturing a two-ply cord does have an appreciable apparent effect on the stress-strain characteristics of a textile.

Proceeding further in the consideration of yarn and single-filament testing, it is known that yarn tests, because of the magnitudes of the forces involved, do not generally obtain the sensitivity with which practically all single-fiber tests have been carried out. Thus, many of the theories advanced to explain the stress-strain relationships of textiles, requiring complicated procedures performed on a sensitive apparatus, accordingly have been worked out for single-filament experiments. These theories, then, are not readily applied to, or obtained from, yarn tests, since, in addition to the complicated procedures, the data for application of these theories are not readily obtainable on commercial yarn testing devices.

The mechanical properties of a number of textile fibers and filaments have been treated successfully on the basis of the theory and methods of the three-element shear model of Eyring and coworkers [1]. This model consists of a spring in parallel with a Maxwell unit of a spring and a non-Newtonian dashpot in series (Figure 1). The theory has been applied to analyze the viscoelastic behavior of single filaments and fibers of cellulose acetate, viscose rayon, wool, and cotton. Application of the three-element model to single-filament experiments involved the location of the "basic spring line." The "basic spring line" may be defined as the locus of "points of no relaxation,"—that is, points within the outer envelope determined by the process of bracketing and at which there is no instantaneous relaxation in

* Presented in part at a joint meeting of the American Association for the Advancement of Science and the American Physical Society, Chicago, December 29, 1947. This partial version appeared in *J. Applied Phys.* **19**, 464 (May 1948).

** American Viscose Corporation, Front Royal, Virginia.

† Fellow of the Textile Research Institute.

‡ Fellow of the Textile Research Institute. Present address: Mallinckrodt Chemical Laboratory, Harvard University.

either direction (*cf.* line *OD* in Figure 2). This technique involved complicated experimental procedures which were not readily applicable to the commercial yarn testers and thus the use of this theory or other similar theories was restricted to single-filament experiments. In the case of cellulose acetate, which is characterized extremely well by the simple three-element model, determination of the spring line through the measurement of "points of no relaxation" is relatively straightforward, particularly on single-fiber testers of the autographic balance or electronic strain-gage type. In the case of viscose rayon, cotton, wool, and other textile fibers, the three-element model is applicable to the first approximation only, because the simple spring line either cannot be determined experimentally or is nonexistent. Although the three-element model is merely a first approach to the problem of the viscoelastic behavior of textile fibers, this behavior can be well characterized through the use of the several spring and viscous constants of the three-element model. Thus a method of applying the theory of Eyring and coworkers to textiles which did not necessitate the location of this spring line would eliminate these two problems and would make the theory more applicable to yarn tests as well as to single-fiber tests, and also would make it applicable as a first approximation to those textiles which do not possess a "basic spring line" as such.

With respect to yarn testing, the present routine laboratory tests to determine the viscoelastic behavior of textile yarns are inadequate and a reduction to basic parameters is necessary. For example, the stress-strain curves of slashed and unslashed yarns are very dissimilar, although both may have been manufactured from the same stock. Again, the

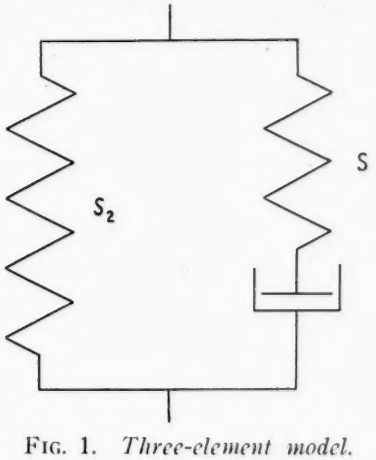

FIG. 1. *Three-element model.*

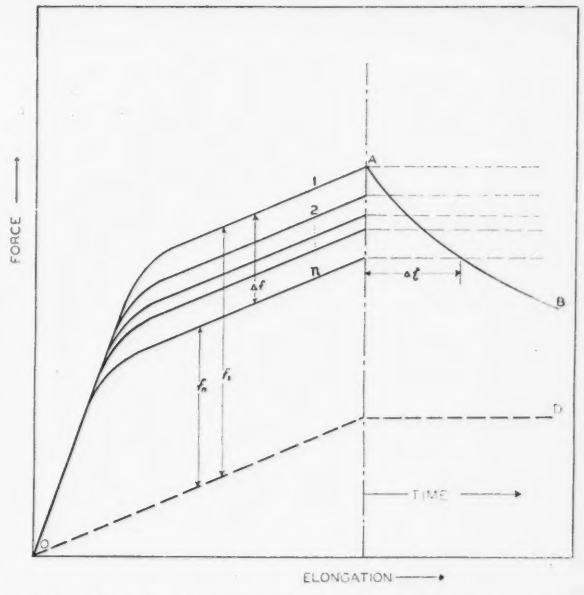

FIG. 2. *Family of stress-strain curves for constant-rate-of-elongation experiments.*

elongation-to-break curves of two rayons may be superimposable, although they may have been manufactured from dissimilar stocks and have very dissimilar elastic or recovery properties.

The spring constants, or elastic moduli, are merely ratios of stress to strain obtained from the slopes of the stress-strain curve. Viscous constants, however, are less familiar terms and require definition. Considering a constant-rate-of-elongation experiment, a viscous constant, β, may be defined by

$$\beta = \rho/K,$$

where ρ is the experimental rate of elongation of the fiber, and K is the rate at which it would lengthen at zero force, if every molecular jump which shortens fibers were suppressed and all jumps which lengthen them were allowed. For constant-rate-of-loading experiments,

$$\beta = P/Kk_2,$$

where P is the experimental rate of loading of the fiber, K is as before, and k_2 is the spring constant of the open spring. A second viscous constant, α, may be defined by the hyperbolic sine law governing the non-Newtonian dashpot, assuming a symmetrical potential barrier opposing flow,

$$\frac{dl_1}{dt} = K \sinh \alpha f,$$

where dl_1/dt is the rate of extension of the dashpot,

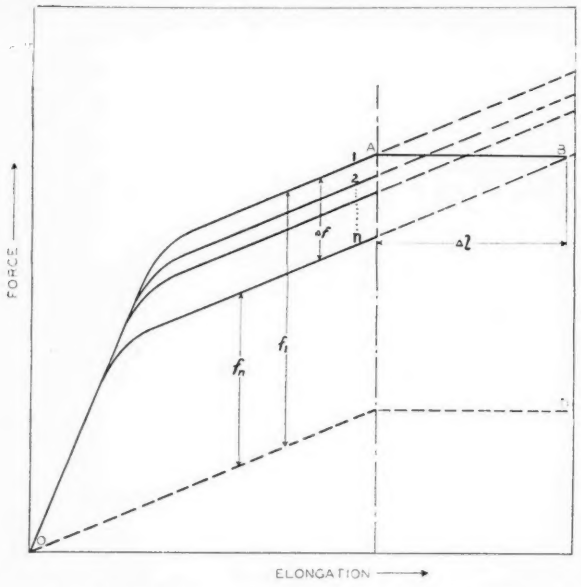

FIG. 3. *Family of stress-strain curves for constant-rate-of-loading experiments.*

and f is the force * acting on it. The constant α is very largely a parameter of the molecular structure. For large values of β,

$$\alpha \approx \frac{1}{f_\infty} \ln 2\beta.$$

The normal method of calculating the viscous constants requires the basic spring line and the two envelopes obtained at two very different rates of loading or elongation. A logical first approach to the problem of determining the viscous constants without resource to an experimentally determined spring line would be to attempt to calculate them from a formula involving three rates of elongation or of loading alone. However, the nature of the equation governing the viscous element is such that the ratio between the rates is independent of the viscous constants [1]. If β is the value of this constant referred to the lowest rate, then for rates m and n times as fast the corresponding values are $m\beta$ and $n\beta$. Thus

$$f_1 = 1/\alpha \text{ arc sinh } \beta,$$
$$f_m = 1/\alpha \text{ arc sinh } m\beta,$$
$$f_n = 1/\alpha \text{ arc sinh } n\beta.$$

* It should be noted that "force" is used in this instance although the term "stress" might be more precise. However, this practice appears to be justified in light of the simplicity of using "force" in plotting the data. No confusion should result from this usage.

The measured ratio R_{mn} is defined as

$$R_{mn} = \frac{f_n - f_1}{f_m - f_1} = \frac{\text{arc sinh } n\beta - \text{arc sinh } \beta}{\text{arc sinh } m\beta - \text{arc sinh } \beta}. \quad (1)$$

To the approximation that

$$\text{arc sinh } \beta = \ln (\beta + \sqrt{1 + \beta^2}) \approx \ln 2\beta,$$

this equation becomes, for large β,

$$R_{mn} = \frac{\ln n}{\ln m}. \quad (2)$$

That is, to a good approximation, the measured ratio remains independent of β and thus this method of calculating this viscous constant fails. Pursuing further the correlation of the stress-strain characteristics of yarn and single-filament experiments of viscose rayon tire cords, another and more successful approach to the problem was suggested by the experimental procedures employed by Reginald Meredith [2]. This approach to the problem and its application to the correlation of yarn and single-filament stress-strain relationships, with reference to its application to Meredith's data, are the subjects of this paper.

II. Theoretical Considerations

Every previous method of determining the various constants involving change of rate required, naturally, a large change in rate of elongation or loading, which in general necessitated the use of two or more samples of the yarn or filament, and a knowledge of the location of the basic spring line. Determining the viscous constants by the method set forth here involves the amount of relaxation in rate-of-elongation experiments or the amount of creep in rate-of-loading experiments per interval of time, requires no knowledge of the basic spring line, and can be carried out on one sample of a particular yarn or filament.

A. Constant-Rate-of-Elongation Experiments

Consider the family of stress-strain curves (Figure 2) obtained in a series of constant-rate-of-elongation experiments from the fast rate 1 down to the fractional rate n, where curve AB represents the relaxation curve from the fast rate. From the theory of

the three-element model [1] the force on the viscous element is given by

$$f = k_1(l - l_1), \tag{3}$$

which upon differentiation yields

$$\frac{df}{dt} = k_1\left(\frac{dl}{dt} - \frac{dl_1}{dt}\right) = k_1\left(\rho - \frac{dl_1}{dt}\right), \tag{4}$$

where $\rho = dl/dt$, the rate of elongation of the sample. In the steady state,

$$\frac{df}{dt} = k_1\rho.$$

Now

$$\left.\frac{df}{dt}\right|_0 = \left.\frac{d\Delta f}{d\Delta t}\right|_0 = k_1\rho, \tag{5}$$

where $\left.\frac{df}{dt}\right|_0$ denotes the initial rate of relaxation, because the instantaneous rate of relaxation is determined by the force, which in the steady state under a constant rate equals $k_1\rho$. Therefore, any

$$\frac{d\Delta f}{d\Delta t} = nk_1\rho_1, \tag{6}$$

where ρ_1 is the rate for the fast rate 1, and $n\rho_1$ gives the rate for the constant rate curve that has the instantaneous value f_n for f_∞.

Now, taking the dimensional datum $\Delta f = f_n - f_1$ as the measured quantity, we have from previous considerations [1]

$$f_n - f_1 = \frac{1}{\alpha}(\text{arc sinh } n\beta - \text{arc sinh } \beta).$$

If the spring line is sufficiently distant from the upper envelope to make β large, then the approximation for arc sinh can be employed, and

$$f_n - f_1 = \frac{1}{\alpha_\infty}\ln n$$

or

$$\alpha_\infty = \frac{\ln n}{f_n - f_1} = \frac{\ln n}{\Delta f}. \tag{7}$$

The symbol α_∞ denotes a limiting value of dimensional α as β becomes very large. Equation (7) may be written

$$n = e^{\alpha_\infty \Delta f},$$

and substitution in equation (6) gives

$$\frac{d\Delta f}{d\Delta t} = k_1\rho_1 e^{\alpha_\infty \Delta f}.$$

Integration gives

$$e^{-\alpha_\infty \Delta f} = -\alpha_\infty k_1\rho_1\Delta t + \text{constant}.$$

When $\Delta f = 0$, $\Delta t = 0$, and the constant = 1. Thus,

$$e^{-\alpha_\infty \Delta f} - 1 = -\alpha_\infty k_1\rho_1\Delta t,$$

where Δf is measured in the negative sense. For positive Δf,

$$e^{\alpha_\infty \Delta f} - 1 = \alpha_\infty k_1\rho_1\Delta t. \tag{8}$$

The magnitude of relaxation, Δf, in time Δt, is measured, $k_1\rho_1$ is known, and a plot of the solution of

$$e^x - 1 = ax, \tag{9}$$

where $x = \alpha_\infty \Delta f$ and $a = k_1\rho_1\Delta t/\Delta f$, can be used to determine α_∞. Values of x vs. a for the equation $e^x - 1/x = a$ are given in Table IV.

B. Constant-Rate-of-Loading Experiments

The family of stress-strain curves obtained in constant-rate-of-loading experiments, from a fast rate 1 down to the fractional rate n, is represented in Figure 3. From the theory of the three-element model, the forces involved can be represented by

$$F - f = k_2 l. \tag{10}$$

Differentiating,

$$\frac{dF}{dt} - \frac{df}{dt} = P - \frac{df}{dt} = k_2\frac{dl}{dt}, \tag{11}$$

where $P = dF/dt$, the rate of loading.

In the steady state

$$P = k_2\frac{dl}{dt}. \tag{12}$$

Therefore, any

$$\frac{d\Delta l}{d\Delta t} = \frac{nP_1}{k_2}, \tag{13}$$

where P_1 is the rate of loading at the fast rate 1, and nP_1 gives the rate for the constant-rate-of-loading curve that has the instantaneous value f_n for f_∞. Since the instantaneous rate of creep is determined by the force, which is given by

$$\left.\frac{df}{dt}\right|_0 = -k_2\frac{dl}{dt}, \tag{14}$$

then

$$\Delta f = -k_2\Delta l. \tag{15}$$

As before,

$$n = e^{\alpha_\infty \Delta f}. \tag{16}$$

Substitution of equation (15) gives

$$n = e^{-\alpha_x k_2 \Delta l}. \tag{17}$$

From equations (13) and (17),

$$\frac{d\Delta l}{d\Delta t} = \frac{P_1}{k_2} e^{-\alpha_x k_2 \Delta l}. \tag{18}$$

Integration gives

$$e^{\alpha_x k_2 \Delta l} = \alpha_x P_1 \Delta t + \text{constant},$$

when $\Delta l = 0$, $\Delta t = 0$, and the constant = 1. Thus

$$e^{\alpha_x k_2 \Delta l} - 1 = \alpha_x P_1 \Delta t.$$

The extent of creep, Δl, in time Δt, is measured, P_1 and k_2 are known, and a plot of the solution of

$$\frac{e^x - 1}{x} = a,$$

where $x = \alpha_x k_2 \Delta l$ and $a = P_1 \Delta t / k_2 \Delta l$, can be used to determine α_x.

III. Experimental Procedure

The apparatus used for the single-filament experiments at constant rate of elongation was the Sookne-Rutherford Autographic Balance and that used for the constant-rate-of-loading experiments on yarn and cord was the commercial Scott IP-4 Tester. The gear box of the IP-4 was modified slightly by removing the catches, which, on being cammed outward, allow the reversal gears to snap back and forth. This allowed the gears to be controlled manually and also allowed them to be placed in a neutral position, which is necessary for the experimental technique, as will be described later. The temperature and humidity conditions used in all the experiments were the same—namely, 75°F and 60 percent relative humidity. The 1170/490 viscose rayon tire-cord yarns were pot-spun. The 1100/490 yarns used in these tests were samples of the 1170/490 yarns described above, which, after being pot-spun, were slashed (that is, essentially, stretched in a wet state and then dried while in a stretched state). The 1650/980 and 2200/980 yarns described here were manufactured by the continuous-spinning method and immediately slashed. All the yarns were given a protective oil finish. The filaments described in this paper were extracted from samples of the above yarns.

The experimental technique necessary for routine laboratory application of the theory is simple; however, it naturally will vary somewhat with the problem under consideration; therefore a standard procedure will not be outlined in this paper. The technique used in testing the theory for this paper contained several modifications of the basic technique. These modifications, at the expense of making the technique slightly more complicated than necessary, were required to test the theory completely and also to allow for further qualitative discussion. The general procedure was as follows:

1. A normal extension-to-break experiment was conducted at one or at several widely different rates of elongation or loading to determine the general shape of the envelope of the stress-strain curve.

2. The following recycling process was carried out (the methods for both constant rate of loading and constant rate of elongation are similar and are therefore combined herein):

   (*a*) The sample (yarn or filament) was elongated at constant rate of elongation (or loaded at constant rate of loading) to a given stress.
   (*b*) It then was allowed to relax (or creep) for a definite period of time.
   (*c*) The sample then was contracted (or unloaded) at constant rate to zero stress (this and the following step were added to allow further qualitative study of the textile, as will be discussed later).
   (*d*) It was allowed to relax (or recover) for a definite period of time (preferably the same period as that for step (*b*)).
   (*e*) Recycling in this manner was continued to break, elongating (or loading) at constant rate to successively higher stresses each time. (Recycling was neither necessary nor required for the application of the theory but it was necessary to show (1) reduction of errors in experimental technique, or (2) departure of the textile from ideal behavior, as will be explained in section IV.)

The technique which Meredith [2] used in his work on the tensile elasticity of fibers was slightly different in that the time of creep for each cycling process varied. The general procedure of loading at constant rate, allowing creep to occur, then unloading at constant rate and allowing recovery to take place, was the same but "a rate of loading of 10 grams per denier per minute was used, the duration of action of the load was ½ minute, and the

recovery time from the start of unloading to reloading was 1 minute." Thus, time of creep diminished as the magnitude of the loading step in each successive cycle increased. As the data given by Meredith in this report are excellent, it would appear that the original curves * from which the data were taken could be analyzed by the method described herein. Although these experimental curves were more than adequate for their problem, they could not be used in this case for, as was stated by the Shirley Institute in subsequent correspondence, "When making a theoretical analysis, as in your case, it is important to know the time cycle exactly, we would go so far as to say that if we were making such an analysis we would redetermine the experimental curves with special attention to the time cycle."

As the exact knowledge of the duration of creep † is important, it would be assumed that the longer the duration of creep the more precise the experimental data would be. However, the rate of creep is very high during only small intervals of time, and small errors in time of starting the unloading or loading cycle would result in large errors in the amount of creep. On the other hand, after a short time the rate of creep becomes very slow—rate of creep varies exponentially with time—and the accuracy of the value obtained depends on the sensitivity and response of the apparatus employed. For this reason, a period of creep of 1 minute was employed throughout the experiment. A period of 30 seconds was observed to be too short, and that of 2 or more minutes was thought to be too long for the latter reason, as well as too time-consuming for commercial testing purposes.

In determining k_2, the second spring constant, the slope used was the straight upper portion of the stress-strain curve, the shorter, more horizontal portion, which occurs in the case of viscose, nylon, wool, and other textiles, being neglected. This is discussed further in section IV.

IV. Discussion

The first experiments that were carried out were normal recyclings to break at constant rate of loading for yarns and constant rate of elongation for single filaments (see Figure 4). Two major observations were made:

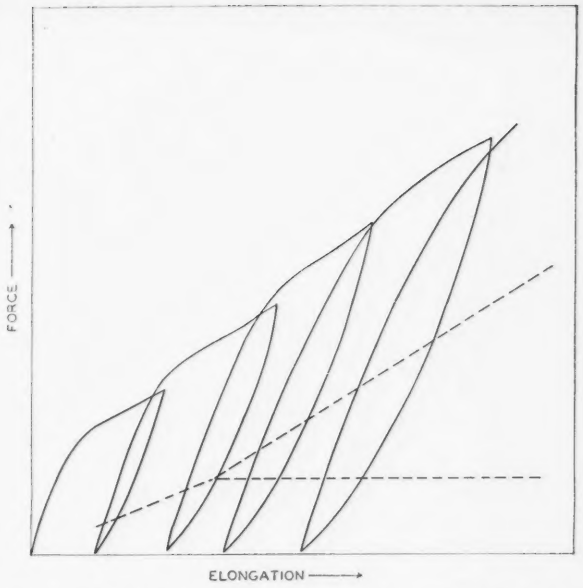

FIG. 4. *Typical recycling stress-strain curve of viscose tire-cord rayon.*

1. The shapes of the envelopes of both the yarn and the single-filament stress-strain curves were the same for any one type of yarn.

2. The return loops of any one stress-strain curve were not superimposable.

The first result was not unexpected, but as the yarns consisted of twisted filaments, a check on the effect of yarn twist on the over-all stress-strain curve was made. It was found that there is no apparent difference in the over-all shape of the stress-strain curve of yarns having degrees of twist varying from zero twist to 5 turns per inch. If the yarn had no twist or only several turns per sample length (generally 100 cm.), the over-all shape of the stress-strain curve was not changed, as stated above, but individual filaments were observed to break long before the yarn breaking point was attained and the sample had a slightly lower breaking strength than a corresponding sample with a higher twist. This is to be expected, a priori, and is consistent with the well-known effect [3] of twist on breaking strength and breaking elongation. Higher twists were not considered; however, a deviation between the single-filament and the yarn stress-strain curves would not be expected until a twist is attained at which the uneven tensions on individual fibers at different positions along a diameter of a cross-section of the yarn

* The Shirley Institute kindly forwarded to us a set of the original curves.

† The word "creep" is used here, and in the following paragraphs of section III, in a general sense to apply to creep, relaxation, or recovery, as the case may be.

TABLE I. UNSLASHED YARN

No.	Denier / Filament	Sample length (cm.)	Rate of loading $\left(\frac{\text{dynes}}{\text{cm}^2\,\text{sec.}}\right)$	Rate of elongation (sec^{-1})	Breaking strength Average $\left(\frac{\text{g.}}{\text{den.}}\right)$	Breaking strength Sample $\left(\frac{\text{g.}}{\text{den.}}\right)$	k_1 $\left(\frac{\text{dynes}}{\text{cm}^2}\right)$	k_2 $\left(\frac{\text{dynes}}{\text{cm}^2}\right)$	Δt (sec.)	Stress $\left(\frac{\text{g.}}{\text{den.}}\right)$	α_∞ $\left(\frac{\text{cm}^2}{\text{dyne}}\right)$
1170/490 yarn											
12	1170/490	100	1.101×10^{8}	—	3.5	>2.7	1.77×10^{11}	2.15×10^{10}	60	1.07	0.670×10^{-8}
									60	1.50	0.703
19	1170/490	50	1.101	—	3.5	3.00	1.33	2.14	300	1.31	0.800*
									300	2.01	0.787*
21	1170/490	50	1.101	—	3.5	2.42	1.21	2.16	30	1.20	0.580
									30	1.67	0.625
22	1170/490	50	1.101	—	3.5	3.08	1.09	2.19	30	1.03	0.645
									30	1.65	0.605
									30	1.89	0.740
									30	2.38	0.612
Single filaments 1170/490 yarn											
3	2.386	6.1	—	5.19×10^{-5}	3.5	2.86	1.16	2.24	290	1.88	0.880*
				4.67×10^{-4}					30	2.16	0.675
									40	2.16	0.690
									50	2.16	0.667
9	2.386	6.45	—	7.42×10^{-4}	3.5	>2.07	1.20	1.65	30	2.07	0.572
									60	2.07	0.678
1	2.386	6.45	—	4.42×10^{-4}	3.5	3.82	1.14	1.90	30	1.70	0.670
									60	1.70	0.624
									30	2.06	0.645
									60	2.06	0.685

vary enough to become effective. Solution of the geometry of yarns necessary to correlate the stress-strain curves of single filaments with those of high-twist yarns would be extremely difficult and has not been attempted. Thus a prediction of the degree of twist necessary to produce such a deviation cannot be made. However, it is logical to expect such deviation with higher twists from a consideration of the phenomena of creping with yarns of extremely high degrees of twist (40–60 turns per inch), since creping is apparently a physical manifestation of the swelling and elastic recovery which are inherent properties of the textile made apparent by the geometry of the high twist.

The second result, however, is not consistent with the three-element viscoelastic theory. For example, in the case of acetate rayon [4] and Loasby's curves on Italian silk [5], both of which obey the theory of the three-element model, the unloading curve at low forces is identical with the unloading curves for each recycling process and, furthermore, the upper portions of the loading curves for each recycling process are identical—that is, the return loops are superimposable. In the case of viscose, both the loading curve, up to the envelope, and the unloading curve, from the envelope, broaden with increasing load. For example, the yield point, as each loading curve reaches the envelope, becomes more gradual as the force attained in each recycling increases, making the return loops nonsuperimposable. However, the return loops of any one type of viscose to any one force, and thus to any one elongation, are superimposable from sample to sample, as is to be expected. Moreover, the over-all shape of a recycling stress-strain diagram of a yarn is the same as that of a filament.

Normally, the next step toward applying the theory of the three-element model is the determination of the "basic spring line." The procedure of determining points of no relaxation revealed that viscose shows no such basic spring line. In fact, after the yield point has been attained, there is an area (see dotted lines in Figure 4) above which a relaxation downward occurs regardless of direction of approach and below which a recovery upward occurs regardless of direction of approach. Within the area, a relaxation or recovery always occurs in the direction opposite to that of approach, but this relaxation or recovery does not approach the limits of the area asymptotically, as is the case with relaxation or recovery outside of the area; that is, through the process of bracketing, a "point of no relaxation"

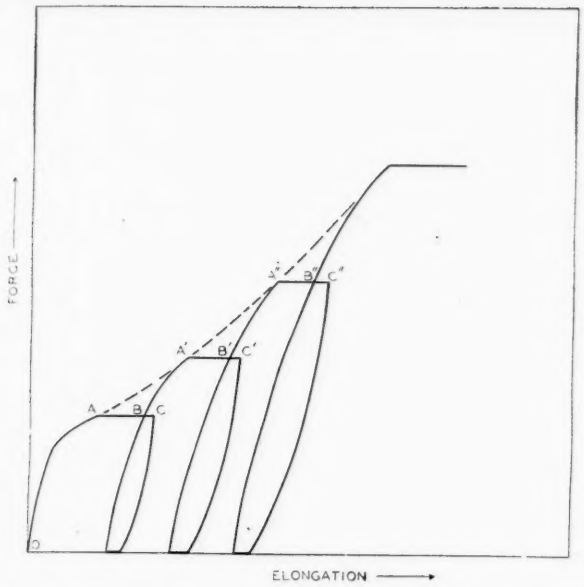

FIG. 5. *Typical experimental curve for constant-rate-of-loading experiments.*

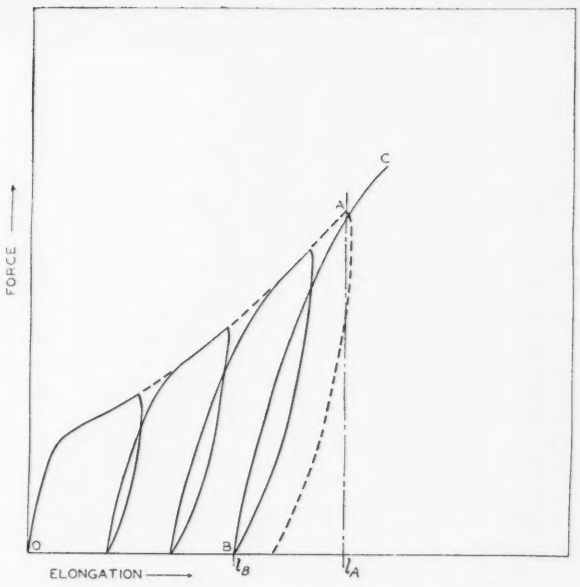

FIG. 6. *Theoretical diagram showing relationship of slashed to normal yarns.*

can be obtained anywhere within the area. This fact, and the previously mentioned lack of superposition, show that the theory of the three-element model is not exactly applicable to viscose and, for an exact representation of the viscoelastic phenomena of viscose, either a poly-element model or another approach is necessary. Either of these two solutions would of necessity be too complicated for easy application to experiment. For this reason, it is considered suitable to use the theory of the three-element model as a first approximation only, and the method of applying the theory without use of, or need for, a spring line is applied to viscose tire-cord rayon in this paper.

Table I lists the values for the two spring constants k_1 and k_2 and that of the viscous constant α_x for single-filament and yarn tests of a normal (1170/490) viscose tire-cord rayon. The values given are

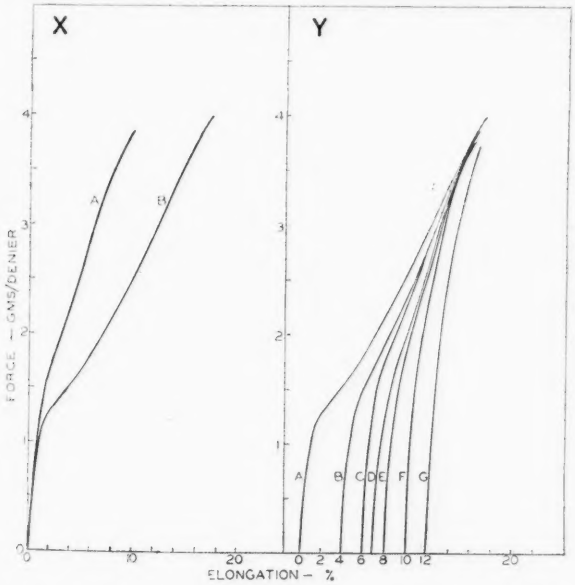

FIG. 7. *Elongation-to-break curves for normal and slashed yarns.*

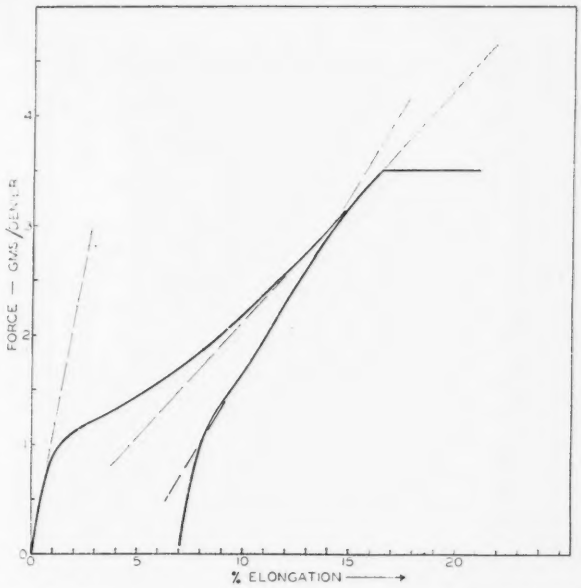

FIG. 8. *True relationship between normal and slashed yarns.*

TABLE II. 1100/490 YARNS

No.	Denier / Filament	Sample length (cm.)	Rate of loading $\left(\frac{\text{dynes}}{\text{cm}^2\ \text{sec.}}\right)$	Rate of elongation (sec^{-1})	Breaking strength Average $\left(\frac{\text{g.}}{\text{den.}}\right)$	Breaking strength Sample $\left(\frac{\text{g.}}{\text{den.}}\right)$	k_1 $\left(\frac{\text{dynes}}{\text{cm}^2}\right)$	k_2 $\left(\frac{\text{dynes}}{\text{cm}^2}\right)$	Δt (sec.)	Stress $\left(\frac{\text{g.}}{\text{den.}}\right)$	α_∞ $\left(\frac{\text{cm}^2}{\text{dyne}}\right)$
Value of k_2 uncorrected—Upper envelope not yet attained											
23	1100/490	100	1.172×10^8	—	3.5	3.20	0.94×10^{11}	3.86×10^{10}	30	1.10	1.23×10^{-8}
										1.76	1.05
										2.01	0.89
										2.54	0.62
6	1100/490	100	1.172	—	3.5	3.26	1.18	3.95	30	1.47	1.18
										2.01	1.10
										2.76	0.405
Value of k_2 corrected—Upper envelope attained											
23	1100/490	100	1.172	—	3.5	3.20	0.94	2.15	30	2.54	1.27
6	1100/490	100	1.172	—	3.5	3.26	1.18	2.18	30	2.76	1.02
20	1100/490	100	1.172	—	3.5	3.32	1.14	2.18	30	2.71	0.925

typical of a number of tests and substantiate the qualitative agreement of yarn and single-filament tests afore-mentioned. The values of α_∞ for three of the creep measurements (marked with asterisks in Table I) are much higher than average, corresponding to low values of the magnitude of the creep per unit of time. The time interval of these same three measurements is large and consideration of the construction of the apparatus used in each case shows that the creep measurements would tend to be in error in the same direction. For this reason, the results cannot be considered as typical and would normally be discarded; however, they are included here to illustrate the magnitude of the errors involved. It might be pointed out that the yarns considered herein have a twist of approximately 5 turns per inch.

The theory thus necessitates only the determination of the two spring constants and the magnitude of the creep or relaxation in a given time to characterize a textile. The accuracy of these two measurements would seem to depend solely on the experimental technique—that is, the dexterity of the operator in obtaining an accurate measurement of the creep or relaxation in unit time and in taking the slopes from the curves. The determination of these constants, however, presents problems which are not always immediately apparent.

One problem in the determination of the spring constant k_2 arises in the fact that the stress-strain curves of most textiles, including viscose rayon, show a slight leveling off immediately after the yield point before taking a longer, straight upsweep to break. This hump or flat portion has been explained on the basis of the three-element model as thixotropy [1], and on the basis of the two-state model as the start of the transition of the one state to another [6]. It is thus neglected in the measurement of the slope for the determination of the spring constant, k_2, of the open spring, and the straight upper portion of the stress-strain curve is used (see Figure 8). Although measurements of the creep made in this rather short, flat portion are fairly accurate, it is not advisable to start creep measurements until the upper straight portion has been attained since the yield point must have been reached before any accurate creep measurements can be made, and this flat portion makes accurate determination of the position of the yield point difficult.

Another problem, which arises in the testing of slashed yarns, involves not only an error in the determination of the spring constant but also in the magnitude of the creep. In a normal stress-strain experiment it is obvious that until the yield point is reached the viscous elements are moving only slightly, or, to be more exact, the viscous elements have not reached a steady state until after the yield point has been passed; thus, almost no apparent creep will take place until after the yield point has been reached. Furthermore, if in a reloading cycle the envelope is not reached, the amount of creep will be less than the true value. This latter point is illustrated for constant-rate-of-loading experiments by Figure 5. An analogous explanation can be obtained for constant-rate-of-elongation experiments through a study of Figure 2. In Figure 5, the distance AC, or $A'C'$, represents the creep from the envelope in time, Δt; the distance BC gives the creep obtained if the en-

TABLE III. SLASHED YARNS

No.	Denier / Filament	Sample length (cm.)	Rate of loading (dynes / cm² sec.)	Rate of elongation (sec⁻¹)	Breaking strength: Average (g./den.)	Breaking strength: Sample (g./den.)	k_1 (dynes/cm²)	k_2 (dynes/cm²)	Δt (sec.)	Stress (g./den.)	α_∞ (cm²/dyne)
1100/490 yarn											
23	1100/490	100	1.172×10^{8}	—	3.5	3.20	0.99×10^{11}	2.15×10^{10}	30	2.54	1.27×10^{-8}
6	1100/490	100	1.172	—	3.5	3.26	1.18	2.18	30	2.76	1.02
20	1100/490	100	1.172	—	3.5	3.32	1.14	2.18	30	2.71	0.925
Single filament from 1100/490 yarn											
7	2.242	6.60	—	7.25×10^{-3}	3.5	>2.15	1.00	2.25	30	2.13	0.792
									60	2.13	0.730
1650/980 yarn											
24	1650/980	100	1.172×10^{8}	—	3.5	3.50	1.43	2.15	30	2.73	1.27
Single filament from 1650/980 yarn											
5	1.685	7.69	—	1.12×10^{-3}	3.5	3.10	1.10	2.30	30	2.21	1.28
									60	2.21	1.11
									30	3.08	0.601
									60	3.08	0.603
2200/980 yarn											
25	2200/980	100	1.172×10^{8}	—	3.5	2.95	0.78	2.25	30	2.68	1.45
Single filament from 2200/980 yarn											
4	2.242	7.01	—	1.22×10^{-3}	3.5	2.75	0.975	2.44	30	2.68	0.828

velope has not been attained on recycling. It can be seen that the closer one approaches the envelopes before making a creep measurement the larger the value of the creep observed. From the equations, it is apparent that the larger the magnitude of the creep the smaller the value of α_∞ obtained for given values of Δt and k_2 at any one rate of stress or strain. In making a test run, first, the yield point must have been passed and, second, the envelope must have been reached.

That this must be taken into account in the first elongation of a slashed yarn is not obvious, unless the previous history of the yarn is considered. In the slashing process, a yarn is stretched while wet, dried while stretched, and then wound on a spindle or spool. The solid line in Figure 6 shows a normal recycling stress-strain curve of a viscose yarn in a constant-rate-of-loading experiment, where l_0 is the original sample length. The theory predicts that if the yarn is stretched to some elongation l_A, allowed to contract and recover for a period of time until no further recovery is apparent so that it attains the elongation (after recovery) of l_B (dotted curve in Figure 6), and that if this sample of yarn is elongated at constant rate (taking a sample length of l_B now, rather than l_0, for obvious reasons), the stress-strain curve will be identical with the normal recycling curve from elongation l_B—that is, line BC, in Figure 6. That this is also the case with a commercially slashed yarn is shown in Figures 7-X, 7-Y, and 8. Figure 7-X shows the stress-strain curve to break for normal (curve B) and for slashed (curve A) yarns using the same sample length for both, with both curves starting at the origin. In Figure 7-Y, curve A is the extension-to-break curve for a normal yarn, and curves B, C, E, F, and G are the extension-to-break curves of yarns which have been stretched while wet and then dried in a stretched state so that their final elongations are respectively 4, 6, 8, 10, and 12 percent greater than the original sample length. Curve D is the extension-to-break curve of a commercially slashed yarn for which the final length is 7 percent greater than the original (that is, curve A of Figure 7-X placed in its proper position in Figure 7-Y). The origin of each of these curves has been placed at an elongation corresponding to the respective elongation attained in slashing. Each of the slashed yarns, including the commercially slashed yarn, was made from a sample of the same yarn which was used to give curve A. Figure 8 is similar to curves A and D of Figure 7-Y, being the stress-strain curves of normal and slashed yarns

alone to better illustrate the relationship between the normal and slashed yarns. The dotted lines show the slopes that would normally be taken for determination of the spring constants. It may be seen from these figures that the slashed yarn does not attain the upper envelope until quite late in the curve, and that the final slope to be used to obtain the spring constant, k_2, of the open spring, is given by the uppermost section of the stress-strain curve for a slashed yarn; furthermore, if the yarn is weak, the upper envelope might never be attained before break (Figure 7-Y, curve G). In addition, any measurements of the creep of a slashed yarn, which are obtained before the upper envelope is attained, would be too small, leading to large values of α_∞.

Tables II and III give the values of the spring and viscous constants for various slashed viscose tire-cord rayon single filaments and yarns. Table II gives the values obtained for a slashed yarn in both cases—that is, where a slashed yarn is considered as a separate entity and where cognizance is taken of the fact that a slashed yarn is in a stretched state and the stress-strain curve does not attain the normal envelope until very high elongations are reached. Table III contains values for the constants of other slashed yarns and single filaments. Apparent discrepancies in the values of α_∞ given are removed when the stress at which each creep measurement has been made is considered. Since at lower stresses the envelope has not been attained and a high α_∞ is expected. The envelope is not attained in the slashed yarns considered here until a stress of approximately 3 grams per denier is reached. Taking this fact into consideration, the values of the two spring constants, k_1 and k_2, and the viscous constant, α_∞, for all of the yarns considered in this paper are essentially the same. The yarns described herein differ only in two ways—namely, the fiber denier varies from 1.685 to 2.386, and one fiber is normal whereas the other three are slashed. These differences would not be expected, from a consideration of the theory, to cause any difference in the fundamental constants.

It was also mentioned earlier that although recycling, or the determination of several creep measurements on one fiber, was not essential to the application of the theory, recycling was necessary for two reasons: (1) to reduce errors in experimental technique, and (2) to determine any breakdown in the fiber from ideal behavior.

TABLE IV. VALUES OF $\frac{e^x - 1}{x}$ VS. x

$\frac{e^x-1}{x}$	x	$\frac{e^x-1}{x}$	x
1.0	0.0000	4.75	2.588
1.01	0.0190	5.00	2.658
1.02	0.0395	5.25	2.722
1.03	0.0596	5.50	2.795
1.04	0.0792	5.75	2.855
1.05	0.0986	6.00	2.915
1.06	0.1150	6.25	2.975
1.07	0.1340	6.50	3.030
1.08	0.1520	6.6	3.050
1.09	0.1700	6.8	3.092
1.10	0.1878	7.0	3.132
1.11	0.2046	7.2	3.170
1.12	0.2210	7.4	3.208
1.13	0.2400	7.6	3.244
1.14	0.2560	7.8	3.280
1.15	0.2735	8.0	3.315
1.16	0.2890	8.2	3.349
1.17	0.306	8.4	3.380
1.18	0.325	8.6	3.413
1.19	0.340	8.8	3.443
1.20	0.355	9.0	3.474
1.25	0.432	9.2	3.504
1.30	0.504	9.4	3.532
1.35	0.575	9.6	3.561
1.40	0.638	9.8	3.588
1.45	0.702	10.0	3.617
1.50	0.763	15.0	4.140
1.55	0.821	20.0	4.510
1.60	0.876	25.0	4.790
1.65	0.930	30.0	5.020
1.70	0.980	35.0	5.210
1.75	1.030	40.0	5.375
1.80	1.082	45.0	5.518
1.85	1.125	50.0	5.640
1.90	1.170	55.0	5.762
1.95	1.206	60.0	5.862
2.00	1.250	65.0	5.960
2.25	1.447	70.0	6.050
2.50	1.615	80.0	6.208
2.75	1.765	90.0	6.351
3.00	1.908	100.0	6.474
3.25	2.028	110.0	6.586
3.50	2.140	120.0	6.690
3.75	2.242	130.0	6.782
4.00	2.335	140.0	6.870
4.25	2.420	150.0	6.950
4.50	2.510	160.0	7.025

It is normally good experimental technique to measure several points rather than a single one if possible, and one method would be to recycle and take several values of one fiber as well as to examine several representative fibers. The values of α_x obtained should all be within experimental error. If this variance is too large for experimental error, the curve should be examined to ascertain whether the envelope was attained before each creep measure-

ment was made. In the first examination of slashed yarns, prior to recognition of the fact that slashed yarns are actually already in a stretched state and that the envelope is not attained until quite late in its stress-strain curve, it was observed that the values of α_x obtained decreased as the stress increased. This could be attributed either to a breakdown of the slashed yarn from ideal behavior as stress, and therefore strain, increases, or, in light of the previous paragraphs, to the fact that the envelope had not been reached before the creep measurements were made. It was this observation, indeed, that led to the previously mentioned examination of slashed yarns. Thus the proper α_∞ values to use to characterize the slashed yarns considered in this paper are those obtained very late in the stress-strain curve after the envelope has been attained. Hence, recycling was used in this case to determine and eliminate errors in experimental technique. Analogous situations would conceivably occur with yarns with an unknown or a neglected previous history.

Considering the second factor—the breakdown of the fiber from ideal behavior—it has been observed for the normal yarns discussed in this paper that the values of α_x obtained remain constant over the entire curve beyond the yield point until just before the fiber breaks, at which point the magnitudes of the measured creep increase and the value of α_∞ decreases sharply. It is plausible that this may be attributed to a breakdown occurring within the fiber. Thus, in a recycling experiment, if the values of α_x change throughout either the latter portion of or the entire stress-strain curve, and it is certain that the envelope has been attained in each case, it would be reasonable to assume (*a*) that the viscous character of the fiber changes with stress and, therefore, strain, and (*b*) that such a decrease in the value of α_∞ shows a definite change of the fiber from its original state.

One section of the experimental curve has not yet been considered—that is, the recovery of the fiber. The experimental procedure included a recovery of force from zero force in constant-rate-of-elongation experiments and a recovery of elongation at zero force in constant-rate-of-loading experiments. For the three-element model, the mathematical treatment of this recovery is identical with that for the creep or relaxation cases considered. Analogous to the creep or relaxation case, the correct value of α_∞ for the recovery is that obtained from the recovery determined after the yield point on the return curve has been attained. For viscose rayon tire cords, which do not obey the three-element model in this range, the yield point of the return curve is never observed experimentally even at quite large elongations. A quantitative analysis of the recovery of viscose rayon tire cords is therefore not feasible. However, by comparing the magnitude of the creep or relaxation with the magnitude of the recovery, a qualitative comparison is possible. With viscous rayon tire cords at the temperature and humidity examined, the magnitude of the recovery was always considerably less than the magnitude of creep or relaxation, and therefore, taking the amount of creep or relaxation as a standard, the recovery would be considered to be poor. Naturally, this does not indicate how poor the recovery properties of viscose rayon tire-cord yarns are as compared to those of other textile types. When experimental data on other textile types are obtained, a relative qualitative comparison can be made.

Further study of viscose rayon tire-cord yarns at a whole series of humidities, as well as other textile yarns at the same series of humidities, is contemplated. It is hoped that both a better insight into the application of the theory to other textiles and a closer approach to the fundamental structure of textiles will be obtained from these studies.

V. Conclusion

A method has been derived for applying the Eyring theory of the three-element model to textiles which, although employing the conventional spring constants, does not necessitate the location of the basic spring line for the determination of the viscous constants. Instead, the method involves the magnitude of the creep in constant-rate-of-loading experiments or the magnitude of relaxation in constant-rate-of-elongation experiments. This simplification of the technique makes the method available for the characterization of textile yarns in routine laboratory tests on the commercial yarn testers. In addition, the apparent relationship between normal and slashed yarns has been brought forth—namely, that slashed yarns are merely normal yarns which have been kept in an apparently metastable stretched state by having been stretched while in a wet state and then dried while still stretched.

Acknowledgment

The authors wish to thank Dr. J. H. Dillon, under whose directions the work described in this paper was carried out; the Office of The Quartermaster General, Research and Development Branch, which sponsored the work in part; the American Viscose Corporation, Front Royal, Virginia, which sponsored the experimental work on the yarns in their Research and Development Laboratory at Front Royal; and the technicians there who carried out the experimental work.

Literature Cited

1. Halsey, George, Non-Linear Viscous Elasticity and the Eyring Shear Model, *J. Applied Phys.* **18**, 1072 (1947).
2. Meredith, R., Comparison of the Tensile Elasticity of Some Textile Fibers, *J. Text. Inst.* **36**, T147 (1945).
3. "Rayon Handbook," 3rd Ed. (Mauersberger and Schwarz, Eds.) New York, Textile Book Publishers, 1939, pp. 567–8.
4. Reichardt, C. H., and Eyring, H., Mechanical Properties of Textiles, XI, TEXTILE RESEARCH JOURNAL **16**, 635 (1946).
5. Eyring, H., and Halsey, G., Mechanical Properties of Textiles, III, TEXTILE RESEARCH JOURNAL **16**, 13 (1946).
6. Burte, H., and Halsey, G., A New Theory of Non-Linear Viscous Elasticity, TEXTILE RESEARCH JOURNAL **17**, 465 (1947).

Cellulose Behavior with Filtered Sunlight

P. J. Fynn, J. E. Sands, and K. S. Campbell*

Southern Regional Research Laboratory,† New Orleans, Louisiana

COTTON TEXTILES exposed out of doors are subject to degradation from each or all of the several destructive forces of weather. Deterioration from microbiological attack, such as mildew, often assumes considerable proportions; the action of wind and rain, the concomitant wetting and drying cycles, temperature changes, dust and other atmospheric contaminants have their effect; but sunlight has long been recognized as a principal degrading factor.

The purpose of the present investigation was twofold: To determine how much of the total degradation suffered by weather-exposed cotton is due to sunlight alone and to determine the relative destructiveness of different regions of the sun's spectrum. For these determinations use was made of a special automatic, normal-incidence, solar-exposure cabinet. A basis of comparison with the cabinet exposures was provided by exposing comparable samples in the open to the total effects of weather.

Exposure Conditions

The special solar-exposure cabinet has been fully described in a previous publication [5]. The samples were fixed in the tightly closed cabinet so that each was irradiated solely with the sunlight transmitted by its particular filter window.

Since there are no glass color filters of high-percent transmission and large area which transmit clear-cut sections of the spectrum, any choice of filters

TABLE I. COLOR FILTER DATA

Filter	Corning Code No.	Transmission % of total sunshine	Degradative index
Corex	9700	95.5	1.00
Ultraviolet	5970	2.5	30.51
Blue	5330	50.0	1.60
Yellow	3482	66.2	0.54
Red	2408	58.9	0.53
Infrared	2540	16.1	1.55

* Present address: Textiles Section, National Bureau of Standards, Washington, D. C.

† One of the laboratories of the Bureau of Agricultural and Industrial Chemistry, Agricultural Research Administration, U. S. Department of Agriculture.

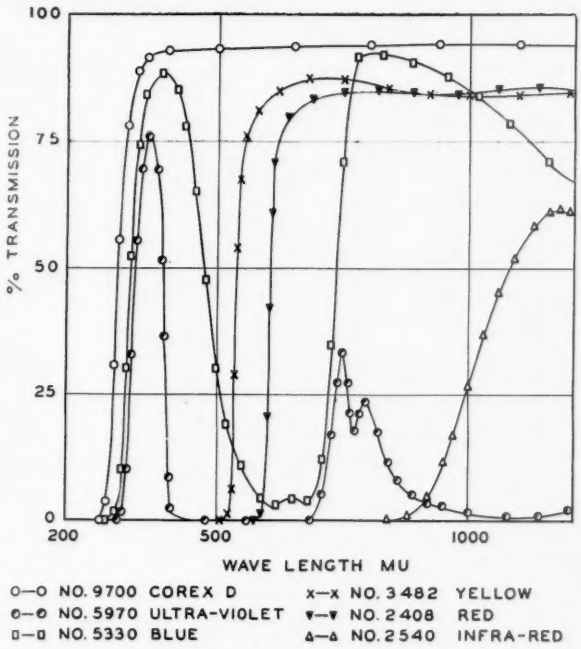

FIG. 1. *Spectral transmission of glass filters.*

is at best a compromise. The filters used in this investigation were selected on a basis of transmission and availability in large areas.

They covered the solar spectrum in five sections, transmitting predominantly in the ultraviolet, blue, yellow, red, and infrared ranges. The sixth filter, Corex D, was highly transparent to all wave lengths of the sun's energy reaching the earth at sea level. Table I lists these filters with their code numbers and Figure 1 gives the percent transmission as a function of wave length.

A pyrheliometer used in conjunction with a strip chart potentiometer and a filter-changing mechanism [5] recorded the cumulative totals of the quantities of solar energy received by each sample beneath its respective filter.

Maximum solar efficiency and minimum losses by reflection from the filter surfaces were assured by having the cabinet so mounted that it constantly maintained a position perpendicular to the sun's rays.

The temperature of the samples was maintained 24 hours daily between 40° and 50°C. by thermostatically heated water circulating through chromium-plated copper cells to which the samples were secured in close contact. Filtered air drawn through soda lime was circulated over the samples, its temperature and humidity subject to a certain amount of control by the water circulating in the cells. The degree of control which was exercised over the relative humidity of the ambient air in the cabinet is illustrated by the reproduction in Figure 2 of typical humidity charts made simultaneously inside and outside of the cabinet.

The samples exposed simultaneously outside to the effects of total weather were fixed in various positions: Some were maintained at normal incidence on frames attached to the outside of the cabinet mentioned above; some were inclined 45° facing south; others were inclined 45° facing south and shielded by glass color filters but otherwise open to the weather; and others were kept vertical facing north and

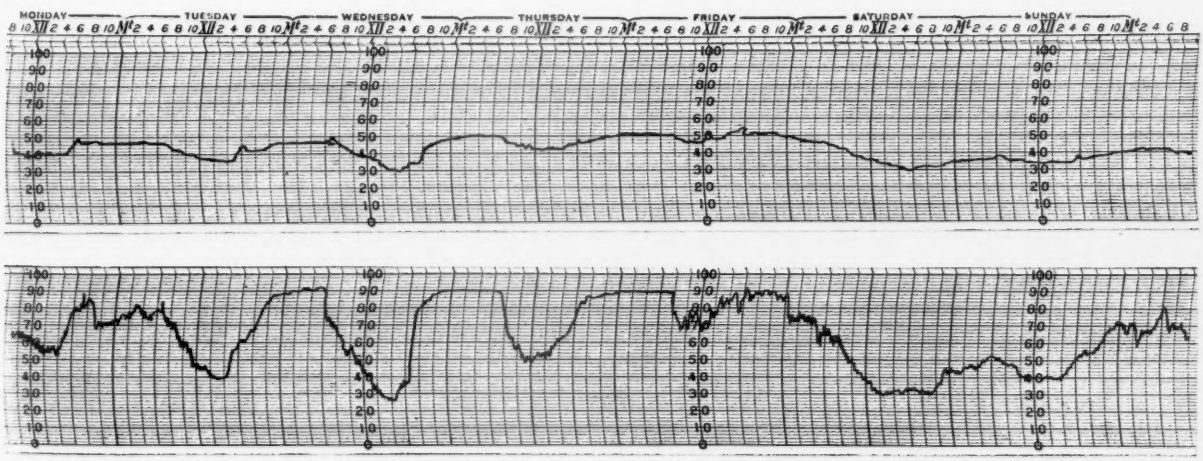

FIG. 2. *Top—Relative humidity of ambient air inside cabinet. Bottom—Humidity of air outside cabinet recorded simultaneously.*

shielded from direct sunlight. All samples were open to free air circulation both front and back. They were fastened to open wooden racks having bars spaced every 6 inches. The glass color filters shielding one set of the samples were supported 4 inches above the surface of its rack to allow access of wind and rain. Portions of fabric for testing were taken only from beneath the centers of the glass, thus avoiding edge effects. Only three filters were used in this stationary rack, the blue, the yellow, and the Corex D.

Materials and Sample Testing

The fabric used for both cabinet and outside exposures was a 48 × 44 cotton sheeting weighing 5.6 ounces per square yard. All fabric used was from the same batch of desized and kier-boiled sheeting especially prepared for the experiment.

At monthly intervals sufficient material was removed from all samples to permit the making of five breaking-strength tests on each. The breaking tests were made on strips cut 6 inches long warpwise by 1½ inches wide and frayed to a thread count equal to the number of warp threads in 1 inch of the original material. The strips were conditioned at a temperature of 70°F and relative humidity of 65 percent for at least 4 hours before breaking on a pendulum-type breaking-strength tester with 3 inches between the jaws. The average of the results of the breaking tests was compared with an average of ten breaks made on the original cloth and the percent breaking-strength loss (% BSL) was computed. The broken strips were extracted in alcohol, reduced to powder in a Wiley mill, and dissolved in cuprammonium solution. The cuprammonium fluidities were obtained by the A.S.T.M. method D539–40T for "The Apparent Fluidity of Dispersions of Cellulose Fibers in Cuprammonium Hydroxide."

Incidental Observations

Apart from data supporting the main objects of the investigation there were several incidental observations of interest.

The cabinet samples, even those exposed 8 months, were still clean and white with a just slightly perceptible yellowing on the exposed surface only. This yellowing had no observed relation to the type of filter used as a screen.

The totally exposed samples were quite gray, particularly those exposed the longest time. With the exception of the vertical north sample, which had a light, mottled, greenish algae-like discoloration on the back, the samples in the cabinet and those totally exposed showed no signs of mildew or other biological action. This is in accord with observations by Dean and Worner [3], Fargher [4], and others that bleached or purified cotton fabrics are not very susceptible to microbiological attack. The absence of biological action is borne out by the results, plotted in Figure 3, in which the cuprammonium fluidity is plotted against the percent loss in breaking strength. According to Searle [7], cellulose fibers attacked by microorganisms have a cuprammonium fluidity of the order of that of undegraded fibers. In Figure 3 the solid lines, taken from data by Dean and Worner [3], show the strength-fluidity relationship for normally weathered cotton fabric and for fabric al-

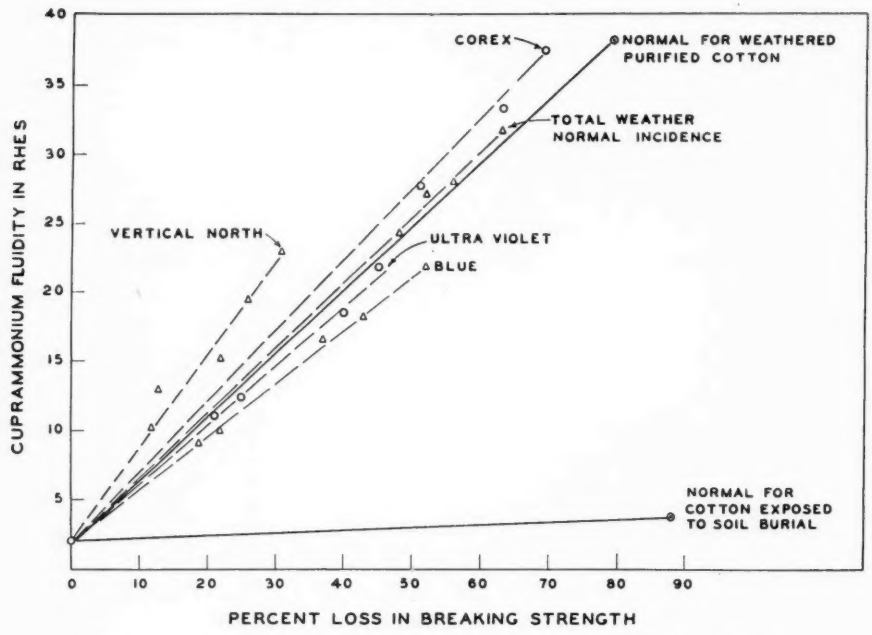

FIG. 3. *Comparison of graphs of fluidity versus loss in strength.*

most completely destroyed by microbiological action; the broken lines show the same relationship for samples exposed in the present experiment. All the broken lines are grouped about the line which represents normal weathering.

It is curious that, contrary to what has just been noted regarding the strength-fluidity relationship of biologically attacked samples, the line in Figure 3 representing the only sample which displayed any visual evidence of biological action, the vertical north sample, had the highest fluidity for a given strength loss. Current work on irradiation of cotton fabrics indicates that the strength-fluidity relationship of light-degraded cotton is influenced by the moisture content of the sample and that for a given strength loss the sample with the highest moisture content during irradiation has the highest fluidity. Therefore the exceptional behavior of the vertical north sample might be explained by the fact that because it was shaded from direct sunlight it generally had a higher moisture content than the other samples. In addition to this, the spotting may have been done by a non-cellulose-destroying organism. Furthermore, north sky light, to which this sample was exclusively exposed, contains a higher proportion of ultraviolet radiation than sunlight.

In early work on sunlight degradation, Turner [8] observed that the fabric appeared to deteriorate with time in a logarithmic fashion. That this observation is verified in the present instance is evidenced by data in Figure 4. Here, plotting the time of exposure on a logarithmic scale against the strength and fluidity data from the cabinet-exposed samples, which are degraded only by sunlight, results in a straight line, thus indicating that in each instance the degradation as measured by both of these criteria proceeds with time in the manner observed by Turner.

Maintaining normal incidence of the samples both within and without the cabinet resulted in an acceleration of the degradation. As shown in Figure 5 and Table II, the loss in strength suffered by the normal-incidence samples in 3 months was not attained by the 45°-south sample until the sixth month. The fluidity value reached by the normal-incidence sample in 3 months was not reached by the 45°-south sample until the eighth month. In both fluidity and strength changes, this acceleration of effect due to normal incidence is the most marked in the early part of the exposure period, the difference between the normal-incidence and the fixed-position exposures

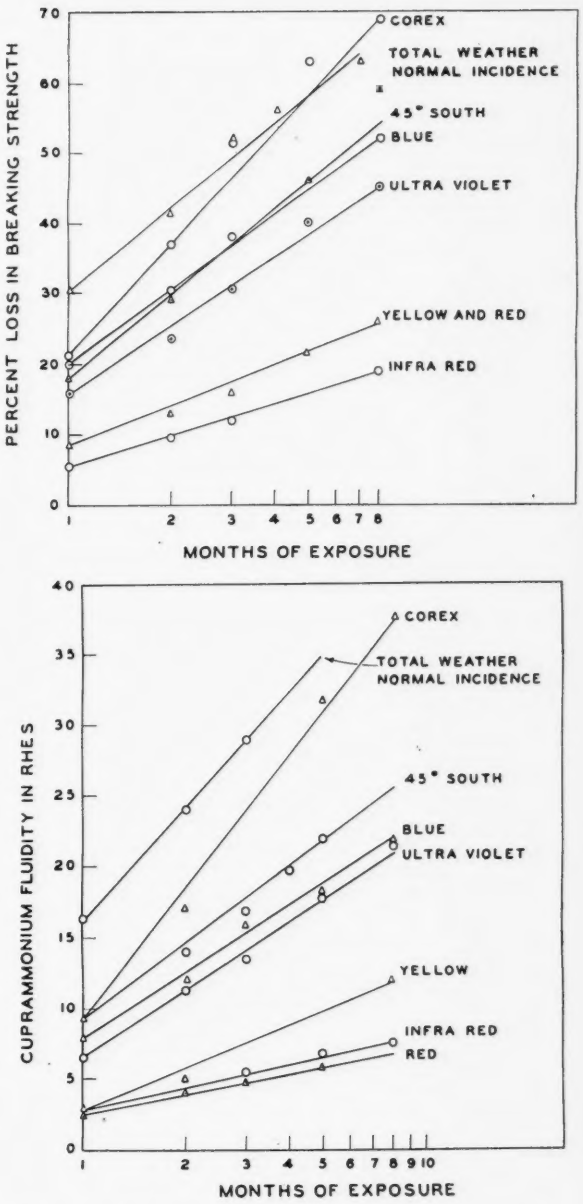

FIG. 4. *Fluidity and loss in strength versus the logarithm of the exposure time.*

diminishing as the exposure time lengthens—a result to be expected from the logarithmic nature of the degrading action.

Degradation Due to Sunlight Only

From Figure 5 it is clear that the samples as exposed beneath Corex at normal incidence in the cabinet are degraded as much as the samples exposed at normal incidence to total weather. It has been pointed out previously that mildew was not a factor

TABLE II. BREAKING STRENGTH LOSS, CUPRAMMONIUM FLUIDITY, AND INCIDENT RADIANT-ENERGY DATA

Samples	Exposure:	1 month			2 months			3 months			4 months			5 months			8 months		
		% BSL	Fl	g. cal./cm² ×10⁻²	% BSL	Fl	g. cal./cm² ×10⁻²	% BSL	Fl	g. cal./cm² ×10⁻²	% BSL	Fl	g. cal./cm² ×10⁻²	% BSL	Fl	g. cal./cm² ×10⁻²	% BSL	Fl	g.cal./cm² ×10⁻²
Set 1 Apr. 9–June 10																			
Cabinet	Corex 9700	22	9.1	192	37	14.4	393												
	U.V. 5970	19	6.9	6	25	12.2	13												
	Blue 5330	19	9.2	101	29	14.0	207												
	Yellow 3482	9	3.1	134	13	5.0	273												
	Red 2408	8	3.0	121	—	—	240												
	Infrared 2540	10	2.8	32	10	4.2	67												
Totally exposed	45° south	15	14.6	—	37	20.4	—												
	Vertically north	13	13.0		18	17.0													
Set 2 May 9–Aug. 12																			
Cabinet	Corex 9700	18	7.5	191	33	17.1	395	52	26.5	605									
	U.V. 5970	15	5.5	6	21	11.1	9	29	17.5	16									
	Blue 5330	19	7.4	100	22	10.0	204	37	16.6	313									
	Yellow 3482	9	2.6	130	14	3.7	266	15	6.7	414									
	Red 2408	8	2.4	115	18	3.2	238	4	4.3	369									
	Infrared 2540	2	2.7	31	5	4.2	62	13	4.9	101									
Totally exposed	45° south	17	9.7	—	21	14.0	—	24	16.8	—	36	19.6	—	44	21.9				
	Vertically north	12	10.3		22	15.4		26	19.5		30	22.6		35	22.6				
	Normal incidence	17	16.4	198	35	24.0	413	52	29.6	638	56	28.0	878	—	—				
Set 3 June 17–Feb. 17																			
Cabinet	Corex 9700							51	27.8	607				63	33.3	935	69	37.5	1294
	U.V. 5970		Not			Not		33	13.5	14		Not		40	18.5	21	45	21.8	27
	Blue 5330		sampled			sampled		43	15.9	314		sampled		43	18.3	484	52	21.9	676
	Yellow 3482		1st			2nd		19	5.7	418		4th		20	7.0	656	26	12.8	918
	Red 2408		month			month		14	5.5	373		month		22	6.7	577	25	7.47	815
	Infrared 2540							8	4.4	104				23	5.8	159	19	8.17	232
Totally exposed	45° south							39	20.7					46	24.6		59	29.1	
	Vertically north							23	18.7	—				31	23.0	—	30	23.8	—
Set 4 July 17–Feb. 17																			
Cabinet	Corex 9700	21	9.3	228	36	14.1	370	39	14.4	565									
	U.V. 5970	20	6.0	6	25	8.2	9	30	8.9	13									
	Blue 5330	22	7.1	120	32	10.2	194	34	10.7	294									
	Yellow 3482	7	2.3	160	12	3.3	260	15	4.7	403									
	Red 2408	10	2.7	140	7	2.9	229	8	3.3	349									
	Infrared 2540	7	2.0	38	7	3.2	63	14	3.9	97								7 months	
Totally exposed:																			
45° south	Corex 9700	15	12.6	—	40	20.2	—	46	27.8	—	49	24.6	—	57	27.8	—	51	30.2	—
Filtered	Blue 5330	16	14.4	—	32	22.7	—	42	28.3	—	56	32.2	—	57	32.7	—	63	34.2	—
light	Yellow 3482	12	8.1	—	12	10.6	—	29	21.2	—	26	18.1	—	28	19.0	—	24	18.3	—
Unfiltered normal incidence		Not sampled			48	24.3	461	52	27.2	624	Not sampled			Not sampled			63	31.6	1153

in this degradation. Therefore it is inferred that, in the absence of any pronounced microbiological action or damage obviously due to corrosive atmospheric contaminants, sunlight accounts for practically all of the degrading effects on cotton fabrics caused by weather exposure, at least for exposure periods exceeding 2 or 3 months.

Spectral Distribution of Degrading Action of Sunlight

As mentioned above, the light filters used in the present experiment were considerably short of the ideal. The extent to which they actually separated the sunlight into distinct spectral regions can be determined from the transmission characteristics (Figure 1).

Data from samples in the cabinet show that, when acting for the same length of time, light from the different filters produces different degrading effects which decrease in the order: Corex, blue, ultraviolet, yellow, red, and infrared (fluidity data rate the infrared ahead of the red (Figure 5)). It is obvious from the percent-transmission data (Table I) that this cannot be the true order of effectiveness of the spectral regions passed by these filters. Cognizance must be taken of the quantity of energy reaching each sample beneath its respective filter. Otherwise a degradative effect interpreted as a selective action due to the quality of the filtered light might in reality be just a quantity effect due to greater or less opacity of the shielding filter. The situation is clarified by considering the degrading effect of the light transmitted by a given filter as a function of the total amount of this light received by the sample. As a means of evaluating this function, a "degradative index" was computed for the light passed by each filter.

For any particular sample, the amount of degradation (in this instance measured as percent loss of tensile strength) is divided by the accumulated total units of radiant energy (gram calories per square centimeter) incident upon it through its particular filter. This results in a number which is a function of the destructive action per unit of energy. If, then, the number computed for the Corex filter, which transmits the entire spectrum, is considered as unity and the numbers for the other filters are reduced to the basis of Corex = 1, the resulting quantities can be used as indices of the degrading power of the

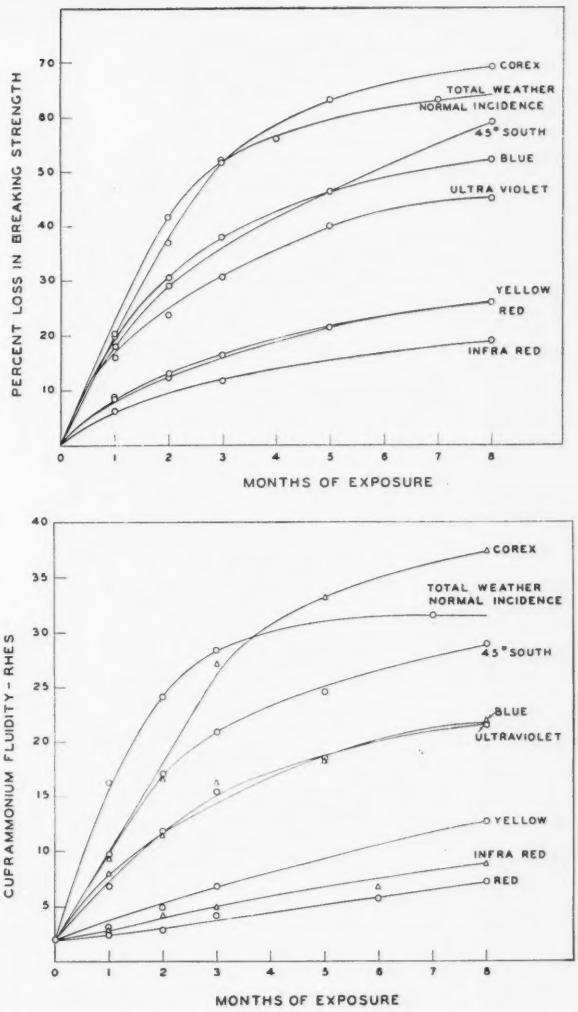

FIG. 5. *Fluidity and loss in strength versus exposure time.*

light from the various spectral regions transmitted by the individual filters.

A comparison of the indices listed in Table I corroborates the accepted view that the short wave-length radiation in sunlight exhibits the greatest degrading efficiency. However, the indices also show that the degrading influence of solar radiation is not limited to the short wave-length portion of the spectrum. In spite of the low degrading efficiency of radiation from the longer wave-length end, this radiation has a not insignificant action. Figure 5 shows that samples exposed to these longer wave lengths of energy as transmitted by the yellow and red filters suffered damage to the extent of at least 20 percent loss of strength in 8 months. It is interesting, also, that the index for the near infrared radiation has a

higher value than that for the energy passed by the yellow or red filters inasmuch as these latter transmit to a considerably higher degree over the whole spectral region in which the infrared filter is transparent. This can be seen in Figure 1.

In a previous paper [2] on the behavior of cellulose with filtered light from a carbon arc (in which were discussed the historical and the general theoretical aspects of this subject) data were presented which indicated the existence of an antagonistic action between energies in the yellow-red portion of the spectrum and those in the ultraviolet-blue portion. It was expected that the present work would demonstrate the existence of this phenomenon in sunlight. The observation made in the present study —viz., that energy from a narrow portion of the spectrum has a higher degrading efficiency than the energy from an enveloping broader portion—might be due to an opposing action of the energies which were added to the narrow portion upon broadening the spectral band, or due to a dilution effect whereby a small quantity of effective energy combined with a large quantity of ineffective energy produces a low resultant efficiency. It is probably due to a combination of both but, because of the overlapping transmission characteristics of the filters employed and because the nature of the samples precludes precise quantitative measurement of the degradation produced, it is impossible to separate the two effects. Under these circumstances, in order for the existence of an antagonistic action to be substantiated, the data should show that samples exposed to a narrow wavelength band of energy are more degraded than other samples simultaneously exposed to the same energy plus energy from the opposing wave-length region.

Some evidence of this nature was obtained from the data for the outdoor exposures beneath filters inclined 45° south (Table I). Here only three filters were involved, Corex, blue, and yellow. Although somewhat erratic, the tensile-strength data, as well as the more consistent fluidity results, showed that there was more degradation of the samples beneath the blue filter than of those beneath the Corex and more, even, than of those totally exposed at 45° south. This was true despite the fact that the blue filter used did not remove all of the yellow-red light and despite the fact that in sunlight the amount of yellow-red light greatly exceeds the amount of ultraviolet light. (The ultraviolet is never greater than 3 percent, whereas the yellow-red averages about 16 percent of sunlight.) The non-appearance of this phenomenon in the cabinet exposures may be in some way related to the difference in humidity conditions between the cabinet-protected samples and the totally exposed samples. As mentioned above, radiation degradation of cotton is considerably influenced by the moisture content of the samples.

The reason why yellow-red light should retard the action of ultraviolet energy, and perhaps the action of the infrared energy, is not known. The source of the antagonistic action must be sought in the mechanism of the photochemical reaction of radiant energy with cellulose. Aston [1] reports a theory advanced by F. A. Lindemann that the cellulose is attacked by ozone produced from oxygen on the surface of the cellulose by the ionizing effect of the ultraviolet radiations, with the most effective frequency for ionization calculated to be 323 millimicrons in the ultraviolet. The most effective de-ionizing frequency for ozone was calculated to be 601 millimicrons lying in the orange region. Therefore it seems that a preponderance of orange light of wave length 601 millimicrons would de-ionize the ozone as fast as it is ionized by energy of 323 millimicrons wave length and before it can react extensively with the cellulose. The present results could be construed as supporting this view except that the relatively high index of the pure infrared region is not explained thereby nor is the fact that the yellow and red regions have any index at all other than zero. Furthermore, Jones [6] demonstrates that the longer visible wavelength radiations can be responsible for considerable cellulose deterioration when the cellulose is "sensitized" or rendered more absorbent to these radiations.

Further progress in the investigation of these antagonistic effects must await the availability of large-area light filters which, although not necessarily monochromatic, will transmit sharply defined spectral regions and be stable to the prolonged action of sunlight and weather.

Summary

Simultaneous exposures of several different samples from the same piece of kier-boiled cotton sheeting were made in sunlight both under fairly well-controlled and under uncontrolled conditions. The controlled exposures were made in a specially constructed cabinet designed to segregate sunlight from other factors of weathering and inside which the samples were kept flat and perpendicular to the

sun's rays during exposure. The uncontrolled exposures were made on open racks, some maintained at normal incidence, some vertically north, and others inclined 45° to the south. A comparison of samples from controlled and uncontrolled exposures indicated that, in the absence of any pronounced microbiological action or damage obviously due to corrosive atmospheric contaminants, sunlight can account for practically all of the degrading effects on cotton fabrics caused by prolonged weather exposure. Considerable acceleration of effect is accomplished by maintaining the sample surfaces perpendicular to the sun's rays.

It is quite demonstrable that radiant energy from some parts of the sun's spectrum is considerably more damaging than the energy from other spectral regions. A "degradative index" was computed from the data which gages the degrading efficiency of light as transmitted by the different filters. It is shown that the degrading influence of solar radiation is not limited to the short-wave portion of the spectrum.

From comparison of the difference in effect on cellulose of solar energy from separate spectral regions acting individually and in combination, evidence is presented which indicates the existence of an antagonism between energies from different portions of the spectrum.

Acknowledgment

The authors wish to thank Mrs. L. D. Wiggins and Miss D. C. Legendre for carrying out the breaking-strength tests; and H. C. Doescher for the fluidity data presented. The cooperation of M. E. Jefferson and coworkers is acknowledged for the measurement of the transmission values of the filters and for the calibration of a thermopile.

Literature Cited

1. Aston, F. W., Dept. Sci. Ind. Research, Great Britain Advisory Comm. for Aeronautics, Reports and Memoranda No. 845, appendix, 1922.
2. Campbell, K. S., and Fynn, P. J., TEXTILE RESEARCH JOURNAL **16**, 450 (1946).
3. Dean, J. D., and Worner, R. K., *Am. Dyestuff Reptr.* **36**, 405 (1947).
4. Fargher, R. G., *J. Soc. Dyers and Colourists* **61**, 118 (1945).
5. Fynn, P. J., and Campbell, K. S., TEXTILE RESEARCH JOURNAL **17**, 158 (1947).
6. Jones, J. I. M., *J. Soc. Dyers and Colourists* **52**, 285 (1936).
7. Searle, G. O., *J. Text. Inst.* **20**, T162 (1929).
8. Turner, A. J., *J. Soc. Dyers and Colourists* **36**, 165 (1920).

A Permeability Method for Determining Fiber Fineness*

John P. Elting and James C. Barnes

Research Department, Kendall Mills, Division of the Kendall Company, Paw Creek, North Carolina

Abstract

An instrument to measure the air permeability of compressed fiber wads is described, together with essential details of construction. An index, F, of fiber fineness is defined following the derivation of an approximate permeability. The roles played by porosity of the plug, the size, shape, and density of the fibers, and their effect on the values of F are discussed with reference to cotton. Errors due to sample weight, moisture, and trash are appraised. An estimate of the instrument precision is obtained by analysis of experimental data. The nature of results obtained from measurements on cotton is described; typical ranges of F observed for several varieties of cotton are noted.

I. Introduction

The practical significance of fiber fineness has been recognized qualitatively for many years; fineness and length of the cotton fiber have been traditionally associated. Only within recent years have the effects on quality of product been adequately described [3, 5]. The textile industry has become acutely aware of the role played by filament size; the wide range of sizes available in synthetic fibers has undoubtedly been largely responsible.

This paper presents a method for measuring the air permeability of a fiber plug, and an index of fiber fineness. The device, with but minor modifications, has been used satisfactorily in these laboratories since 1939. A large sample of cotton is tested; no special cleaning or preparation is required. Measurements of adequate precision are obtained and may be carried out quickly and with ease.

The word "fineness" implies smallness of dimension—a state or degree of attenuation when applied to a fiber. The term is rather loosely used, to refer to the concept of dimension, and as a synonym for fiber weight per unit length, for fiber "diameter," for cross-sectional area or perimeter, or for specific surface or surface per unit mass of fiber. It is essential to note that each of these measures is associated with the size of the fibers; each will exhibit a general, if not precise, correlation with all of the others. Since stresses within a yarn or cord made from staple fibers must act across the fiber surfaces, any measure of dimensions would seem to possess practical significance.

Because permeability, or its reciprocal, does not uniquely describe the transverse dimension of a fiber, this characteristic will be referred to in the following pages as the F-value, or fineness index. The F-value is inversely proportional to the permeability.

II. Previous Work and Apparatus

Balls and Goshawk [1] developed an instrument in 1928 called a Porometer to measure the flow of liquids through a plug of parallel fibers. The instrument was used to measure the change in cross-sectional area of the fibers on absorption of water.

Wiggins, Campbell, and Maass [17] in 1939 described the application of the Kozeny equation relating specific surface and permeability to wads of glass fibers, wool, and rayon. Their results agreed within experimental error with microscopical measurements of specific surface.

Fowler and Hertel [6] proposed a measure of surface per mass of fibers as a fundamental measure of fiber size and described an apparatus for its measurement which has since become known as the Arealometer. Sullivan and Hertel [14, 15] and Sullivan [16] developed the theory of the measurements in a series of papers. The Hertel instrument requires only a very small sample, a feature which makes it of great value when only limited samples are available, as in many breeding problems.

Apparatus similar to the Arealometer, described by Mary Anna Grimes [7], has been used to measure

* Presented in part at the Fall Meeting of The Fiber Society, Princeton, New Jersey, September 4, 1947.

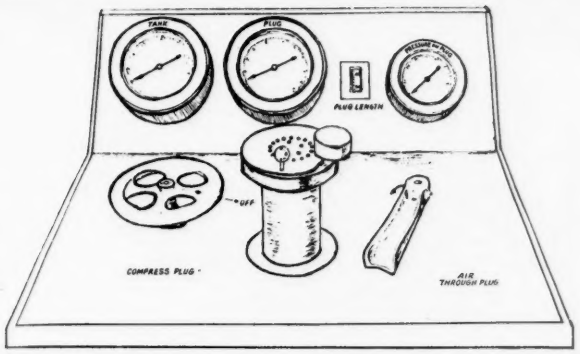

FIG. 1. *Sketch of cabinet top showing end of sample chamber and controls.*

the fineness of various cottons. She reports a high correlation between the pressure drop across the wad of cotton and the fiber weight per unit length as measured by the technique developed by the U. S. Department of Agriculture [12].

Cassie [2] has used the measurement of permeability to derive the "diameter" of wool fibers.

Pfeiffenberger [11] discusses an apparatus for measuring the resistance to air flow of a mass of well-fluffed cotton. This device is a modification of the Schiefer apparatus [13] for measuring the permeability of fabrics. He finds a good correlation between pressure difference across the cotton and fiber weight per length.

A new instrument, called the Micronaire, has currently appeared on the market. The response of this instrument depends on the resistance offered to the passage of air through a compacted wad of fiber.

Work on a method of appraising fineness of cotton was undertaken in this laboratory in 1936, following suggestions made by Hertel. The early work consisted largely of attempts to appraise cottons using experimental designs of sample chamber, methods of measurement, and various air "circuits."

The present instrument, built in 1939, has been used continuously as a routine test device. The fineness index or *F*-value has been a corollary development.

III. Description of Kendall Mills Instrument

The device consists of three principal components: (1) a sample chamber which holds the fibers in a tightly compressed wad, and the mechanism for securing this compression; (2) an orifice which is used to determine the rate of flow of air through the fiber plug; and, (3) the two pressure gages, one

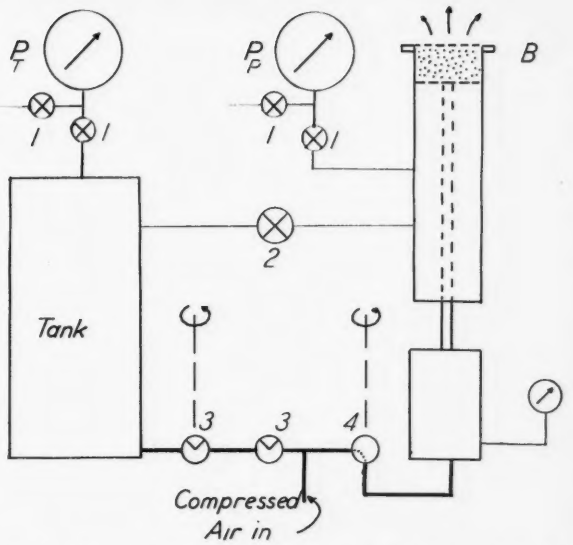

FIG. 2. *Diagram of air circuit: (1) stopcocks, (2) metering orifice, (3) needle valves, (4) four-way valve.*

which measures pressure at the inflow side of the fiber plug and the other which measures it at the inflow side of the metering orifice. These elements, with the necessary valves, are mounted in a cabinet. Figure 1 shows the location of the gages, the top of the sample chamber, and the controls. Figure 2 is a schematic diagram showing how the air flows through the system.

The sample chamber is a steel tube with an inside diameter of 2.5 inches. Compression of the sample is obtained by an air-actuated piston. The top of the chamber is a perforated swinging plate. The depth of the chamber is 1 inch, accurately controlled by a stop on the piston rod. The perforations in the piston and cover consist of 22 holes in each, ¼ inch in diameter, arranged as shown in Figure 3.

The piston, which compresses the cotton in the chamber, is actuated by a separate air cylinder attached below the sample chamber. A total compressing force of about 200 pounds is required. The stroke of the piston is 2.5 inches.

The metering orifice is a standard ¼-inch stopcock. Compressed air from an outside source is admitted to the actuating cylinder through a standard two-way valve. The air which is passed through the metering orifice is reduced to a comparatively low pressure by a needle valve. The flow of this air is controlled by a second needle valve in series with the first.

The pressure gages are standard commercial items. The one which measures the pressure at the inflow

side of the metering orifice (tank pressure) has a range of 30 inches of water; that on the inflow side of the sample chamber (plug pressure) has a range of 20 inches of water. A third gage is incorporated in the instrument to show the pressure in the actuating cylinder.

In routine use the procedure followed consists in obtaining two determinations for each sample at slightly different but specified values of pressure at the inflow side of the metering office. These pressures are 26 and 27 inches of water.

The operations consist, first, in the weighing of the sample. This weight is 0.90 ± 0.01 ounce. The cotton has been conditioned at 70°F and 65 percent relative humidity. The sample is then inserted into the sample chamber; the cover is swung into the closed position and tightly clamped. The cotton is next compressed by admitting air to the actuating cylinder until the piston firmly strikes the stop. Air at reduced pressure is then made to pass through the compressed fiber wad by opening the needle valve until the specified pressure on the inflow side of the metering orifice is reached, at which time the pressure gages are read. The needle valve is opened slightly more until the second specified pressure is obtained, and again the gages are read. From these data, two values of F are computed according to equation (11) and averaged. In this equation (ΔT) and (ΔP) are the pressures on the inflow side of the metering orifice and the fiber plug, respectively; B is the barometric pressure in atmospheres.

Calibration of the instrument is effected by means of a standard or calibrating orifice. This is made in the form of an inverted tumbler fitting snugly inside the sample chamber when the piston is in its bottom position. A small hole drilled in the top of the inverted tumbler provides the orifice.

IV. The Fineness Index

A rational basis for the fineness index, F, is found by recourse to Darcy's law governing the flow of fluids through porous media. Darcy's law is usually written in the form [10]:

$$Q = c\Delta p \frac{A}{L}. \qquad (1)$$

Here, Q is the rate of flow of water, c is a constant, Δp is the pressure drop through the medium, and A and L are the area and length of the medium.

Darcy's law states that the rate of flow is proportional to a constant. This constant is dependent on the size, shape, and disposition of the particles constituting the porous medium. In general, the smaller the particles, the smaller become the interparticle spaces and the greater becomes the resistance offered to the passage of a fluid, and, consequently, the smaller the value of the permeability.

1. Permeability

For the case of isothermal flow of air through a porous medium of length L and cross section A, Darcy's law may be written:

$$k = \frac{2\mu L Q_m}{\gamma_0 A (P_1^2 - P_2^2)}, \qquad (2)$$

in which the ratio k/μ takes the place of the constant c of equation (1). In this equation, μ is the viscosity of the air in centipoises, γ_0 is the density of the air at a standard or reference pressure and temperature in grams per cubic centimeter, L and A are length and area of the porous plug in centimeters, P_1 and P_2 are absolute pressure in atmospheres on the inflow and outflow sides, and Q_m is the mass flow of air in grams per second.

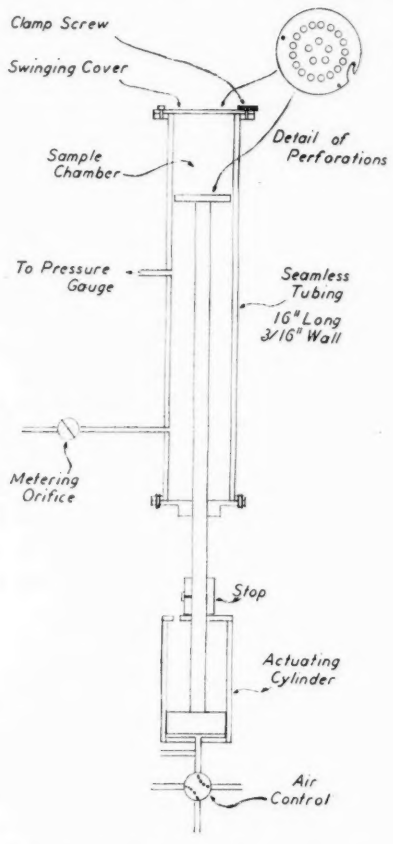

FIG. 3. *Schematic drawing of sample chamber and actuating cylinder.*

When the above units are used, k, the permeability, is in darcys and has the dimensions:

$$(\text{cc/sec})/\text{cm}^2/(\text{atmos/cm}).$$

If the barometeric pressure is represented by B and the volume rate of flow of gas, or air, of density γ_0 is Q, equation (2) becomes:

$$k = \frac{2\mu L}{A}\frac{Q}{(P_1^2 - P_2^2)}. \tag{3}$$

By reference to the diagram in Figure 2, it is seen that $P_1 = P_P$, $P_2 = B$.

The "tank pressure," P_T, is that on the inflow side of the metering orifice; the flow through the metering orifice may be expressed as a function of the pressure drop across it. If, then, Q' represents a volume of gas at the pressure P_P, and assuming isothermal flow, the volume of air passing through the orifice can be written as a function, g, of the pressure difference, thus:

$$Q' = g(P_T - P_P). \tag{4}$$

Again, with the assumption of isothermal flow and an ideal gas, the change of volume in passing through the porous fiber plug is:

$$Q'P_P = QB. \tag{5}$$

Solving equations (4) and (5) for Q, one obtains

$$Q = P_P g(P_T - P_P)/B.$$

Substituting this equation in equation (3) yields:

$$k = \frac{2\mu L}{A}\frac{P_P g(P_T - P_P)}{B(P_P^2 - B^2)}. \tag{6}$$

If it is now assumed that the function given in equation (4) is linear—that is,

$$g(P_T - P_P) = \beta(P_T - P_P),$$

where β is a constant, equation (6) becomes:

$$k = 2\alpha\frac{P_P(P_T - P_P)}{B(P_P^2 - B^2)}, \tag{7}$$

where $\alpha = \mu L\beta/A$ is a constant of the apparatus.

In the above equations all pressures are absolute and in atmospheres. The pressure gages, however, measure the difference in pressure over the existing barometric pressure. If C is the factor to change gage-scale units to atmospheres, the following conversion equations may be written:

$$P_T = B + C(\Delta T)$$

and

$$P_P = B + C(\Delta P), \tag{8}$$

where (ΔT) and (ΔP) represent the pressure-gage readings. Substitution of equations (8) in equation (7) yields:

$$k = 2\alpha\frac{[B + C(\Delta P)][C(\Delta T) - C(\Delta P)]}{B[2BC(\Delta P) + C^2(\Delta P)^2]}. \tag{9}$$

In making fineness measurements, the tank pressure $C(\Delta T)$ is held constant at a value near 0.07 atmosphere. The plug pressure $C(\Delta P)$ varies with the permeability of the fiber plug, its usual range being from 0.01 to 0.05 atmosphere. Equation (9) may be simplified by assuming that

$$B \gg C(\Delta P),$$

from which it follows that $\frac{B + C(\Delta P)}{B}$ is approximately unity and that $C^2(\Delta P)^2$ is so small that it may be neglected, with the result that

$$k' = \alpha\frac{1}{B}\frac{(\Delta T) - (\Delta P)}{(\Delta P)}, \tag{10}$$

where k' denotes the approximate value of the permeability k.

2. Fineness Index

The reciprocal of the approximate permeability, $1/k'$, is taken to be a measure of the resistance offered by the fiber plug to the flow of air. In accordance with the preceding discussion, the finer the fiber the greater the resistance, and therefore

$$F = \frac{B(\Delta P)}{(\Delta T) - (\Delta P)} \tag{11}$$

has been chosen as the index of fineness. At locations near sea level the factor B may be assumed to be equal to unity, an uncertainty of about 3 percent being introduced owing to fluctuations in barometric pressure.

Other than for the barometric pressure in the above equation, this value of F corresponds to resistance in the analogous electrical circuit.

3. Calibration and Adjustment

The metering orifice was adjusted arbitrarily so that the average value of F for cotton would fall in the neighborhood of unity. A reference or calibrating orifice was then constructed as previously described, to replace the cotton, and its F-value was determined. The size of this orifice was chosen

so that its value, F_o, also would be close to 1. While the instrument is being calibrated, the tank pressure is held midway between standard values and the metering orifice is adjusted until the plug pressure has a value

$$(\Delta P) = F_o(\Delta T)/(F_o + B). \tag{12}$$

4. Porosity

The total porosity, f, of a fiber plug is defined as

$$f = 1 - \frac{\gamma_P}{\gamma_f} = 1 - \frac{V_f}{V_P}, \tag{13}$$

where γ_f and V_f are the density and volume of the fibers, and γ_P and V_P are the apparent density and volume of the fiber plug.

The Kozeny formula, which shows an explicit variation of permeability k with porosity given by

$$k \sim S\frac{f^3}{(1-f)^2}, \tag{14}$$

where S is a shape factor, makes it apparent that in the inference of fineness from permeability the porosity of the fiber plug must be controlled.

The apparent density of the compressed cotton plug is 0.32 gram per cubic centimeter. If a value of 1.32 gm./cm^3 is taken for fiber density [6], the porosity of the cotton plug is found to be 0.76. It is significant to note that if fibers other than cotton are to be measured in this apparatus the amount used depends on fiber density, and may be estimated from equation (13).

5. Effects of Fiber Shape and Density

The shape of the fiber cross section affects the flow of air through the fiber plug and thus alters the permeability, as indicated by equation (14). It is of practical significance to note that, for cotton, flat immature hairs, even when these have a relatively large perimeter, exhibit high values of F—as high as or frequently higher than the values exhibited by normally mature but actually small fibers.

The F-value is also dependent on the density of the fiber, as shown in equation (13). It is reasonable to assume for cotton that no appreciable flow of air occurs through the lumen. The density involved in estimating porosity from equation (13) must therefore be an over-all fiber density, not the density of cellulose itself.

It is not the purpose of this paper to establish a value of fiber density. It is pertinent to point out that the area of the lumen is generally assumed to be 10–20 percent of the total cross-sectional area of the fiber [1, 9]. From a limited number of measurements of fiber cross section in this laboratory, assuming a cellulose density of 1.55 gm./cc., an average fiber density of 1.35 gm./cc. was obtained. Clegg and Harland [4] calculated from similar measurements a low average value of 1.05. Calculations based on data presented by Karrer and Bailey [8] indicate a range in fiber density from 1.29 to 1.49. These represented extremes from linear fibers having large lumens to elliptical fibers with small lumens. Their data would indicate an average density of about 1.43. Measurements by Fowler and Hertel [6] of linear density and cross-sectional area led them to choose a value for fiber density for some specific cottons of 1.32 gm./cc.

The possible variations in fiber density indicated above, if they do occur, would result in an appreciable change in F-value. From equations (13) and (14) it is seen that a change in F-value of about 25 percent may be accounted for as the result of assuming a 10-percent change in fiber density.

It is evident that the F-value depends not alone on the size of the fiber but also on its shape and density. The effects of these three variables cannot be separated by permeability measurements alone. However, this fact does not reduce the practical utility of this measure, but rather emphasizes that it must be supplemented by other information or measurements if the results are to be unambiguous. The fact that the F-value does depend on these three variables permits different interpretations of results, depending on the type of supplementary information available. Thus, F-value may be used as a measure of size if shape and density are approximately constant; if, however, some knowledge of size is had—from knowing the variety of the

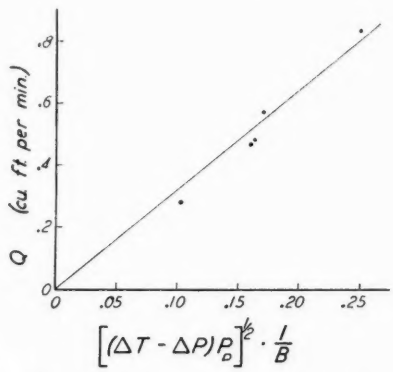

FIG. 4. *Flow characteristic of metering orifice.*

cotton, for example—then differences in F may be used to indicate shape and density.

V. Precision

1. Effect of Sample Weight

The particular weight of the cotton sample (0.9 ounce) and the volume of the sample chamber (80.44 cm³) were those found experimentally to be satisfactory. Smaller amounts of cotton permit "channeling" and yield fictitiously low and unreproducible values of F. The cotton sample is weighed on a platform balance which is sensitive to, and carries a scale graduated to, 0.01 ounce.

Samples of cotton are conditioned at 70°F and 65 percent relative humidity. Variations in moisture content of approximately ±1 percent may occur. Under these conditions, a 1-percent error in sample weight would produce about a 2-percent error in the value of F.

2. Effect of Time

The relative humidity of the air passing through the fiber plug may be assumed to be nearly at saturation. A measurable increase in the F-value is observed if the air is allowed to flow through a cotton plug for several minutes. The tank pressure

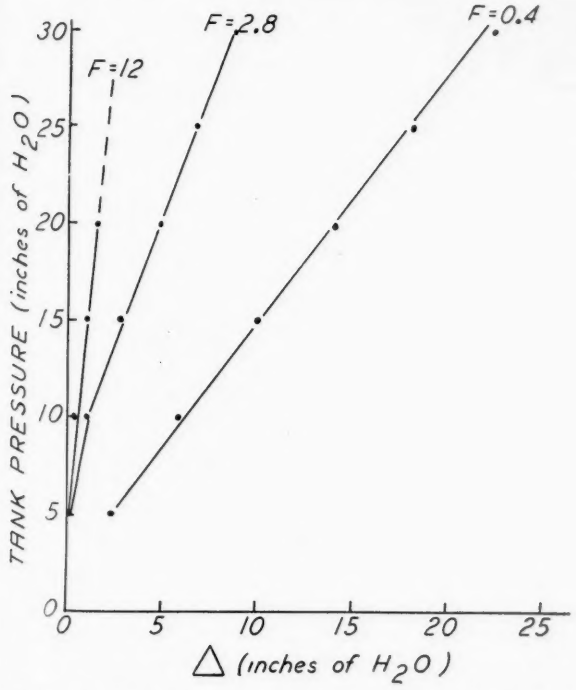

FIG. 5. *Illustration of method used to determine F-value above range of instrument.*

may, however, be brought easily and quickly to the desired standard values (26–27 inches of water) and the gage readings may be made within 10 or 15 seconds. A uniform technique eliminates all sensible error from this source.

3. Effect of Trash

In the determination of the F-value of cotton, trash appears to have little effect in the range of grades of most general interest. One sample was taken from each of 31 bales on the floor of an opening room. Grades ranged from low middling to middling. Samples were taken from picker laps made from these same bales. F-valves observed before and after the opening, cleaning, and picking operations were:

	Average F-value	Maximum	Minimum
Average of 31 *B C* taken from opening room	0.926	1.49	0.62
Average of 17 samples taken from picker laps	0.921	0.97	0.83

The reduced spread between maximum and minimum values is attributed to the mixing of the cotton during the operations.

The effects of trash removal are also shown by measurements of F before and after cleaning with a machine similar to the Shirley Analyzer.

Twenty-five samples were tested; 5 samples represented each of the five grades: strict good ordinary, low middling, strict low middling, middling, and strict middling. The average difference in F-value before and after cleaning was 0.04, with an average standard deviation of the difference, by grades, equal to 0.10. This precision is of the same magnitude as that found for repeated tests on the same sample without cleaning.

4. Effects of Fiber Alignment

It is assumed that the fibers in the plug are oriented in all directions. If fibers are aligned as the result of combing or drafting operations, they become packed together more closely than when randomly oriented. Cotton from bales, picker laps, and card slivers appears to be satisfactory; drawing slivers and rovings must be most thoroughly disarranged.

5. Experimental Reproducibility

To determine the instrument precision and to obtain an estimate of the variability of test results

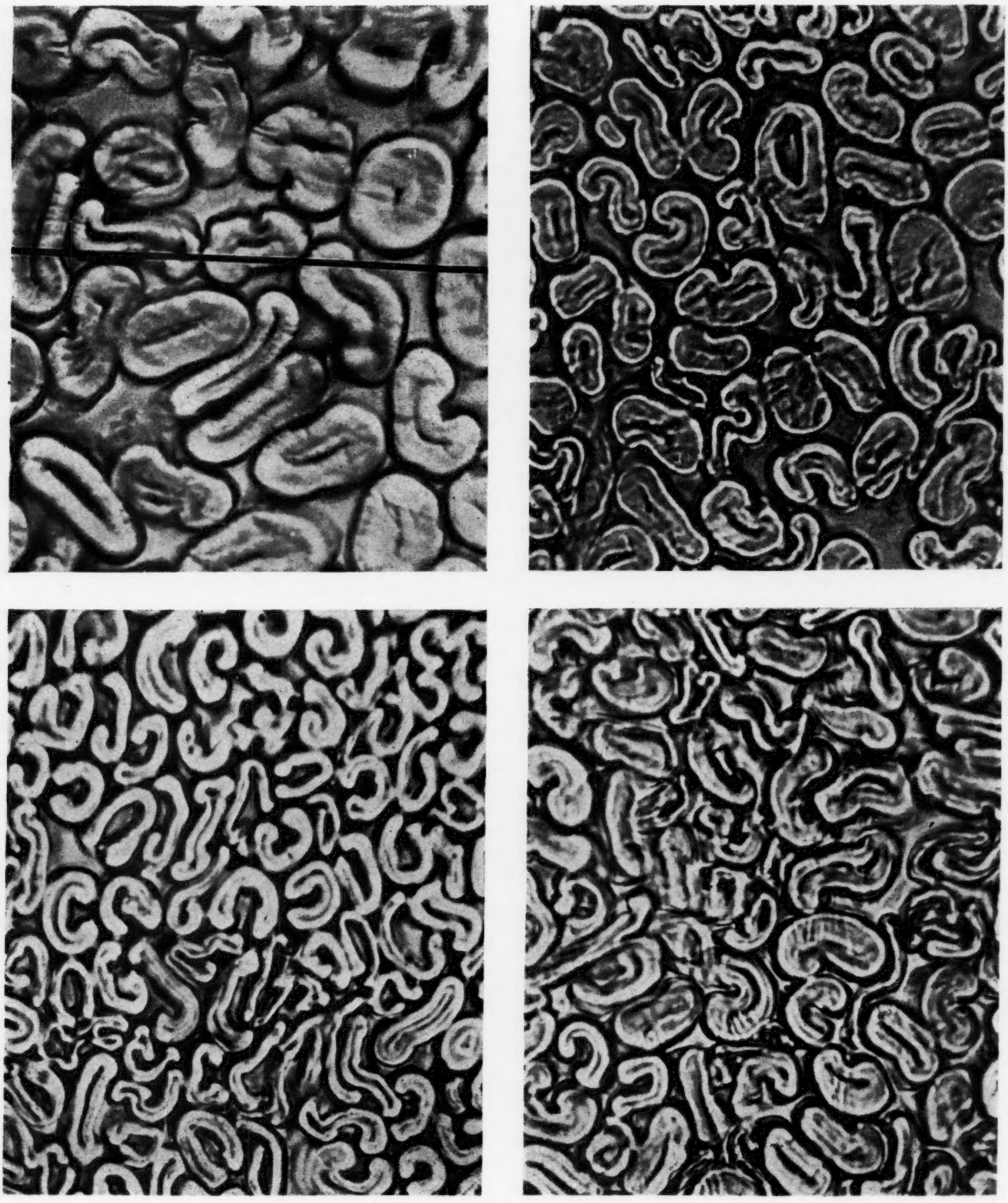

FIG. 6. *Cotton cross sections, magnified 750×: A (upper left)—F = 0.28; B (upper right)—F = 0.63; C (lower right)—F = 1.23; D (lower left)—F = 2.5.*

arising from different operators, the following experiment was performed: six measurements of F were made by each of three operators on each of 10 cotton samples drawn from an assumed homogeneous parent lot. Each measurement included a redrawing from the samples and a weighing of the cotton for the plug. The tests were made on different days. A variance analysis of the 180 items

of data gave the following results:

Source	Sum of squares	Degrees of freedom	Estimate of variance	Component of variance
Operators	0.34344	2	0.1717	0.0027
Cottons	4.76074	9	0.5289	0.0288
Days	0.17310	5	0.0346	0.0008
Residual	1.63234	163	0.0100	0.0100

The components of variance in the last column are estimates of the variation due to the separate factors listed. It is immediately apparent that operators and inhomogeneity of the cotton contribute the greatest uncertainties; that due to the cotton is of no concern here other than that its effect is eliminated.

Of the three operators, two were known to be careful workers. Inspection of the original data showed that the larger portion of variance due to operators may be attributed to the third individual. Part of this variance may also be presumed to be due to the repeated handling of the cottons. Each sample was handled eighteen times, thus imposing a more severe condition than exists under usual operating circumstances.

The effect of making the measurements on different days is negligible. The residual error variance of 0.01 may be considered to measure the reproducibility of the instrument itself.

VI. Miscellaneous—Nature of Results

1. Characteristics of the Metering Orifice

The flow of air through the metering orifice is proportional to the square root of the pressure drop across it, not a linear function, as assumed in equation (7). A calibration curve is shown in Figure 4.

2. Extremely Fine or Coarse Fibers

Extremely coarse cotton fibers, below the sensitivity of the instrument, have not been observed. The practical lower limit of the present instrument is an F-value of about 0.04. The coarsest cotton so far observed has been an India variety with an F-value of 0.28.

Extremely fine (or extremely immature) cottons are occasionally found which require a lower-than-standard tank pressure in order to keep the plug pressure-gage on scale. The upper limit of the instrument when the standard tank pressure is used is an F-value of approximately 3. When such fibers are encountered it is necessary only to observe and plot, as in Figure 5, the pressure drop across the metering orifice for two or three values of tank pressure. The relation between these is linear. The straight line is then extrapolated to the standard tank pressures and the corresponding plug pressures are read. The computation of F is then made in the usual manner.

3. Range of F-Value for Cotton

F-values of cotton have been observed from 0.28 to 12. Varieties exhibit typical ranges of F-value; within a variety the degree of maturity has considerable effect. Approximate ranges for several varieties of cotton are:

Approximate Range of F-value for Normally Mature Cottons of Several Varieties

India or China	0.2–0.4
American Upland	
Rowden	0.6–0.8
Coker 100	0.9–1.2
Acala	1.1–1.4
Egyptian	1.3–1.6

Cross sections of four cottons are shown in Figure 6. Figure 6A shows the large, well-developed sections of an India cotton. Figures 6B and 6C are American Uplands of the same type but with different average maturity, the maturity being less for the higher F-value. The section shown in 6D is of an extremely immature cotton.

VII. Acknowledgment

The authors wish to express their appreciation to Messrs. J. A. LeConte, Jr., and J. J. Such for their able assistance in the development of the instrument described in this paper and in the statistical analyses of data.

Literature Cited

1. Balls, W. Lawrence, "Studies of Quality in Cotton," London, Macmillan Co., 1928.
2. Cassie, A. B. D., *J. Text. Inst.* **33**, T195 (Dec. 1942).
3. Cassie, A. B. D., *J. Text. Inst.* **37**, P154 (July 1946).
4. Clegg, G. C., and Harland, S. C., *J. Text. Inst.* **14**, 498 (1924).
5. Finlayson, D., *J. Text. Inst.* **37**, P168 (July 1946).
6. Fowler, J. L., and Hertel, K. L., *J. Applied Phys.* **11**, 496 (July 1940).
7. Grimes, Mary Anna, TEXTILE RESEARCH **13**, 12 (Nov. 1942).

8. Karrer, E., and Bailey, T. L. W., Jr., TEXTILE RESEARCH **8**, 381 (Sept. 1938).
9. Osborne, G. G., TEXTILE RESEARCH **5**, 292 (Apr. 1935).
10. Muskat, M., "The Flow of Homogeneous Fluids Through Porous Media," New York, McGraw-Hill, 1937, p. 56.
11. Pfeiffenberger, G. W., TEXTILE RESEARCH JOURNAL **16**, 338 (July 1946).
12. Richardson, H. D., Bailey, T. L. W., Jr., and Conrad, C. M., *U.S.D.A. Tech. Bull.* **545** (Jan. 1937).
13. Schiefer, H. F., and Boyland, P. M., Natl. Bur. of Standards Res. Paper, RP 1471 (May 1942).
14. Sullivan, R. R., and Hertel, K. L., TEXTILE RESEARCH **11**, 30 (Nov. 1940).
15. Sullivan, R. R., and Hertel, K. L., *J. Applied Phys.* **11**, 761 (Dec. 1940).
16. Sullivan, R. R., *J. Applied Phys.* **12**, 503 (June 1941).
17. Wiggins, E. J., Campbell, W. B., and Maass, O., *Can. J. Research* **17**, Sec. B, 318 (1939).

An Electron-Microscopical Examination of Rayon

Charles W. Hock

Hercules Experiment Station, Hercules Powder Company, Wilmington, Delaware

Abstract

By metallic shadow-casting of specimens for electron-microscopical examination, fibrils a few hundred Angstroms in diameter were demonstrated in cuprammonium and in viscose rayons. Fibrillation was more distinct in the rayons having a high degree of orientation. The fine fibrils in the fibers of both these regenerated celluloses were similar to those previously observed in native cellulose fibers.

A comparison of surface replicas of the fibers revealed distinct differences. Whereas the cuprammonium rayon fibers were relatively smooth except for occasional markings which gave them a scaly appearance, the viscose rayon fibers were rougher, and showed an irregular netlike pattern.

IN A recent electron-microscopical study of natural cellulose fibers [8], metallic shadow-casting of the specimens was found to be helpful in delineating fiber structure. This method has since been applied to rayon fibers, for the purpose of comparing the fine structure of regenerated cellulose with that of natural cellulose and as a means of observing structural dissimilarities in rayons of different types.

Metallic shadow-casting offers a means of increasing the contrast in electron-microscopical images, thereby enhancing the detail which can be resolved by the instrument. Lack of contrast is particularly objectionable in organic structures such as cellulose, where details of structure are often indistinct even though they are larger than the resolving power of the instrument. In the metallic shadow-casting technique [15], a metal of high atomic weight is evaporated onto the surface of the specimen at such an angle that elevated points on the surface prevent the metal vapor from depositing in regions to the leeward. These metal-free areas, or "metallic shadows," are, in contrast to the metal-coated areas, considerably more transparent to the electron beam. Small variations in surface elevation of the specimen cause sufficient variation in metal deposition so that the increased contrast in the image reveals details of structure not ordinarily detected in unshadowed objects.

In the present study, the metal shadow-casting technique was applied to cuprammonium rayon, regular textile viscose rayon, and to high-tenacity viscose rayon. In order to free the fibers of any oils which might interfere with their examination, especially in the study of surface replicas, the samples were treated for 3 hours with absolute ethyl ether in a Soxhlet extractor. Because individual fibers are too thick to be examined directly with the electron microscope, they were mechanically disintegrated by beating in water in a Waring Blendor for 20 minutes. Small drops of the aqueous dispersion were placed on a glass slide which previously had been coated with a thin film of nitrocellulose (0.3-percent Parlodion in amyl acetate). After the water evaporated, leaving the finely dispersed fiber cellu-

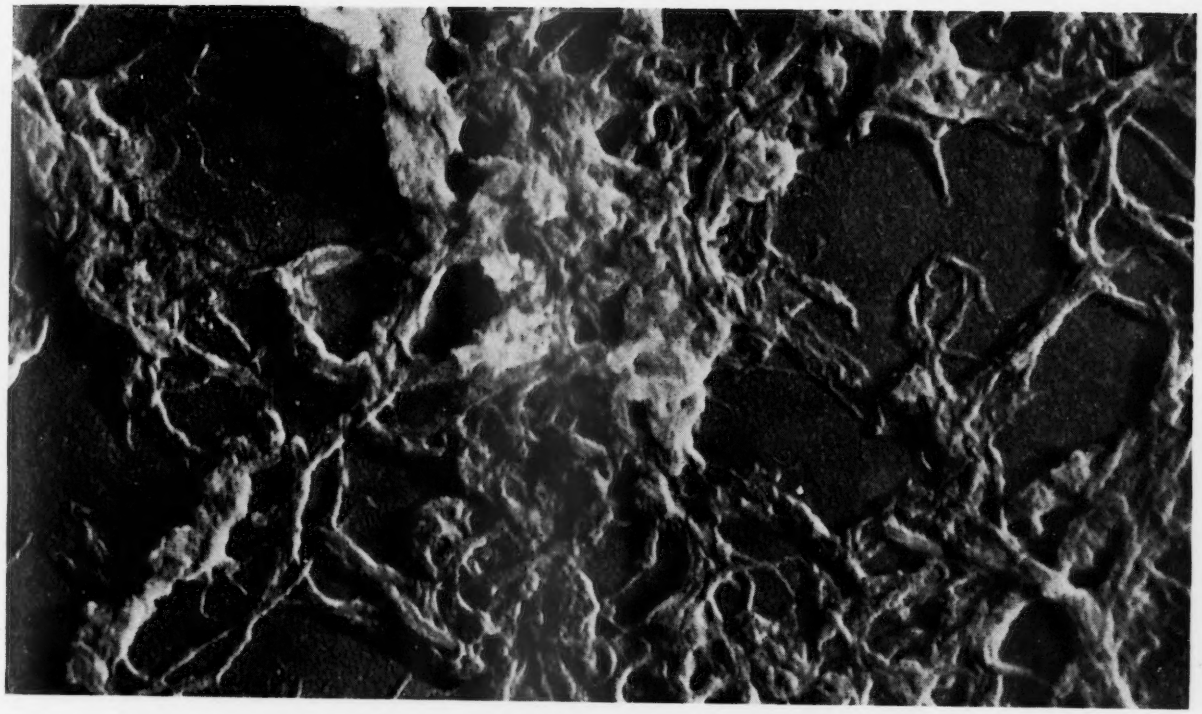

FIG. 1. *Beaten cuprammonium rayon shadowed with chromium. Magnification × 53,000.*

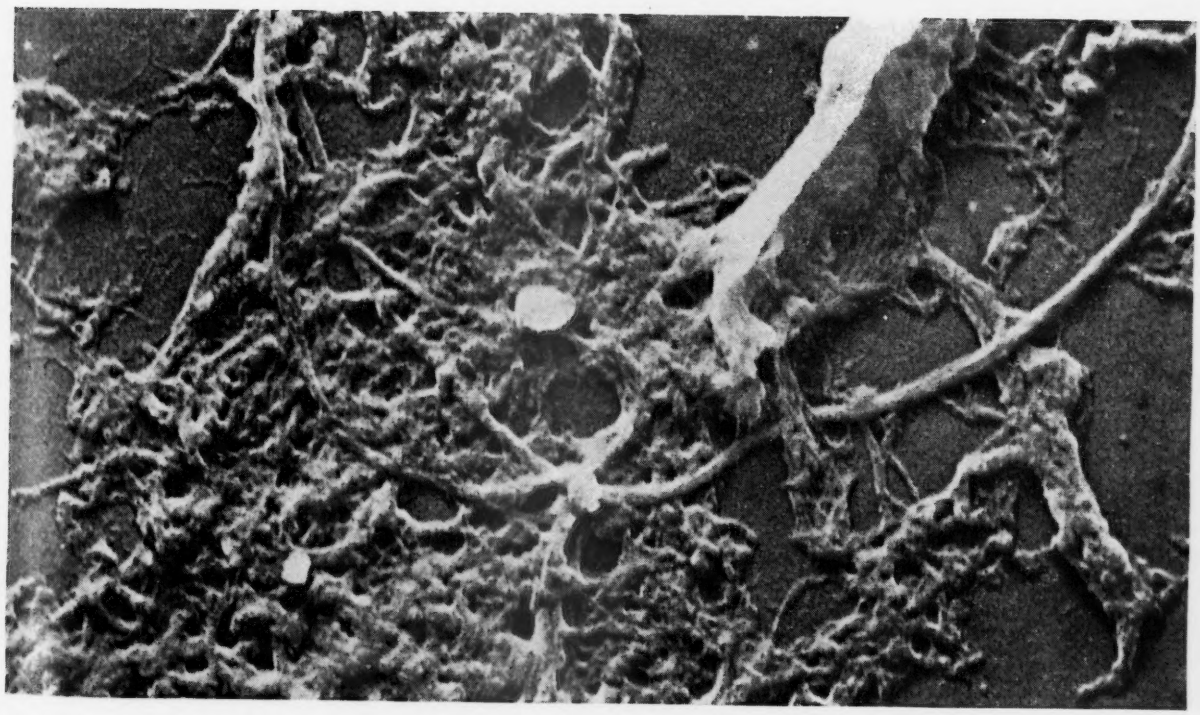

FIG. 2. *Beaten regular textile viscose rayon shadowed with chromium. Magnification × 53,000.*

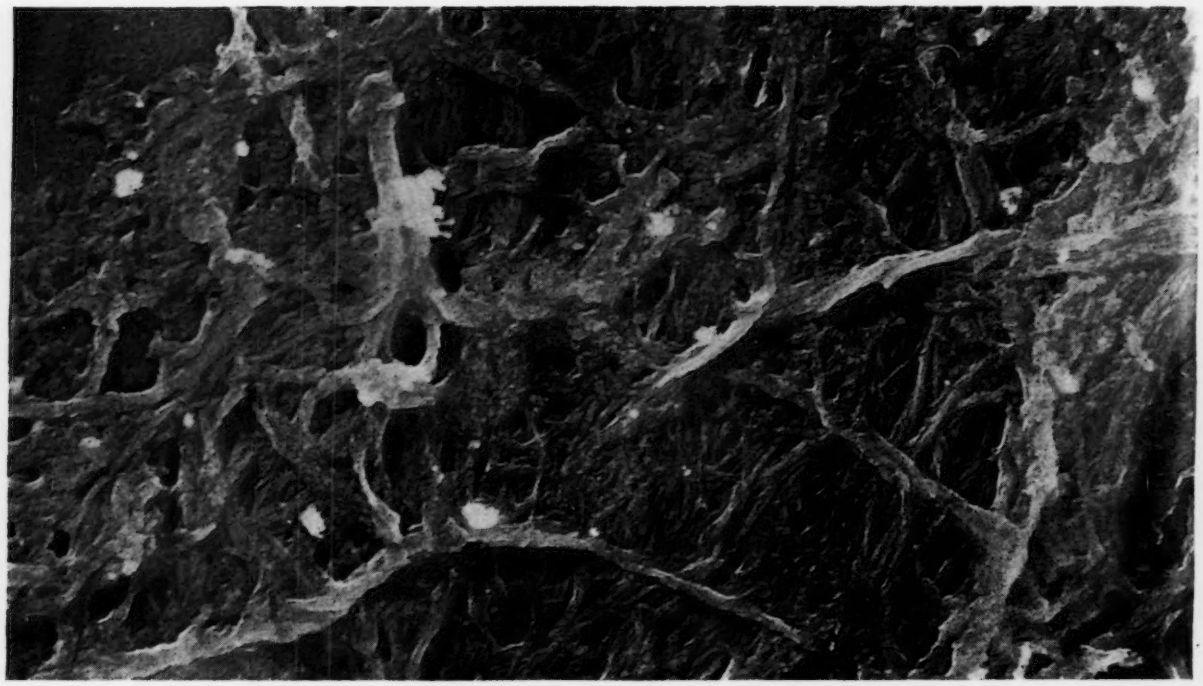

FIG. 3. *Beaten high-tenacity viscose rayon shadowed with chromium. Magnification* × *53,000.*

lose on the supporting film, the specimens were shadowed with chromium, at an angle of 25°. Subsequently, the film was floated off the glass slide and prepared, by the usual methods, for electron-microscopical examination.

The surface character of the fibers was studied by means of replicas. A glass microscope slide was coated with a solution of 3.0-percent Parlodion in amyl acetate. The fibers to be examined were floated on the surface of the liquid. As the solvent evaporated, the fibers were drawn onto the surface of the nitrocellulose film. After drying, the fibers were stripped from the films, whereupon the replicas were shadowed with chromium at a 25° angle.

In order to obtain pictures in which the shadows were dark, prints were made from positive transparencies which, in turn, had been made from the original negatives obtained with the microscope. As a result of photographic reversal, the specimens look as if they were illuminated by light at an oblique angle. This creates the illusion of three dimensions, which, besides being pleasing to the eye, is helpful in interpreting the pictures.

Figures 1, 2, and 3 are representative electron micrographs of the chromium-shadowed rayon specimens. In all of them, fibril-like structures with diameters of a few hundred Angstroms are evident. The fibrils in the cuprammonium rayon were rather distinct but appeared to be shorter than the corresponding structures in high-tenacity viscose rayon. The regular textile viscose rayon had the appearance of a network—that is, there was considerable lateral cohesion and crossing over of the fibrils. These variations in distinctness of fibrillation are probably related to different degrees of crystallite orientation of the fibers. It should be pointed out, however, that the same fibrillate pattern may not prevail in all regions of the fiber. In obtaining these specimens by beating in a Waring Blendor, most of the fine fragments which were used for electron-microscopical examination came from the fiber surface. The occurrence of a "skin" which is more highly oriented than the core is well established, and has been demonstrated in cross sections of rayon fibers by optical [10] and electron-microscopical methods [4].

The surfaces of the fibers were compared by means of chromium-shadowed replicas. Figures 4, 5, and 6 illustrate the results obtained. In interpreting the pictures, it should be borne in mind that replicas and not the actual fiber surfaces are being viewed. The surface character of the cuprammonium rayon appears to be markedly different from that of the viscose fibers. Except for occasional irregularities which give it a kind of scaly appearance, the surface

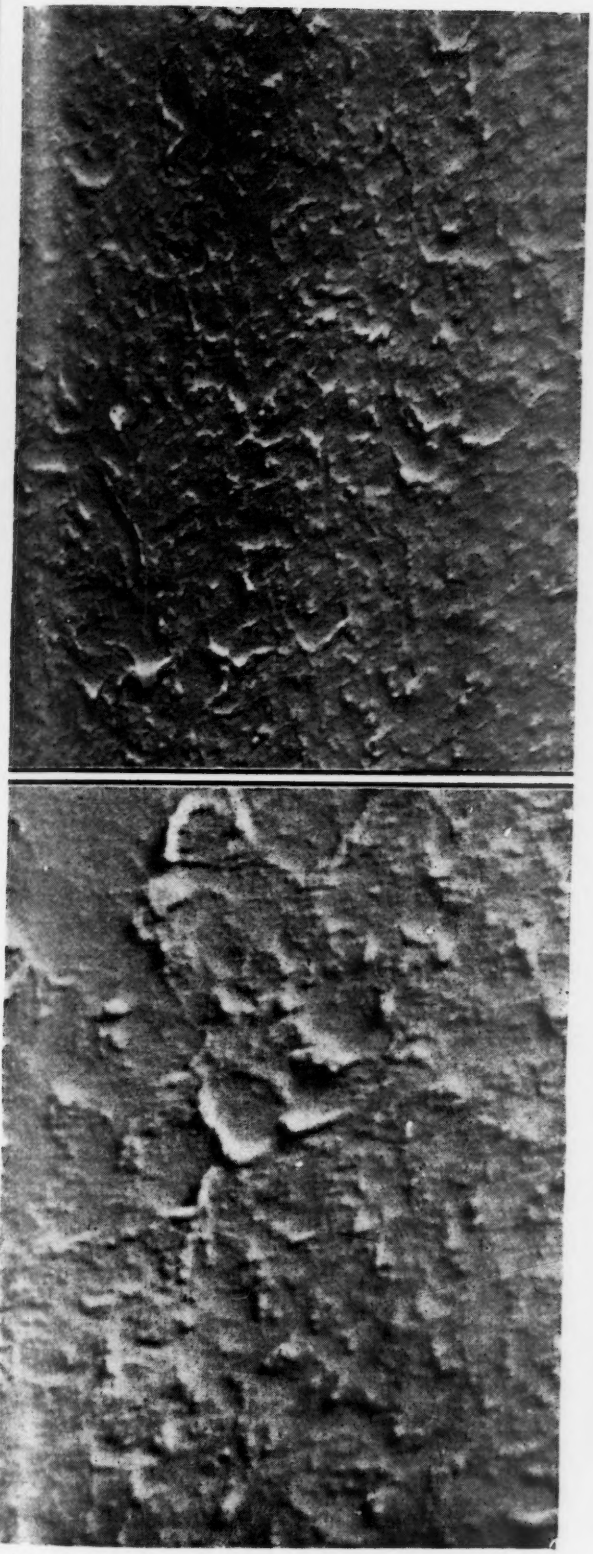

FIG. 4. *Chromium-shadowed nitrocellulose replica of surface of cuprammonium rayon fiber. A (top)—Magnification × 27,000. B (bottom)—Magnification × 53,000.*

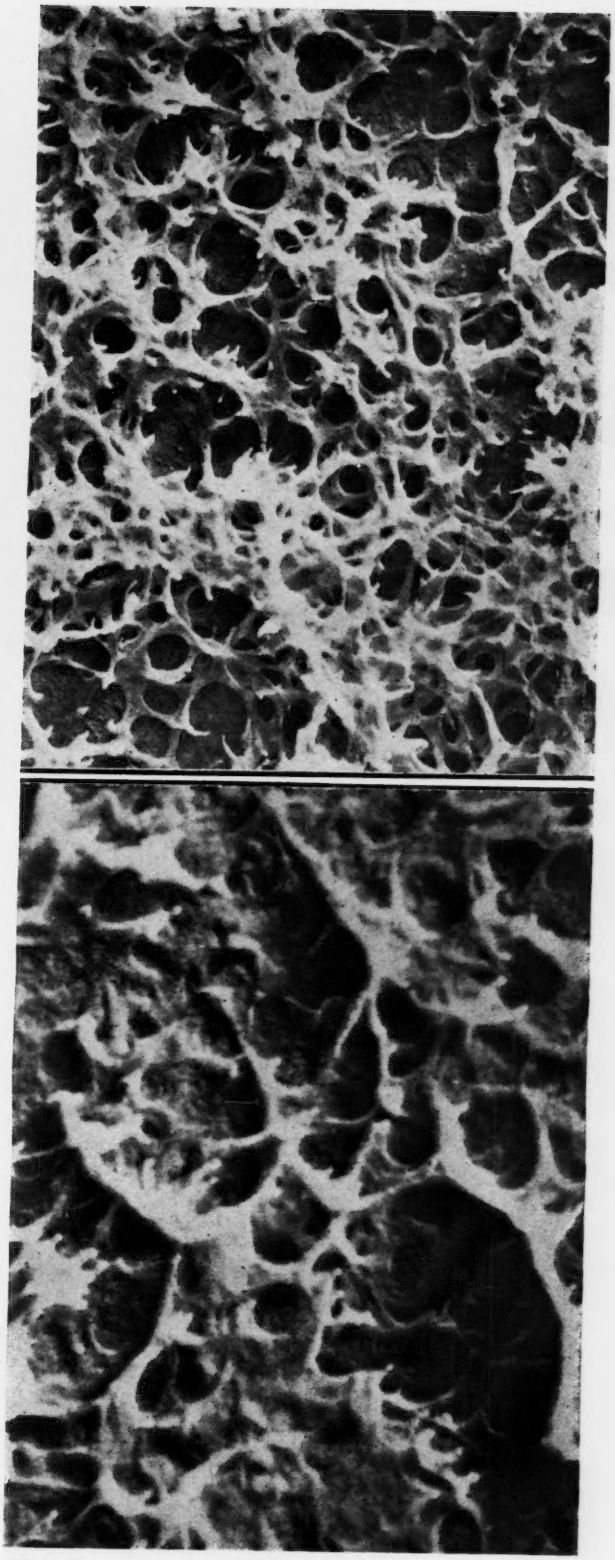

FIG. 5. *Chromium-shadowed nitrocellulose replica of surface of regular textile viscose rayon fiber. A (top)—Magnification × 27,000. B (bottom)—Magnification × 53,000.*

which can be observed with the light microscope, and into still finer fibrils which are resolved by the electron microscope, is of practical as well as theoretical interest in understanding the nature of regenerated fiber formation and in interpreting their mechanical properties.

In natural cellulose fibers such as purified cotton, surface replicas clearly reflected the fibrillate nature of the unbeaten cellulose [8]. Surface replicas of the regenerated fibers, on the other hand, did not reveal a fibrillate structure so clearly. Although the cuprammonium rayon, for example, broke down into fibrils upon beating (Figure 1), little or no evidence of fibrils was apparent in replicas of the fiber surface (Figure 4). Fibrils were faintly discernible, however, in the viscose rayons, particularly in the high-tenacity sample (Figure 6). These differences, aside from being of interest in themselves, illustrate the usefulness of the replica method as a means of observing dissimilarities among fibers and of following changes which they undergo during various stages of processing.

Acknowledgment

The author wishes to acknowledge the help of Mr. A. N. Abbott in preparing the specimens for electron-microscopical examination and in obtaining the micrographs.

Literature Cited

1. Eisenhut, O., and Kuhn, E., *Angew. Chem.* **55**, 198 (1942).
2. Hermans, P. H., TEXTILE RESEARCH JOURNAL, **16**, 545 (1946).
3. Hess, K., *Melliand Textilber.* **24**, 333 (1943).
4. Horio, M., Kobayashi, K., and Kondo, T., TEXTILE RESEARCH JOURNAL **17**, 264 (1947).
5. Husemann, E., *J. makromol. Chem.* [3], **1**, 16 (1943).
6. Husemann, E., *J. makromol. Chem.* [3], **1**, 158 (1944).
7. Jentgen, H., *Kunstseide u. Zellwolle* **23**, 76 (1941).
8. Kinsinger, W. G., and Hock, C. W., *Ind. Eng. Chem.* In press.
9. Kuhn, E., *Melliand Textilber.* **22**, 249 (1941).
10. Morehead, F. F., and Sisson, W. A., TEXTILE RESEARCH JOURNAL **15**, 443 (1945).
11. Roseveare, W. E., Waller, R. C., and Wilson, J. N., TEXTILE RESEARCH JOURNAL **18**, 114 (1948).
12. Schwarz, E. R., TEXTILE RESEARCH **13**, 4 (1943).
13. Wallner, L., *Melliand Textilber.* **23**, 261 (1942).
14. Welch, L. M., Roseveare, W. E., and Mark, H., *Ind. Eng. Chem.* **38**, 580 (1946).
15. Williams, R. C., and Wyckoff, R. W. G., *J. Applied Phys.* **17**, 23 (1946).
16. Wuhrmann, K., Heuberger, A., and Mühlethaler, K., *Experientia* **2**, 105 (1946).

A Microscopical Technique for Determining Latex Distribution in Tire Cords

Ines V. deGruy and Mary L. Rollins

Southern Regional Research Laboratory, New Orleans, Louisiana*

Abstract

A dye-staining technique is described which permits the microscopist to locate the extent of penetration of latex in tire cords. Photomicrographs illustrate the results obtained.

MICROSCOPICAL TECHNIQUES have been successfully employed in the study of tire cord for determining the degree of penetration of rubber into the cord [1, 2]. These methods, however, have not been effective in determining the penetration of latex because of the transparency and lack of color of this dipping material. Embedding and staining of latex-dipped threads and yarns have been reported [4, 5], but the methods used involve procedures which are complicated when applied to routine laboratory tests on plied cords. An investigation of latex-dipped cords has resulted in the development of a simple microscopical technique which may be of interest in

* One of the laboratories of the Bureau of Agricultural and Industrial Chemistry, Agricultural Research Administration, U. S. Department of Agriculture.

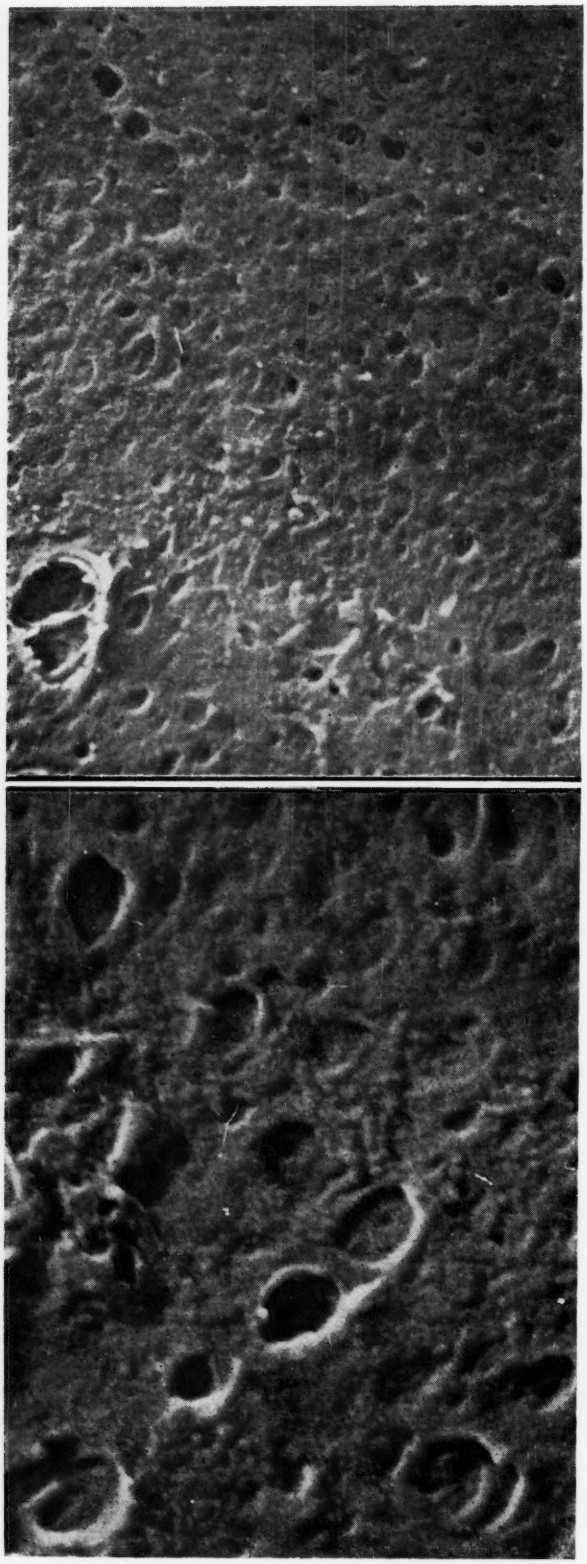

FIG. 6. *Chromium-shadowed nitrocellulose replica of surface of high-tenacity viscose rayon fiber. A (top)—Magnification* × *27,000. B (bottom)—Magnification* × *53,000.*

of the cuprammonium fibers is relatively smooth. On the other hand, the replicas of the viscose rayons are more uneven and reflect a netlike structure. This pattern is more pronounced in the regular textile viscose than in the high-tenacity viscose rayon. It is interesting to note that cuprammonium fibers which, as shown here, have relatively smooth surfaces, are, in general, glossier than viscose rayon fibers.

Previously, in specimens of natural cellulose which had been shadowed with metals or treated with electron stains, a transverse spacing was detected at approximately 150-Å. intervals along the long axis of the fibrils [8]. Although suggestions of a similar structure are shown faintly in some of the micrographs of regenerated cellulose, a pattern as distinct as that in natural cellulose was not obtained. Some of the surface replicas—for example, Figure 6B—likewise give indications of a periodicity. The pattern revealed in the surface of the viscose fibers resembles to a certain extent the network structure recently demonstrated in the surface of regenerated cellulose film [11]. Additional work and a refinement of the experimental technique are required to clearly elucidate the small-scale structure of the rayons which were examined in this investigation.

The breakdown of natural cellulose fibers into fibrils, by the action of chemical or mechanical agents, is well established as a result of numerous optical and electron-microscopical investigations [8]. Indeed, in appropriate specimens, fibrils can be detected in cell walls which have not received specific chemical or mechanical treatments to aid in the delineation of these structures. Although the occurrence of fibrils in artificial fibers has been denied [3, 7, 12, 16], there is increasing evidence that fibrils do occur in certain types of regenerated fibers. Thus, by light microscopy, it has been clearly demonstrated that rayon fibers having high crystallite orientation can, in contrast to unoriented rayons, be separated into fibrils similar to those in cotton and ramie [14]. By means of electron microscopy, several investigators have detected fibril-like structures in certain types of rayon [1, 2, 5, 6, 9, 13]. The breakdown of rayons into fibrils is given additional support from this study. Although somewhat less uniform, these fine fibrils are similar in many respects to those previously observed in chromium-shadowed specimens of natural cellulose fibers [8]. That regenerated cellulose fibers break down into coarse fibrils

distinguishable from that of the cord filaments. These alien fibers serve to fill the extra space in the sectioning device and prevent crushing of the cord. Nylon is more suitable for this purpose than other commercially available synthetics because of its uniformity, unmistakable circularity, and lack of dye affinity. After insertion of the tongue so that the sample is held securely in place, the bundle is trimmed close to the metal with a single-edge razor blade. The bar holding the auxiliary plunger is then attached (Figure 3, lower view) and only one step remains before the sample is ready for sectioning.

In cross-sectioning, the fibers will separate if they are not cemented together with a plastic embedding material. "Neg-O-Lac," * which is normally used at this laboratory since it dries quickly and leaves a clear, flexible film, is not suitable in the present method because it causes bleeding of the stain, thus making detection of the degree of penetration uncertain. The most satisfactory embedding material proved to be a cellulose acetate solution prepared by dissolving 3 grams of cellulose acetate (commercial type, high acetyl) in a solution containing 85 parts of acetone, 15 parts of ethyl alcohol, and 5 parts of ethyl acetate.

Cross sections 3 to 5 microns thick are prepared under a wide-field microscope (magnification 45 ×) in the following manner:

With the thumb screw, the plunger is propelled so as to force the specimen a few microns above the surface of the metal plate. The coating material is applied and, thereafter, each time before sectioning. A safety-razor blade is used for cutting and the sectioning is performed free-hand with a synchronized two-way motion, the blade and the device being moved toward each other simultaneously. A smooth section is obtained if the blade rides on the metal plate and is held at a 45° angle with respect to the sample. After each section has been cut it is mounted in paraffin oil on a glass slide and examined at a magnification of 125 ×. This examination reveals the exact depth of penetration of the latex solids represented by the dark portions shown in Figures 1 and 2. Fibers occurring at the interstices of the plies appear in longitudinal view because of the angle of twist in the cord. Permanent mounts may be prepared by ringing the cover slip with "Neg-O-Lac" or some other suitable varnish medium.

Whereas the chemist measures the amount of latex solids in terms of percentage or take-up, the microscopist, using the technique described here, shows its location in the cord. Thus he may be of assistance by providing a means of studying in detail the effectiveness of chemical treatments.

* Trade name for a nitrocellulose lacquer used in coating negatives as a protection against scratching.

Acknowledgment

The authors wish to thank the members of the laboratory staff, especially the Chemical Properties Section, for their helpful suggestions.

Literature Cited

1. Dieterich, E. O., Estimation of the Degree of Penetration of Rubber into Fabrics, *Ind. Eng. Chem.* **2**, 102–3 (1930).
2. Bailey, T. L. W., Jr., and Rollins, M. L., Some Applications of Microscopy to Cotton Research, TEXTILE RESEARCH **15**, 1–6 (1945).
3. Hardy, J. I., "A Practical Laboratory Method for Making Thin Cross Sections of Fibers," U. S. Department of Agriculture, Circular **378** (1935).
4. Stevens, H. P., Textile Finishes Research, *Rubber Chem. Technol.* **7**, 330–41 (1934).
5. Van Nederveen, G., Impregnation of Cotton Yarns with Latex, *Rubber Chem. Technol.* **15**, 323–31 (1942).

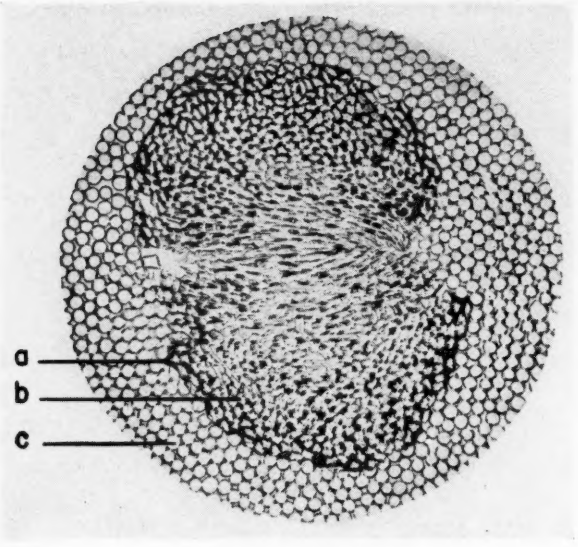

FIG. 1. *Cross section of 2-ply rayon tire cord surrounded by nylon showing (a) latex solids, (b) rayon filaments, (c) nylon filaments. Cord dipped without tension. Magnification 125 ×.*

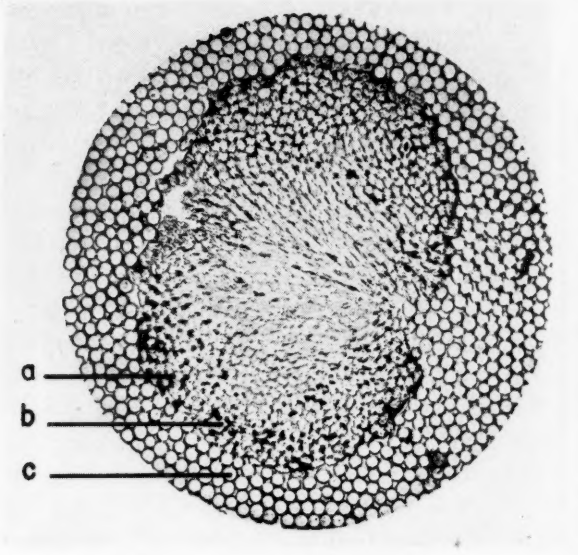

FIG. 2. *Cross section of 2-ply rayon tire cord surrounded by nylon showing (a) latex solids, (b) rayon filaments, (c) nylon filaments. Cord dipped under 150 grams tension. Magnification 125 ×.*

evaluating different latices for cord dipping or various cord constructions for latex adhesion. The procedure involves differential staining and cross-sectioning of the cord to demonstrate the location of latex solids *in situ*.

During the course of investigations on cotton tire cord and its comparison with other tire cords, it was observed in a series of 2-ply rayon cords commercially dipped in latex under varying tensions that the extent of penetration decreased with an increase in tension. Figure 1 represents a cross section of a cord of this series dipped without tension in which the latex has penetrated throughout both plies. Figure 2, representing a cross section of a cord dipped in latex under a tension of 150 grams, shows only partial penetration in the outer edge of the cord.

The sample is prepared for staining by first removing finishing agents having the same dye affinity as latex. This can be accomplished either by extracting or soaking the cord in acetone for 1 hour. It is then immersed overnight in a 0.25-percent solution of Calcogas Red 0.5078 in 95-percent ethyl alcohol. After drying at room temperature the stained sample is carefully rinsed three times in 95-percent ethyl alcohol to remove excess dye and again is allowed to dry.

A hand microtome (Figure 3) is used for sectioning the sample. First introduced by Hardy [3] and modified by Bailey [2], this device consists of two metal plates fitting snugly together when the tongue of one is inserted into the slot of the other. The sample to be sectioned is held in a small circular opening at the base of the slot; a removable auxiliary plunger attached by means of a small screw serves for advancing the bundle.

The sample of cord in the circular opening is surrounded by synthetic fibers of a cross-sectional shape

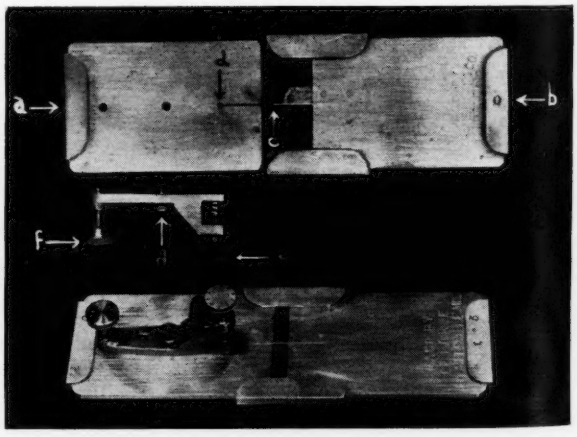

FIG. 3. *Modified Hardy microtome. Upper view shows device unassembled: (a, b) metal plates, (c) tongue, (d) hole for sample, (e) thumb screw for propelling plunger, (f) centering pin, (g) attachment screw. Lower view shows device assembled.*

Book Reviews

Chemical Aspects of Light. E. J. Bowen. 2nd Edition. New York, Oxford University Press, 1946. 200 pages. Price, $6.00.

(Reviewed by M. T. O'Shaughnessy, Polytechnic Institute of Brooklyn)

In the field of textile chemistry there are several general problems in which a knowledge of the nature of light, of the processes of absorption, emission, reflection, refraction, and scattering of light, and of the chemical effects of light absorption are of direct importance. As obvious examples one may mention dyes and dyeing, bleaching, and the photochemical degradation of dyes and of the fiber substance; less obvious but of fundamental interest is the investigation of molecular orientation by measurement of optical birefringence. Greater, however, than this direct interest is the indirect importance to chemists in general of an understanding of the interactions of light and matter. Experiments in this field developed, in the first instance, most of the facts upon which our modern knowledge of the structures and energies of atoms and molecules is based, and there is probably no field of study which is more fruitful in sharpening the individual chemist's insight into the ultimate physical nature of atoms and molecules and of the forces which are responsible both for their stability and, under appropriate conditions, for their reactivity.

This book is a condensed exposition of these portions of the theory of light and of the interactions of light with matter and the effects following upon these interactions which are of most interest to the chemist. It consists of (1) two chapters on physical optics and light sources; (2) a long chapter on the absorption and emission of light by atoms and molecules, followed by another on the transformation of absorbed radiation; and (3) shorter chapters discussing the luminescence of solids, photochemical reactions, photosynthesis, the photographic process, the reaction of the eye to light, photocells, and chemi-luminescence. The method throughout is one of concise verbal exposition with a minimum use of mathematical equations. The chapter on the absorption and emission of light begins with a discussion of the quantum mechanical theory of atomic and molecular structure, profusely illustrated with energy-level diagrams and with diagrams illustrating the nature of the standing waves of electron probability amplitude represented by solutions of the Schrödinger equation for certain simple molecules. The author points out that these diagrams are oversimplifications of a complex subject; the reviewer feels that, as such, they are very suggestive and useful. This same chapter contains an excellent discussion of the absorption of light by resonating organic molecules and a classification of dyes according to the type of resonating system involved. The brief topical chapters convey vivid, if necessarily incomplete, pictures of the state of knowledge in the fields they cover.

The book is as easy to read as the subject permits; it necessarily presupposes considerable physical and chemical knowledge on the part of the reader. The author's purpose appears to have been to convey a maximum of insight into the structure of matter and the interactions of light and matter with a minimum of irrelevant detail, and in this purpose he has, in the reviewer's opinion, succeeded admirably.

The Chemistry and Technology of Waxes. Albin H. Warth. New York, Reinhold Publishing Corporation, 1947. 519 + viii pages. Price, $10.00.

(Reviewed by Raymond A. Pingree and Maurycy Bloch, Warwick Chemical Company)

Here, gathered into a single volume, is a wealth of information covering our present knowledge of the natural and synthetic waxes, waxlike materials, and related compounds. Dr. Warth exhibits an intimate working knowledge of these materials in his broad and intelligent treatment of the subject.

The major portion of the book is devoted to the naturally occurring waxes, which have been grouped under "The Natural Waxes" (vegetable, animal, marine), "Fossil Waxes, Earth Waxes, and Lignite Paraffins," and "Petroleum Waxes."

The first chapter deals with the chemistry of waxes and contains an interesting discussion of the biological formation of the long-chain acids, alcohols, esters and hydrocarbons which go into the building of the wax compounds. Chemical and physical characteristics of practically all of the known compounds which enter into the structure of the natural waxes are listed in several tables.

Biological derivation, sources of supply, and methods of extracting and refining are described at some length. A comprehensive listing of one hundred and twenty-two naturally occurring waxes, from beeswax to tubercle bacillus wax, shows their physical and chemical characteristics, available technical grades, and other pertinent data.

Similar detailed treatment is accorded to the hydrocarbon waxes, which are classified under "Fossil," "Earth," "Lignite Paraffin," and "Petroleum" waxes. Of particular interest in these chapters is the section devoted to the refining and manufacturing techniques employed in the preparation of various types of petroleum waxes.

The field of synthetic waxes is well covered in a chapter describing the chemical structure, methods of preparation, properties, and uses of these compounds. Most of the known synthetic wax types are mentioned, including alkaryl acid amides, alkyl acid amides, polyethylene glycols, polyethylene oxides, chlorinated diphenyl, chlorinated paraffins, montan wax esters, glycol esters, and synthetic paraffins from the Fischer-Tropsch synthesis.

In the chapter "Emulsifiable Waxes" are given the compositions of many commercial preparations of this type and several wax emulsifying agents are mentioned. Included in this same chapter is a short résumé of the preparation, physical properties, and uses of metallic soaps.

Chapter 8 is devoted to a description of standard test methods for determination of physical and chemical characteristics of waxes, including x-ray examination for crystal spacings. Many types of standard test instruments are illustrated.

A wealth of useful information is contained in the final chapter, which examines briefly the multitude of industrial applications involving wax compositions. The types of waxes which enter each field of use are mentioned and many working formulas are given.

The usefulness of this book is multiplied many fold by the excellent bibliography at the end of each chapter, which includes literature references up to 1946, and the complete author and subject indexes at the end.

A few inaccuracies which do not materially detract from the value of the book have been noticed. These include a tabulation on page 8 which shows "b.p." of several materials at "0 mm.," and on page 28 the statement "dihydroxy acids generally result from the saponification of unsaturated fatty acids."

In spite of the few inaccuracies it contains, this book should prove to be a useful reference work to all who are interested in the subject of waxes, for it includes information which heretofore could be obtained only by extensive search of the literature.

The Story Of Wool. William .F. Leggett. New York, Chemical Publishing Company, 1947. 304 pages. Price $5.00.

The author of this book has made a unique contribution to the textile industry in that he has prepared a history of wool from its alleged origin, about 4,000 B.C., to the machine age in England. The book consists of thirty-six chapters and a bibliography and includes the use and the preparation of wool in various countries, such as India, Greece, Assyria, Rome, medieval Italy, Spain, France, England, and America. A chapter is also provided on Australian wool and other chapters on exotic wool, which includes cashmere, mohair, llama, vicuna, alpaca, and other animal fiber. Perhaps the most interesting chapters concern sheep and their ancestors, the Merino sheep, the alteration fleece, wool and its allies, and information on wool and worsted as well as felt. The book does not contain any technological data, as it was not written for that purpose, but is one of a series of histories which include linen, silk, and cotton.

1152*h* (through *Chem. Abstr.* **42**, 1530*g* (Mar. 10, 1948)).

Recent publications on this subject are cited.

Text. Research J. June 1948

End-Effect in Rotational Viscometers

End-effect in rotational viscometers. Charles H. Lindsley and Earl K. Fischer. *J. Applied Phys.* **18**, 988–96 (Nov. 1947).

In the classical equations for the traction on concentric cylinders by a viscous substance, it is assumed that traction on the top and bottom of the inner cylinder (bob) is negligible in comparison with that on the curved surface. In viscometers of practical dimensions, however, it is necessary to compensate for the end-traction or end-effect by adopting one of several expedients in design or by determining the magnitude of the effect and accounting for it in terms of increased length of bob. In the experiments reported in this paper, the method of multiple bobs has been used, and the variation of end-effect with the following factors studied: (1) radius of bob; (2) clearance between cylindrical surfaces; (3) separation between bottom of bob and cup; and (4) viscosity. The magnitude of the end-effect increases with radius and with clearance. For separations at the bottom greater than 1 cm. and for viscosities above 1 poise the end-effect is nearly constant, but must be determined for each cup and bob combination. At lower viscosities the correction must be determined either by calibration with a standard liquid of about the same viscosity as the unknown, or by the multiple-bob method. It is shown that trapping a layer of air beneath the bob is not effective in making the traction on the bottom negligible. The end-effect is almost as large for a bob with an open bottom as for a closed one. When the method of multiple bobs is used, data with an accuracy of $\pm 2\%$ can be obtained without calibration. When the instrument constant is determined with standard liquids or computed from a value for the end-effect previously found, data of somewhat lower accuracy result, but the uncertainty should be within $\pm 5\%$. Authors

Text. Research J. June 1948

Wetting Time Test

Wetting of textiles. Practical tests with different types of fabrics. Peter Fink. *Tids. Textilteknik* **5**, 65–7 (July–Aug. 1947).

A simple, rapid method for investigating wetting agents for fabrics consists in placing a fabric sample 3 cm. in diameter into a funnel 6 cm. in diameter, then turning the latter upside down and placing it into a beaker containing 500–600 cc. of a wetting-agent so that the sample remains pressed down below the surface of the liquid. The wetting power of the product is determined by the time which passes until the fabric sinks down, measured by a stop watch. For fair accuracy these time intervals must lie within 0.20–2 min. and this can be achieved by use of a concentration corresponding to 2 g. Igepon T, 200% per liter.

Text. Research J. June 1948 Ilse Zeise

X-Ray Diffraction

Self-printing x-ray diffraction interplanar scale. A. P. DeBretteville, Jr. and S. Benedict Levin. *Rev. Sci. Instruments* **19**, 120–1 (Feb. 1948).

An instrument is described which prints an interplanar scale in angstrom units on $\frac{1}{2}$ of an x-ray diffraction photograph while the sample is being x-rayed in a Debye-Scherrer camera. The energy for the printing comes from the scattered radiation in the camera. An approximate value of interplanar spacings of the x-ray diffraction rings is obtained by inspection of the photograph. L. P. Witnauer

Text. Research J. June 1948

A means of eliminating "paper grain" from x-ray diffraction films. Karl E. Beu. *Rev. Sci. Instruments* **18**, 453 (June 1947).

Using fogged Kodalith instead of black paper to protect film from light fogging during x-ray diffraction exposures, the author observed that the background irregularity was much less. L. P. Witnauer

Text. Research J. June 1948

Tackiness Meter

An improved tackiness meter. Joseph M. Lambert and Richard A. McDonald. *Rev. Sci. Instruments* **19**, 119–20 (Feb. 1948).

An improved tackiness meter with which the actual tack measurement is performed automatically is described. The tackiness meter has been used to give a quantitative measure of the difference in "tack" exhibited by several polyvinyl ethers. L. P. Witnauer

Text. Research J. June 1948

CHEMICAL AND PHYSICAL RESEARCH

★

Equilibrium Adsorption Isotherms

The heats of reaction and affinities of direct cotton dyes for cuprammonium rayon, viscose rayon, and cotton. W. J. Marshall and R. H. Peters. *J. Soc. Dyers and Colourists* **63**, 446–61 (Dec. 1947).

Equilibrium adsorption isotherms for 14 direct cotton dyes have been determined in the presence of sodium chloride on cuprammonium and viscose rayons, cotton, and mercerized cotton at temperatures ranging from 50°C to 100°C. The standard free energy changes (or affinities) of dyeing have been calculated by the thermodynamic treatment of Peters and Vickerstaff. The treatment gives good agreement with experiment at all the temperatures investigated in the case of 6 dyes, agreement at the higher temperatures with only 5 dyes, and poor agreement at all temperatures with the remaining 3 dyes. The deviations are ascribed to aggregation of the dyes in solution. From these results, heats of dyeing and entropy changes have been calculated. The

ABSTRACTS

SERVICES AVAILABLE

Reprints of the original articles abstracted in TEXTILE RESEARCH JOURNAL *are often available from the publishers. Otherwise, it may be possible to secure copies of the periodicals. Orders should be sent direct to the publishers.*

Photostat negatives of articles abstracted will be furnished to members of the Institute at a cost of 25 cents per page for pages not exceeding 7 inches in width and 50 cents per page for larger sizes up to 11½ x 14 inches. Photostats of patents are 50 cents per page. The library's service charge will be added.

Microfilm copies and paper enlargements of microfilm may be obtained from: Microfilms Inc., 313 N. First St., Ann Arbor, Mich.; New York Public Library, New York, N. Y.; Yale University Library, New Haven, Conn.; Harvard University Library, Cambridge, Mass.; and Library of Congress, Washington, D. C. Translations may also be obtained from the above sources.

The JOURNAL *is again offering to its subscribers reprints of the Abstracts and Book Reviews sections, printed on one side of the sheet so that the items may be clipped, pasted on cards, and filed for permanent reference. Subscriptions to this service for 1948 are $3.00 each. Orders for this special service should be mailed at once to Textile Research Institute, Inc., 10 East 40th Street, New York 16, N. Y.*

A list of periodicals abstracted, the abbreviations used in references to articles, and the addresses of publishers of English language publications is given in the January, 1948, issue, page 48.

ANALYSIS: TESTING: LABORATORY METHODS

★

Dielectric Measurements

Resonant cavities for dielectric measurements. C. N. Works. *J. Applied Phys.* **18**, 605–12 (July 1947).

For the measurement of dielectric constant and dissipation factor in the frequency range of 100–1,000 megacycles, a fixed and variable length re-entrant resonant cavity is described. Applying the susceptance variation method to these cavities results in a rapid measuring technique with simple relations for calculating the values of the dielectric properties. The sensitivity of the cavities is so great that very small disc-shaped samples can be used. The results of the measurements of a few typical dielectrics are given. L. P. Witnauer

Text. Research J. June 1948

Electronic Computer

An electronic computer for x-ray crystal-structure analyses. R. Pepinsky. *J. Applied Phys.* **18**, 601–04 (July 1947).

An electronic computer is described which when coupled to a cathode-ray oscillograph produces a visual presentation of the atoms in a crystal structure. The computer sums the two-dimensional Fourier series representing the projection on a lattice plane of electron densities in a crystal unit cell and has the great advantage of immediately observing the effects of change in signs of one or any number of Fourier coefficients on the projection. L. P. Witnauer

Text. Research J. June 1948

Test for Glucuronic Acid

A specific color reaction for glucuronic acid. Zacharias Dische. *J. Biol. Chem.* **171**, 725–30 (1947) (through *Chem. Abstr.* **42**, 1847*b* (Mar. 20, 1948)).

A specific color test for glucuronic acid is described. Mannose and glucuronic acid are made to react in concentrated H_2SO_4 solution with a solution of thioglycolic acid. A deep pink color develops; in the absence of glucuronic acid a greenish-yellow color results. The pink color developed in the presence of an excess of mannose is specific but may be mistaken for the pink color produced with pentoses. The color should be measured in a spectrophotometer.

Text. Research J. June 1948

Molecular-Weight Distribution

A suggested new method of determining molecular-weight distribution. Francis Breazeale. *J. Polymer Sci.* **3**, 141–2 (Feb. 1948).

The decrease in viscosity of solutions of macromolecules with increasing velocity gradient is caused by (1) solute molecular orientation to positions parallel to the direction of flow; (2) lessening of tritanglement or bonding of solute molecules. Since the size and dimensional ratios of the macromolecules influence both of these, it is concluded that the viscosity gradient-viscosity relationship should be related to the molecular-weight distribution. A scheme for determining molecular-weight distribution of high polymer from velocity gradient-viscosity data is given. E. D. Klug

Text. Research J. June 1948

Monosaccharides from Cellulose

Analysis of mixtures of monosaccharides obtained in the hydrolysis of cellulose and related products. A. Roudier. *Chim. anal.* **29**, 279 (1947); cf. *C.A.* **42**, 489*b*,

Polyacrylonitrile

Synthetic fibers. II. Hydrolysis of acrylonitrile with caustic soda. Yasumi Mamiya. *J. Soc. Chem. Ind. Japan* **44**, 860–2 (1941); cf. *C.A.* **38**, 3481[8] (through *Chem. Abstr.* **42**, 2108*e* (Mar. 20, 1948)).

To improve the resistance of polyacrylonitrile fiber to alkaline solution, the reaction velocities of saponification of acrylonitrile with NaOH were determined. The results satisfy the relation $K = x/ta(a - x)$, where a is the initial concentration in mol./l. of nitrile or NaOH, and x is molecule of NH_3 liberated in t min.; thus, in the presence of H_2O, a bimolecular reaction takes place between acrylonitrile and NaOH to form Na acrylate and NH_3. The values of K calculated for 60°, 80°, and 100° are 0.00686, 0.0402, and 0.182, respectively. The activation energy ΔH for the hydrolysis calculated according to the Arrhenius equation $R \ln K_1/K_2 = -H(1/T_1 - 1/T_2)$ is 20,300 cal./mol. which is much greater than ΔH = 3,500 cal./mol. for the hydrolysis of propionitrile by KOH calculated from the data obtained by Peskoff and Meyers (*C.A.* **7**, 1652). Hence the C≡N bond in acrylonitrile is stronger than in propionitrile.

Text. Research J. June 1948

Polymeric Amides

Polymeric amides from omega-amino acids. D. D. Coffman, N. L. Cox, E. L. Martin, W. E. Mochel, and F. J. Van Natta. *J. Polymer Sci.* **3**, 85–95 (Feb. 1948).

The preparation of fiber-forming polymeric amides by condensing ω-amino acids, the corresponding amino acid, the amino ester, the amino nitrile, the *N*-formyl amino acid, and the lactam is described. Methods of preparing the monomer are given in many cases.

Text. Research J. June 1948 E. D. Klug

Hydrolysis of Soap

The hydrolysis of soap solutions. II. The solubilities of higher fatty acids. Lucille M. John and James W. McBain. *J. Am. Oil Chemists Soc.* **25**, 40–1 (Feb. 1948).

The solubilities of capric, lauric, myristic, palmitic, and stearic acids in water at 25° and 50°C were determined by use of conductivity measurements. Correction was made for carbon dioxide; and total solubilities, together with the concentration of dissociated and of undissociated acid, were calculated. Their solubilities range from 359×10^{-6} M for capric acid to 2.1×10^{-6} M for stearic acid at 25°C. The solubility of lauric and myristic acids is approximately doubled by an increase in temperature from 25° to 50°C; that of capric, palmitic, and stearic acids increases by 25 to 40%.

Text. Research J. June 1948 Authors

The hydrolysis of soap solutions. III. Values of pH and the absence of fatty acid as free liquid or solid. James W. McBain, P. Laurent, and Lucille M. John. *J. Am. Oil Chemists Soc.* **25**, 77–84 (Mar. 1948).

The pH of the laurates, myristates, palmitates, and stearates of sodium and potassium at 25° and 50°C was determined by use of a glass electrode. pH: concentration curves were constructed, and hydroxyl ion activity was calculated. In general the concentration of hydroxyl ion ranges from 0.001 to 0.0001N; for the less dilute solutions of the higher soaps, the upper limit is exceeded by several fold, and in the more dilute solutions the concentration may fall beneath the lower value. Solubilized hexane reduced the pH of potassium and sodium laurate only very slightly. Potassium or sodium chloride reduced the pH of soap solutions over a certain range but caused a slight increase in a narrow intermediate range. Using the pH values obtained, the actual concentration of fatty acid in the soap solutions was calculated, and was found to be less than the saturation concentrations obtained by conductivity measurements through the entire range investigated. Free fatty acid therefore never separates as such from pure soap solutions unless acted upon by excess of acid such as carbon dioxide. Percentage hydrolysis was calculated and curves were constructed. In general, the potassium soaps are hydrolyzed more than the corresponding sodium soaps; the difference is slight for the laurates but is considerably greater for the myristates, palmitates, and stearates in higher concentrations at 25°C. The difference is appreciably smaller at 50° than at 25°C. Percentage hydrolysis for the laurates is very much less than for the higher soaps. Authors

Text. Research J. June 1948

The hydrolysis of soap solutions. IV. The composition of acid potassium laurates and acid sodium oleates as determined by conductivity measurements. Lucille M. John and James W. McBain. *J. Am. Oil Chemists Soc.* **25**, 141–3 (Apr. 1948).

The effect of excess lauric and oleic acids on the conductivity and on the pH of 0.2–0.02N potassium laurate and 0.1–0.01N sodium oleate systems was observed. The decrease in the specific conductivity corresponded with the formation of the acid soaps, 2KL·HL, KL·HL, 2NaOl·HOl, NaOl·HOl, and the mixed soaps 2KL·HOl and 2NaOl·HL. The mixed soaps resemble the oleates in appearance. All of these systems, even with 100 or 150 moles percent excess acid, were slightly alkaline. Authors

Text. Research J. June 1948

Starch Chemistry

Starch. XXXV. Degradation of amylose by α-amylase. P. Bernfeld and H. Studer-Pécha. *Helv. Chim. Acta* **30**, 1895–1903 (1947) (through *Chem. Abstr.* **42**, 931*g* (Feb. 10, 1948)).

The findings of Myrbäck (*C.A.* **37**, 5884[5], 4270[9]) contradict results obtained by K. H. Meyer earlier in this series of papers. The present paper affords evidence to harmonize these differences. It is shown that a competition is involved between the hydrolysis of amylose by α-amylase and the ageing of the amylose in solution to α-amylase-resistant

affinities and heat of reaction of any one dye are approximately the same on all 4 fibers, which fact supports the hypothesis that the mode of attachment of the dye to all the fibers is the same. Therefore, the energetics of the process are the same and the difference in dyeing behavior must be accounted for by purely physical differences between fibers. The results are consistent with the view that the dye is attached to the cellulose by hydrogen bonds and the magnitude of the heats of reaction (10–30 kg. cal.) suggests that at least 2 such bonds are involved. Authors

Text. Research J. June 1948

Dyeing of Wool

The chemistry of wool and its importance for the textile industry. Bailli Nilssen. *Textilteknik* **5**, 101–8 (Nov. 1947).

The chemistry of wool keratin is discussed on the basis of the theory of W. T. Astbury and J. B. Speakman, with respect to its importance to the various textile-chemical processes, in particular to dyeing and milling. Two new possibilities of dyeing wool are suggested. Amino and carboxyl groups, as well as a number of other groups contained in wool, offer the possibility of binding dyes, not only by ionogen bonds but also with formation of direct homopolar compounds; e.g., wool keratin combines with diazonium salt, forming dyed compounds. This dyeing is due to the combination of the oxyphenyl group of tyrosine with the diazonium salt.

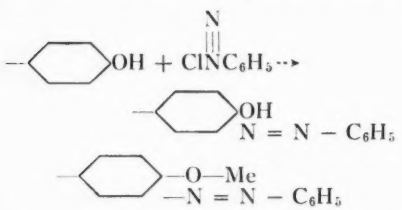

When the *p*-position is occupied, the combination will give *o*-oxyazo compounds, which can be subjected to an after-treatment with metals, some of which give improved fastness properties. Another possibility is the reaction of tyrosine radicals with HNO_2 with formation of an *o*-nitrosophenol group, which also reacts with different metal ions, forming complex compounds.

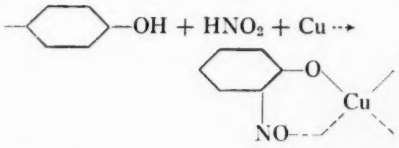

Since this group occupies only 2 of the 4 or 6 coordination valences of the metal atom, it is possible to vary the dyeing to a much greater extent with the use of other complex components. Mordant dyes can also be used. The method seems economical since a full depth of dyeing is obtained and toning with small amounts of mordant dye yields almost any desired shade. Ilse Zeise

Text. Research J. June 1948

Fracture Statistics

Statistical aspects of fracture problems. Benjamin Epstein. *J. Applied Phys.* **19**, 140–7 (Feb. 1948).

In recent years there has been an increasing interest in the development of statistical theories of strength mainly to explain such phenomena as the dependence of the strength of specimens on their volume or length. In this paper it is pointed out that the problems posed by these models are equivalent to an important problem in mathematical statistics; namely, the distribution of the smallest value in samples of size n drawn from a population having some probability density function $f(x)$. The calculations made by mathematical statisticians give a far more complete description of the results to be expected than do the estimates to be found in the technical literature. Author

Text. Research J. June 1948

Cellulose Glycolates

Some applications of ultracentrifugation to the study of salts of celluloseglycolic acids. M. Banderet. *J. chim. phys.* **44**, 52 (1947) (through *Chem. Abstr.* **42**, 1479*h* (Mar. 10, 1948)).

Two samples of an aqueous solution of commercial Na celluloseglycolate (in 2*N* NaCl) containing approximately 0.9—OCH_2CO_2Na group per glucose residue were precipitated ultracentrifugally. The solution, down to 0.1% solute, consists of a micellar portion suspended in a molecularly dispersed, nonprecipitable portion; both have the same glucose:glycolate ratio. From the constants of sedimentation and diffusion the degree of polymerization of the nonprecipitable fraction is calculated to be 336 and 725 for the 2 samples. The ratio of the coefficient of friction of the molecules to that of spherical molecules of the same mass is 3.9 and 4.1, respectively, for the same 2 samples. When the samples were completely solubilized by forming the nitrate esters, the degree of polymerization in each case was the same order of size as that of the nonprecipitable fraction; hence the micelles must be composed of aggregates of the smaller particles. The η was also determined and the limiting η at 0 concentration was calculated.

Text. Research J. June 1948

Nylon Raw Materials

Raw materials for synthetic fiber. I. Preparation of sebacic acid and decamethylenediamine from castor oil. Kiichiro Sugino, Hiroshi Murotani, Keijiro Odo, and Mutsuo Tachika. *J. Soc. Chem. Ind. Japan* **44**, 706–8 (1941) (through *Chem. Abstr.* **42**, 2108*c* (Mar. 20, 1948)).

Na ricinoleate, obtained almost quantitatively by saponification of castor oil, fused with 40–60% of KOH gave 41% of the theoretical yield of sebacic acid (the yield was based on the assumption that castor oil consists entirely of ricinoleic acid glyceride). The acid was converted to the chloride by $POCl_3$, and the chloride treated with NH_4OH gave the diamide in 86% yield. The diamide was converted to the dinitride in 73% yield (by means of PCl_5), and the dinitrile reduced with Na to the diamine, and this gave the dihydrochloride in 75% yield. Equimolecular quantities of the diamine and sebacic acid heated at 200°C in *N* gave a polyamide that could be drawn to a fiber.

Text. Research J. June 1948

in vitro by heating the solution with dilute acids, but this restoration was not successful with dyed textiles. The sensitivity of dyes to alkalies is connected with their structure, especially for compounds containing nitro groups located near azo groups. Compounds with nitro groups in the meta and para positions generally darken; *o*-nitro derivatives become lighter than the original color. The same observations were made on naphthol AS, naphthol AS-D, and naphthol AS-BO, even if bound to various diazotized bases. The results do not seem to affirm the quinoid structure. Probably the theory of Radulescu-Alexa is correct, the possible explanation being that nitro groups change the quinone hydrazones to hydroxy azo compounds, and simultaneously increase the alkali-binding capacity, as observed in the case of nitrated phenols.

Text. Research J. June 1948

Natural Dyes

Natural dyes and synthetic dyes applied to wool. A. M. Baron. *Teintex* **12**, 400 (1947) (through *Chem. Abstr.* **42**, 1739*g* (Mar. 10, 1948)).

Synthetic vat dyes are superior to natural indigo and madder. Cochineal is fast to light but sensitive to alkali; alizarin dyes are fast to washing.

Text. Research J. June 1948

Garment Dyeing

Processes and hints regarding the scouring and dyeing of clothes containing cellulose acetate. Paul Joly. *Teintex* **12**, 371 (1947) (through *Chem. Abstr.* **42**, 1740*i* (Mar. 10, 1948)).

Discussion of several hints resulting from careful studies and daily usage at the "Atelier d'applications des sociétés Rhodiacéta et Tubize."

Text. Research J. June 1948

Viscose Rayon Dyeing

Some factors affecting the dyeing of viscose rayon. Parts I and II. J. M. Preston, P. Pal, and A. H. Kapadia. *J. Soc. Dyers and Colourists* **63**, 430–8 (Dec. 1947).

Various changes in the structure and treatments of viscose rayon fibers are found to vary the rates of dyeing. These rates vary directly as the available surface and inversely as the degree of orientation. Some viscose fibers which show marked differences in rates of dyeing show insignificant differences in the equilibrium dyeing values. The orientation of the cellulose molecules in viscose rayon fibers is shown to affect both the rate of dyeing and the equilibrium dye uptake. Authors

Text. Research J. June 1948

Dyeing Properties on Chlorinated Wool

The dyeing properties of chlorinated wool. J. Barritt and F. F. Elsworth. *J. Soc. Dyers and Colourists* **64**, 19–33 (Jan. 1948).

Modification of the surface structure of wool fibers which occurs on chlorination renders the fiber more accessible to penetration by dye molecules and dye aggregates, which in turn results in the different behavior of chlorinated wool in dyeing. When applied under the conditions normally used for their application to unchlorinated wool, most dyes are taken up more rapidly by chlorinated wool; secondly, chlorinated wool absorbs dyes under conditions which would not be suitable for their application to unchlorinated wool. Thus, chlorinated wool takes up, under neutral conditions, metalliferous dyes, many direct cotton dyes not absorbed by unchlorinated wool, and certain chrome dyes which cannot normally be applied by the metachrome method. The colloidal acid dyes are taken up much more readily at lower temperatures. Determination of the total combining capacity of wool and chlorinated wool for acid and acid dyes indicates that chlorination does not increase the basic properties of the wool. With metachrome dyes it is shown that there is a definite correlation between dyeing properties and chemical constitution. Thus, sulfonated metachrome dyes are taken up by chlorinated wool more rapidly than they are by unchlorinated wool, whereas nonsulfonated metachrome dyes are taken up very rapidly and at the same rate by both types of wool. When dyed on chlorinated wool, the fastness to wet treatments of most wool dyes tends to be lower than when they are dyed on unchlorinated wool. With acid dyes of the level-dyeing type the loss in fastness is appreciable, but with the faster types, e.g., chrome dyes and metalliferous dyes, the change in fastness properties is negligible. No significant change has been observed in the fastness to light. Methods for the production of tone-in-tone and two-color effects by piece-dyeing material containing wool and chlorinated wool are reviewed in detail.

Text. Research J. June 1948 Authors

American Dyeing Practice

Modern American dyeing practice. H. F. Clapham. *J. Soc. Dyers and Colourists* **63**, 469–72 (Dec. 1947).

In modern American dyeing practice, practically all the changes that have been made have been aimed at improving quality or increasing production. Volume production tends to decrease costs and thereby increase markets, whereas improved quality heightens customer satisfaction, which also broadens the market. Outstanding in American practice is the trend towards continuous processing. Improvements in the continuous dyeing methods for vat and sulfur dyes, characterized by the development of the pad-steam technique, have resulted in greatly increased use of continuous processes. The multi-lap machine promises to fulfill a similar requirement for wool, synthetic fiber, and union dyeing. In general, the dyeing of loose fibers and yarn tends strongly towards the use of pressure-type dyeing machines. All of these methods are directed toward decreasing man-power requirements and thereby reducing costs, and at the same time increasing production and consumption of high-grade textiles. Authors

Text. Research J. June 1948

particles. This explains the dependence of the extent of scission on the concentration of the enzyme.
Text. Research J. June 1948

Constitution of Starch

Some points on the constitution of starch. R. Sutra. *Bull. soc. chim. biol.* **29**, 221–31 (1947) (through *Chem. Abstr.* **42**, 1752*h* (Mar. 10, 1948)).

From the experimental data of author and others cited, it is concluded that starch is a homogeneous substance and that the substances called amylose and amylopectin are degradation products; that the methylation method is not suitable for determining the length of the chains or the kind of branching, if any; that the common conceptions of straight chains and branched chains in starch molecules are only interpretations; that starch can be completely converted to maltose by amylases under suitable conditions; and that root starch and seed starch are different types of starch. Other commonly accepted ideas are disputed. 35 references.
Text. Research J. June 1948

Swelling and Solution of Viscose

The swelling and solution mechanism of xanthated soda cellulose fibers. W. Schramek and Annelies Stenzel. *Melliand Textilber.* **28**, 383–8 (1947) (through *Chem. Abstr.* **42**, 2100*d* (Mar. 20, 1948)).

Photomicrographs are reproduced of Sedura, Vistra HB, normal B-staple rayon, Duraflox, Schwarza W 1, Lanusa, Cuprama, and an experimental spun fiber. An attempt is made to find relationships between fiber properties, fiber structure, and spinning conditions. During storage, the viscosity of a freshly prepared viscose solution decreases, remains stationary for a brief period, and then increases rapidly. It is assumed that, in the freshly prepared cellulose solution, the final distribution of the native cellulose aggregates has not taken place, and that after it does occur large cellulose aggregates are formed. The decrease and increase of viscosity show a chemical degradation of cellulose xanthate. During the regeneration of the cellulose molecules from the xanthate, these molecules regain their aggregation powers. Technical viscose represents a micellar dispersed state of aggregation of cellulose containing varying amounts of primary and secondary aggregates. The possibility of a fundamental difference between such aggregates is discussed. The undestroyed native fiber is broken up first into fragments with fracture surface running nearly vertical to the fiber axis. Then the decomposition of the fragments takes place along a direction approximately parallel to the fiber axis (probably preceded by interfibril or intercrystalline cleavage) and also parallel to the molecular crystallite longitudinal axes. Afterwards, cross-sectional cleavages are possible, producing not only long fibril sections that become progressively thinner but also sections that become progressively shorter. These new cross-sectional cleavages can lead to new longitudinal cleavages which finally lead up practically to the formation of separate molecules. The disappearance of x-ray diagrams during the dissolving of cellulose xanthate is no proof for the molecular solution of cellulose. Since the dissolving process does not cause an essential shortening of the molecules and the decomposed product has very few still-connected molecules, it appears that the primary particles must correspond to the dimensions of the molecules (1,000 and 1,500 Å. long, 15 Å. broad, and 5 Å. thick) and consist of flat rods or ribbons whose long boundary planes represent true crystalline cleavage planes. It is very probable that only very few and proportionally short molecular pieces project from the ends of these very long ribbons. Reaggregation possibilities of cellulose particles in viscose and the formation of supermolecular structure in spun fibers are discussed. The primary aggregates are considered to be the basis for the formation of secondary conglomerations.
Text. Research J. June 1948

BLEACHING: DYEING: FINISHING

★

Continuous Bleaching

Continuous bleaching of cotton cloth. Georges Mairesse. *Teintex* **12**, 410 (1947) (through *Chem. Abstr.* **42**, 1742*a* (Mar. 10, 1948)).

A description of equipment used for continuous bleaching of cotton cloth.
Text. Research J. June 1948

Bleaching Animal Fibers

The bleaching of animal fibers by modern methods. M. H. Wilkinson. *J. Soc. Dyers and Colourists* **64**, 8–13 (Jan. 1948).

Hydrogen peroxide bleaching of wool and silk is discussed and formulas are given. The importance of pH+, temperature, volumetric and time controls is stressed. Borax is suggested for use as a buffer. The bleaching of pigmented fibers such as alpaca, cow hair, etc. in a peroxide bleach without a mordant and with hot and cold iron sulfate mordant baths indicates considerable progress with these types of fibers.

J. A. Woodruff
Text. Research J. June 1948

Aniline Black

The significance, from the point of view of research technique and industrial history, of aniline black in textile printing and dyeing. Rudolf de Dax. *Monatsschr. Textil-Ind.* **56**, 45–8, 72–4, 109–12, 131–2 (1941) (through *Chem. Abstr.* **42**, 1428*i* (Feb. 20, 1948)).
Text. Research J. June 1948

Naphthol AS Dyes

Alkali sensitivity of developed naphthol AS dyes containing nitro groups. Zoltán Csuros. *Magyar Chem. Folyóirat* **50**, 25–33 (1944) (through *Chem. Abstr.* **42**, 1057*h* (Feb. 10, 1948)).

Most ice colors undergo color changes in the presence of dilute (even 5%) solutions of Na_2CO_3. The original color could be restored

equivalent all-worsted yarn. In terms of count this means that fabrics can be woven on power looms with a single 70s worsted number in the warp. Advantages of blending nylon and wool during spinning are discussed. L. A. Fiori

Text. Research J. June 1948

End Breakage in Spinning

The spinning end-breakage test and some typical results. A. F. Coulson. *J. Text. Inst.* **38**, P535–48 (Dec. 1947).

This discussion deals with the development of an end-breakage test which could be made to show how spinning performance varies with spindle speed, traveler size and type, type of ring, twist in roving, new and run-in rings, and other factors. Information derived from this test results in the scientific fixing of work loads since it evaluates the frequency of occurrence of each type of end breakage. General conclusions are: (1) the average of the breaks per 100 spindles per hr. taken over the doff varies from a low of about 2.5 to a high of 15, and (2) the end-breakage rate tends to be higher for fine counts than for coarse counts, but a rate of 6 to 8 would be acceptable for 30s and a rate of 3 to 5 for 12s. The comparison of specially black-coated rings and brightly polished rings showed that for the first month of its life the former gave better performance but after that the position reversed itself and the latter yielded a slightly lower number of end breaks. Over a longer period (3 mos.) there was no significant difference in the performance of the 2 rings. End-breakage rate increases with spindle speed, slowly at first, but rapidly after a certain critical speed is reached. The standard traveler on a 1½ flange ring gave good results, indicating that the use of other special travelers, such as the elliptical, would not be much advantage. Results show that new rings give consistently higher end-breakage rates than run-in (old) rings. At the end of a 6-mo. test period, the old rings still gave better performance. An unexpected result is that at the same spindle speed the larger lift ring frame gave a lower end-breakage rate than the smaller frame. A 5% reduction in roving twist gave a 51% improvement in spinning. Detailed statistical charts and graphs illustrating the characteristics of the end-breakage curve are included. It is pointed out that it takes from 2 to 5 yrs. to "break in" new rings and that there was no correlation between ends down and relative humidity, although the moisture content in the roving might conceivably mask this correlation. L. A. Fiori

Text. Research J. June 1948

An analysis of technical factors controlling spinning breaks at the ring frame. F. Charnley. *J. Text. Inst.* **38**, P556–60 (Dec. 1947).

Lack of yarn uniformity caused by inherent drafting waves of the textile fibers that make up the length of yarn between the drafting rollers and the bobbin is responsible for increasing the tension at this point to a degree exceeding the breaking strength of the yarn. Factors which affect thread tension at the ring frame for a given count are: spindle speed, ratio of ring diameter to bobbin diameter, type and weight of traveler, and the condition of the ring. Spinning breakages are more numerous with higher ring spindle speeds. At spindle speeds of 7,000, 8,000, 9,000, and 10,000 the breakage rates were 1.6, 2.2, 6.9, and 9.2, respectively, per 100 spindles per hr. To minimize tension when winding on to the bare bobbin, bobbin diameter is usually chosen in relation to the ring diameter so that the path of the yarn between traveler and bobbin makes an angle of not less than about 27° with the radius. Traveler speed has an upper limit of 80 ft. per sec. The C-shaped traveler is the one most universally used. The bow-diameter traveler was found to be not important in fine counts but beneficial in reducing end breakage in coarse counts. Highly polished rings are desirable. Worn or rusty rings caused excessive spinning breakages. The fundamental causes of yarn irregularity which affect tension—namely, the cotton itself, roller settings employed, quality of carding, and the presence of mechanical defects—are analyzed. Also reviewed are the miscellaneous causes of end breakage such as temperature and humidity, creel packages, and clearer waste.

Text. Research J. June 1948 L. A. Fiori

End breakages at the ring frame. Their effect on P.M.H. James Baines. *J. Text. Inst.* **38**, P549–55 (Dec. 1947).

The factors influencing the number of spindles which can be operated by a ring spinner are discussed. The relative importance of these factors are illustrated with the aid of data taken from work studies. It is shown that P.M.H. (production per man hour) at the ring spinning process may possibly be increased by (1) introducing larger creel packages which would not only reduce the total work of the spinner but would save 7.46% of the total work load, (2) providing auxiliary labor to perform the cleaning and oiling duties, and (3) maintaining the rate of end breakages below 30 per 1,000 spindles. Based on a reduction of the end-breakage rate from 100 to 30 per 1,000 spindle hrs., a 48% increase in P.M.H. is possible.

Text. Research J. June 1948 L. A. Fiori

Some factors affecting end breakage in ring spinning. J. U. Steiger. *J. Text. Inst.* **38**, P561–75 (Dec. 1947).

In order to save time in determining the causes of end breakages by direct observation, the following methods of investigation were found to be useful: (1) examination of the broken end, (2) recording the location of the breaks, (3) use of a yarn tension meter, and (4) variation of speeds, settings, etc. Summarized in table form are detailed observations of a ring spinning frame spinning 32s, spindle r.p.m. of 9,000, hank roving 4.5, and in which occurrences were 62 with 75 breaks per 1,000 spindle hrs. Broken roving accounts for 2 broken ends, roller laps for 10, traveler-off for 1, after doffs for 5, hard ends for 14, thin places for 11, and other factors for 33. In spite of careful examination,

Research in Dyeing and Finishing

Basic research in the coloring and finishing of textiles. M. L. Crossley. *Papers of AATT* **3**, 9–17 (Dec. 1947).

A brief discussion of the use of laboratory apparatus such as the Dyeometer and optical microscopes in the study of dyeing and finishing practices. J. A. Woodruff

Text. Research J. June 1948

Screen Printing by the Urea Process

Some suggestions for screen printing by the urea process. J. H. Bingham. *Textile Age* **2**, 82, 84–7 (Feb. 1948).

A commentary on the methods and practices developed for screen printing synthetic fibers by the urea process. The types of dyes which may be used successfully are described. A. L. Landau

Text. Research J. June 1948

Textile Drying Methods

Textile drying methods compared. Anon. *Am. Wool and Cotton Reptr.* **6**, 11–12 (Feb. 5, 1948).

Evaporation, or drying, is affected by the temperature, humidity, velocity of circulation of the air, and by the characteristics of the material being dried. Heat for drying may be supplied by contact, air flow, or radiation. Infrared drying is most useful as a predrying agent in front of existing machinery, as there is little penetration. High-frequency drying is electrical drying accomplished by passing an electrical current through the material to be dried. This raises the temperature throughout the material and causes the moisture to migrate to the surface of the fabric, whence it is removed by an air current.

A. L. Landau

Text. Research J. June 1948

Waterproofing Rayon

Chemicals for textile treatment. I. Hexadecyl 3-hydroxy-2-naphthoate. Yoshibumi Oshima and Mosuke Hayashi. *J. Soc. Chem. Ind. Japan* **44**, 821–2 (1941) (through *Chem. Abstr.* **42**, 2108*g* (Mar. 20, 1948)).

Hexadecyl 3-hydroxy-2-naphthoate, greenish-white flaky crystals, melting at 72°–3°C, soluble in C_6H_6, glacial AcOH, and petroleum ether, sparingly soluble in cold EtOH, insoluble in H_2O, was prepared by action of cetyl alcohol on 3 - hydroxy - 2 - naphthoyl chloride (from the acid and $SOCl_2$). The ester applied to rayon in quantities of 10% or more is a good waterproofing agent. The ethyl and dodecyl esters of the same acid had little or no waterproofing effect.

Text. Research J. June 1948

FIBERS: YARNS: FABRICS: MECHANICAL PROCESSES

★

Fancy Yarns

Fancy yarns and furnishing fabrics. Anon. *Textile Weekly* **41**, 532 (Mar. 19, 1948).

Described briefly are background details for dyeing, designing, and weaving procedures when using fancy yarns. L. A. Fiori

Text. Research J. June 1948

Ply-Yarns

Conditions for maximum lustre and maximum strength of ply-yarns. B. K. Chakrabarti. *Indian Text. J.* **58**, 241–4 (Dec. 1947).

In this report an attempt has been made to arrive, from theoretical considerations, at the conditions for maximum luster and maximum strength of ply-yarns having not more than 6 components, with special reference to jute yarns. Formulas are given for final twist in single yarns after doubling, for maximum luster, and for maximum strength. These relations are true only when the "take-up" is small. Details of the effect of this "take-up" and other relevant points will be published later. Mathematical derivations, proofs, and theories substantiating the formulas are given; also a practical illustration of the application of the formulas.

Text. Research J. June 1948 L. A. Fiori

Vinyon N Yarn

Vinyon N yarns revealed. Anon. *Textile Age* **12**, 44–8, 50, 51 (Mar. 1948).

Vinyon N yarn is manufactured from a copolymer resin consisting of 60% vinyl chloride and 40% acrylonitrile, and may be produced in either the continuous filament or the staple fiber form. Varying characteristics indicate that many versatile uses are possible.

A. L. Landau

Text. Research J. June 1948

Yarn Twists

The determination of twist in yarns. Tentative (textile) specification No. 12, 1947. Anon. *J. Text. Inst.* **38**, S21–2 (Dec. 1947).

This specification is intended to cover the determination of twist (as turns per unit length) of both spun and continuous-filament yarns in single, ply, and cabled constructions, plain or fancy. Apparatus, sampling technique, number of tests, method of testing, and manner of expressing results are described in detail. L. A. Fiori

Text. Research J. June 1948

Nylon-Wool Blends

Nylon in the wool fabric field. Anon. *Text. Mercury and Argus* **118**, 225, 227, 242 (Feb. 13, 1948).

Experiments indicated that the best method in making use of nylon as a carrier in fine yarns was to lead the nylon into the worsted yarn at the nip of the spinning-frame front roller. This avoids any drawing action on the nylon. An alternate method of doubling the nylon and worsted yarn in a separate operation proved to be unsatisfactory in many ways, especially during dyeing. The most striking improvement noted when combining nylon with wool is the increase in tensile strength. In some cases this was found to be 100% greater than an

Card Clothing

Types of card clothing. R. S. Audley. *Fibres* **9**, 56–9 (Feb. 1948).

A detailed résumé of types of card clothing, method of calculating points per sq. in. from clothing data, differences between Continental and English types of fillet, methods of applying clothing to carding machines, and the merits of metallic card clothing. Illustrations of various types of clothing are given. L. A. Fiori

Text. Research J. June 1948

Fats, Oils, and Soaps

Annual review of the literature on fats, oils, and soaps. Part I. M. M. Piskur. *J. Am. Oil Chemists Soc.* **25**, 129–41 (Apr. 1948).

Text. Research J. June 1948

Silicates in Soap

Silicates in soaps. R. C. Merrill. *J. Am. Oil Chemists Soc.* **25**, 84–95 (Mar. 1948).

A review. 61 references.

Text. Research J. June 1948

Silicones

The chemistry of silicones. Feodora Sos. *Rubber Age* (London) **28**, 240–2 (1947) (through *Chem. Abstr.* **42**, 1757*c* (Mar. 10, 1948)).

A review with 20 references.

Text. Research J. June 1948

Weighting of Silk

Determination of the constituents of tin salt loading in silk. P. Cardoni. *Chimica, e industria* (Milan) **27**, 4–6 (1945); *Chimie & industrie* **57**, 161 (1947) (through *Chem. Abstr.* **42**, 2110*f* (Mar. 20, 1948)).

Qualitative tests are made to determine what elements are present in the ash. Each element is determined differently according to the other elements present.

Text. Research J. June 1948

Laminated Wood

Hydulignum. Anon. *Textile Weekly* **41**, 440, 442 (Mar. 5, 1948); *Text. Mercury and Argus* **118**, 354–5 (Mar. 5, 1948).

Hydulignum, a laminated, densified wood which is manufactured by taking selected hardwood veneers and consolidating them into a homogeneous block, by use of synthetic resin and compression under heat, is especially suited for such items as picking sticks, shuttles, undersleeves, race boards, and other wooden loom parts. Because it can be made with any desired density and grain, this material has resilience, strength, and capacity to take a high polish—all particularly valuable in the case of multi-shuttle looms.

Text. Research J. June 1948 L. A. Fiori

Low-Density Plastics

Low-density plastics. R. A. Clark, T. J. McCuistion, and L. E. Cheyney. *India Rubber World* **117**, 361–3 (1947) (through *Chem. Abstr.* **42**, 1757*d* (Mar. 10, 1948)).

An illustrated review and discussion of present developments in the manufacture and uses of plastic products with sponge and cellular structures. Tabulated data show some of their important physical properties.

Text. Research J. June 1948

Nylon Plastics

Nylon in the food industry. John S. Trevor. *Food* **17**, 20–1 (1948) (through *Chem. Abstr.* **42**, 1671*c* (Mar. 10, 1948)).

The advantages of brushes and sieves made from nylon, and of molded nylon for piping, for table coverings, for lining vessels, for insulating wires and cables, and for the manufacture of many articles used in the food industry are pointed out.

Text. Research J. June 1948

Mothproofing

Modern mothproofing agents. History of the development of "Eulan." H. Stötter. *Angew. Chem.* **A59**, 145–50 (1947) (through *Chem. Abstr.* **42**, 1701*e* (Mar. 10, 1948)).

A comprehensive review of the field based largely on European patent literature. 30 literature and patent references.

Text. Research J. June 1948

Multiple Way Stopcock

A compact multiple way metal stopcock. S. H. Bauer. *Rev. Sci. Instruments* **19**, 52 (Jan. 1948).

A compact multiple way metal stopcock which may be used with a continuously pumped vacuum system is described and illustrated.

L. P. Witnauer

Text. Research J. June 1948

Carbon Disulfide Poisoning in Rayon Plants

Two outbreaks of carbon disulfide poisoning in rayon staple fiber plants in Poland. Emil A. Paluch. *J. Ind. Hyg. Toxicol.* **30**, 37–42 (1948) (through *Chem. Abstr.* **42**, 2101*d* (Mar. 20, 1948)).

A total of at least 152 cases of CS_2 poisoning are described.

Text. Research J. June 1948

Vacuum Seal

Metal-ceramic vacuum seal. Neal Williams. *Rev. Sci. Instruments* **18**, 394–7 (June 1947).

The procedure used in preparing a metal-ceramic seal is outlined and some precautions are noted.

L. P. Witnauer

Text. Research J. June 1948

PATENT REFERENCES

★

Decorative Fabric

Manufacture of decorative fabric articles having a design in relief. Frederick H. Untiedt. U.S. 2,434,527 (Jan. 13, 1948).

A fabric is applied to a sheet of unvulcanized foam rubber. The fabric surface is then embossed, collapsing the rubber foam wherever pressure is applied and forming a design on the surface. Vulcanizing

it is usually found that the "unknown" is the largest class of breaks. Results of ring-frame overhauling showed improvement of end breaks per 1,000 spindle hrs., from 114 to 51 on 10s filling, 144 to 51 on 13s warp, and 118 to 60 on 25s warp. Spindle speed exerts considerable influence on end breakages, which increase with speed. The use of tubes which taper to a relatively small diameter at the top is to be deprecated from the point of view of end breakages. With a twist multiplier of 4.5, end breakage decreases and further increases in twist multiplier up to 4.75 showed significantly fewer breakages, thus supporting the view that some increase in conventional twist multipliers would result in better spinning. A comparison between leather and cork roller coverings indicated no appreciable differences in end breakages; however, a comparison of cork and synthetic rubber coverings showed a small but significant advantage for the latter. Count variation, high spinning drafts, roving piecings, and the outer layers on roving bobbins also contribute toward increases in end breakages.

Text. Research J. June 1948 L. A. Fiori

The analysis of the results of end-breakage tests. A. Ormerod. *J. Text. Inst.* **38**, P576–82 (Dec. 1947).

This paper is concerned with multiple breaks and the behavior of the two ends of yarn and drafted roving after the break. On examining the effects of multiple breaks on work load and running efficiency, it was found that 8.6% primary single end breaks developed into multiple breaks and that 77 multiple breaks pulled down no fewer than 220 ends. If multiple breaks could be eliminated, there would be a 13.8% reduction in ends down. It is concluded that if each "spindle unit" could be isolated from the influence of the 2 adjacent units the reduction in end breakage would represent a reduction in work load of 5%. Main causes for multiple breaks are failure of the underclearers to remove the drafted roving from the spinning zone, lashing of the twisted end into the adjacent balloons, and lashing of a roving end in the vicinity of the traveler. When pneumatic clearing units were used multiple breaks did not develop to the same degree, owing, no doubt, to an 8% reduction in work load. The disposal of drafted roving after end breakage, as observed with yarn spun at 2 twist multipliers and with revolving and pneumatic underclearers, gave surprising results with 21% of the breaks forming crowlaps and 79% forming laps on the leather roll for the hard twist. When revolving top clearers were replaced by specially designed stationary clearers no leather roller laps occurred and all the roving ends were drawn away by the suction equipment. L. A. Fiori

Text. Research J. June 1948

Motor speed control in ring spinning as an aid to reducing yarn breakages. F. J. Stevenson. *J. Text. Inst.* **38**, P586–9 (Dec. 1947).

Three distinct methods are available for controlling the starting and running of a motor individually driving a ring frame: (1) smooth starting by controlled acceleration, (2) variable speed (definite graduation over a range of speed), and (3) change speed (preselection of 2 or more definite running speeds). Yarn breakages are influenced both by the nature of the drive and spindle r.p.m. For the experimental tests selection was made of a "change speed" drive with an increase of 10% in the normal spindle speed. With a typical speed cycle for a run—that is, 10 min. of initial slow speed for the build up, 105 min. top speed for the middle run, and 10 min. slow speed for the tail off—the frame's total run of 125 min., compared with a normal single speed frame run of 138 min. operating under the same conditions, resulted in a 10% increase in production, with the same end breakage for the change speed drive frame. On another frame having a slightly revised speed cycle, the net increase in production was 5¼%, with an improved rate of end breakages. Electric motor designs for variable, changing, and standard speeds are considered in some detail. L. A. Fiori

Text. Research J. June 1948

End breakages in cotton ring spinning. Anon. *J. Text. Inst.* 38, P590–1 (Dec. 1947).

Causes of end breakages compiled from records of tests under actual mill conditions are listed. The minimum rate of occurrence of end breakages of all classes that may be expected is about 30 per 1,000 spindle hrs. L. A. Fiori

Text. Research J. June 1948

End breakages in cotton ring spinning. E. G. Hegedus. *J. Text. Inst.* **38**, P592 (Dec. 1947).

A device which imparts false twist to the drafted roving with attendant strengthening during the final twisting operation is driven independently of the spindle drive and is located in place of the ordinary fixed thread guide at the top of the balloon. This small twist unit consists of 3 discs, the largest being responsible for the drive. It receives the yarn through a diagonal slit and retains it by means of suitable thread guides. Claims made are (1) an increase of production by 15 to 20% and P.M.H. (production per man hour) by 50 to 100%, (2) the number of end breaks is reduced by 50 to 80% without change in spindle speed or twist inserted, and (3) the spindles may be run at speeds up to 20% above normal if twist multiplier is retained at the normal value. L. A. Fiori

Text. Research J. June 1948

MISCELLANEOUS

★

Uniform Cotton Blending

Cotton classification plus inventory equals uniform blends. S. Carter. *Textile World* **98**, 118, 119, 194, 196 (Feb. 1948).

An outline of a method of recording the number of bales of different lots of cotton on hand and of proportioning the bales so that a uniform blend will always be maintained. A simplified method of calculating the blend is given. A. L. Landau

Text. Research J. June 1948